Attaining Record-High Magnetic Exchange, Magnetic Anisotropy and Blocking Barriers in Dilanthanofullerenes

Sourav Dey and Gopalan Rajaraman*

Department of Chemistry, Indian Institute of Technology Bombay, Powai, Mumbai-400076.
Email: rajaraman@chem.iitb.ac.in

Attaining Record-High Magnetic Exchange, Magnetic Anisotropy and Blocking Barriers in Dilanthanofullerenes

Table of Contents

Computational Details

Scheme S1: The qualitative MO scheme of the formation of various spin states from the spin of two Gd centres and one unpaired electron between them.

The energy of a spin state of $Gd_2@C_{59}N$ and $Gd_2@C_{79}N$ is represented by Equation (2) with the Hamiltonian Equation (1);[1, 2]

$$H = -J(S_A S_B O_A + S_A S_B O_B) + BT_{AB} \dots\dots (1),$$

$$E(S, \pm) = -\frac{J}{2}S(S+1) \pm B\left(S + \frac{1}{2}\right) \dots\dots (2),$$

Here, J and B is the interaction and delocalisation parameter respectively. A and B correspond to the Gd1 and Gd2 centres, respectively. S is the total spin multiplicity (see scheme S1), where the additive combination is represented by E(S,+), and the subtractive combination is represented by E (S, -). Consider a spin state S = 13/2, which can be formed by two combinations; $\left[\left(S_{Gd1} = \frac{7}{2}\right) + \left(S_{Gd2} = \frac{5}{2}\right) + \left(S_{rad} = \frac{1}{2}\right)\right]$ or

$[\left(S_{Gd1} = \frac{7}{2}\right) + \left(S_{Gd2} = \frac{7}{2}\right) - \left(S_{rad} = \frac{1}{2}\right)]$. The former one is represented as E(S,+) while the latter one is denoted as E (S, -).

Here T_{AB} is the electron transfer operator

$$T_{AB}|S_A S_B S >^A = \left(S + \frac{1}{2}\right)|S_A S_B S >^B \quad \text{....... (3)}$$

and $\quad T_{AB}|S_A S_B S >^B = (S + \frac{1}{2})|S_A S_B S >^A \quad \text{.........(4)}$

O_A and O_B electron localisation operator

$$O_B|B, S, M_s > = |B, S, M_s > \quad \text{.......... (5)}$$

$$O_B|A, S, M_s > = 0 \quad \text{........... (6)}$$

The delocalisation parameter B is determined with Equation (7), where the energies of E(S,+) and E(S,-) states has been computed by ab initio CASSCF calculation.

$$B = \frac{E(S, +) - E(S, -)}{2S + 1} \quad \text{.......... (7)}$$

On the other hand, using Heisenberg Hamilton $\hat{H}^H = -J_1(S_{Gd1}S_{rad} + S_{Gd2}S_{rad}) - J_2 S_{Gd1}S_{Gd2}$, the energy of a spin state (S) is computed with Equation (8); [3]

$$E^H(S, \pm) = \pm\left(\frac{J_1 - J_2}{2}\right)\left(S + \frac{1}{2}\right) - \frac{J_2}{2}\left[S(S + 1) - S_{max}^{DE}(S_{max}^{DE} + 1)\right] \text{.....(8)}$$

where J_1 is the metal-radical exchange, and J_2 is the metal-metal exchange interaction. The DE represents double exchange, S_{max} represents maximum spin multiplicity. Comparing Equation (2) and (8), one can derive

$$J_1 = 2B + J_2 \quad \text{.......... (9)}$$

$$J_2 = \frac{1}{S}[\{(E(S - 1, -) - E(S, -)\} - B] \quad \text{............... (10)}$$
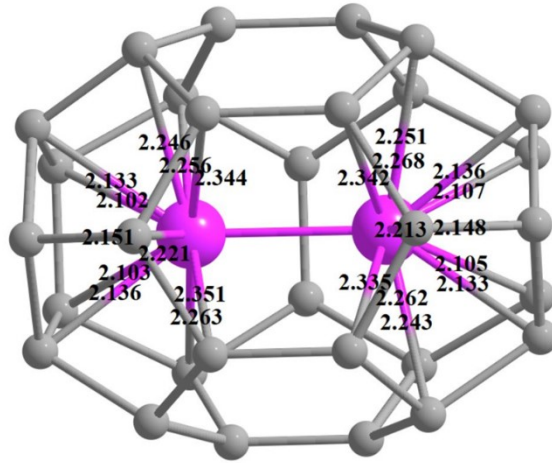
Figure S1: The optimised structure of $Gd_2@C_{30}$-C_{2v}. The Gd-C bonding interactions are obtained from AIM analysis. The Gd-C bond lengths are shown in the angstrom unit. Colour Code: Gd-pink, C-grey.

Table S1: The number of Gd-C bonds in all $Gd_2@C_{2n}$ computed from the BCPs of AIM analysis. It is important to note that Gd^{3+} ion in all $Gd_2@C_{2n}$ binds with a five-membered ring in η^5 fashion except for $Gd_2@C_{34}$-C_s (Gd1), $Gd_2@C_{36}$-D_{2d}, $Gd_2@C_{60}$-I_h, $Gd_2@C_{80}$-D_{5h} where the binding is in η^6-fashion (see Figure S3-22). The third type of η^2 bindings with a six-membered ring was detected in $Gd_2@C_{44}$-D_2, $Gd_2@C_{52}$-D_{2d}, and $Gd_2@C_{80}$-C_{2v}. In this regard, the maximum number of Gd-C BCP has been found in $Gd_2@C_{38}$-D_{3h}, in which both Gd1 and Gd2 form 15 bonds with the carbon atoms in the C_{38} fullerene cage (see Table S1 and Figure S9-10).

$Gd_2@C_{2n}$	Gd1-C	Gd2-C
$Gd_2@C_{30}$-D_{5h}	13	13
$Gd_2@C_{30}$-C_{2v}	12	12
$Gd_2@C_{32}$-C_2	7	10
$Gd_2@C_{32}$-D_3	12	12
$Gd_2@C_{34}$-C_s	7	8
$Gd_2@C_{34}$-C_2	7	7
$Gd_2@C_{36}$-C_s	6	10
$Gd_2@C_{36}$-D_{2d}	6	6
$Gd_2@C_{38}$-C_1	9	6
$Gd_2@C_{38}$-D_{3h}	15	15
$Gd_2@C_{40}$-D_3	8	8
$Gd_2@C_{40}$-C_{2v}	6	6
$Gd_2@C_{42}$-D_3	5	6
$Gd_2@C_{42}$-C_1	7	5
$Gd_2@C_{44}$-C_s	6	8
$Gd_2@C_{44}$-D_2	2	2
$Gd_2@C_{46}$-C_s	9	5
$Gd_2@C_{46}$-C_1	5	6

Gd$_2$@C$_{48}$-C_{2v}	7	7
Gd$_2$@C$_{48}$-C_1	6	6
Gd$_2$@C$_{52}$-C_s	12	8
Gd$_2$@C$_{52}$-D_{2d}	6	6
Gd$_2$@C$_{60}$-I_h	6	6
Gd$_2$@C$_{80}$-C_{2v}	2	2
Gd$_2$@C$_{80}$-D_{5h}	6	6

Table S2: Endohedral fullerenes Gd$_2$@C$_{2n}$ with the number of APRs. The number of APR becomes zero in the case of Gd$_2$@C$_{2n}$, 2n $\geq$ 60.

| Gd$_2$@C$_{2n}$	APR	Hexagon
Gd$_2$@C$_{30}$-D_{5h}	12	5
Gd$_2$@C$_{30}$-C_{2v}	12	5
Gd$_2$@C$_{32}$-C_2	12	6
Gd$_2$@C$_{32}$-D_3	12	6
Gd$_2$@C$_{34}$-C_s	12	7
Gd$_2$@C$_{34}$-C_2	12	7
Gd$_2$@C$_{36}$-C_s	12	8
Gd$_2$@C$_{36}$-D_{2d}	12	8
Gd$_2$@C$_{38}$-C_1	12	9
Gd$_2$@C$_{38}$-D_{3h}	12	9
Gd$_2$@C$_{40}$-D_3	12	10
Gd$_2$@C$_{40}$-C_{2v}	12	10
Gd$_2$@C$_{42}$-D_3	12	11
Gd$_2$@C$_{42}$-C_1	12	11
Gd$_2$@C$_{44}$-C_s	12	12
Gd$_2$@C$_{44}$-D_2	12	12
Gd$_2$@C$_{46}$-C_s	10	13
Gd$_2$@C$_{46}$-C_1	11	13
Gd$_2$@C$_{48}$-C_{2v}	12	14
Gd$_2$@C$_{48}$-C_1	11	14
Gd$_2$@C$_{52}$-C_s	10	16
Gd$_2$@C$_{52}$-D_{2d}	8	16
Gd$_2$@C$_{60}$-I_h	0	20
Gd$_2$@C$_{80}$-C_{2v}	0	30
Gd$_2$@C$_{80}$-D_{5h}	0	30
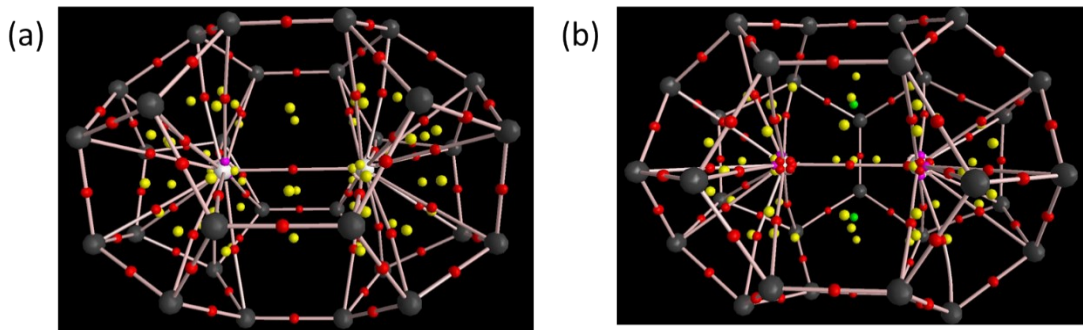
Figure S2: (a) Molecular graph of Gd$_2$@C$_{30}$-D_{5h}. (b) Molecular graph of Gd$_2$@C$_{30}$-C_{2v}.

Table S3: The electron density ($\rho(r)$ in eÅ^{-3}), Laplacian of electron density ($\nabla^2\rho(r)$ in eÅ^{-5}), kinetic energy (G(r) in a.u.), potential energy (|V(r)| in a.u.) of the Gd-C BCPs (bond critical points) in Gd$_2$@C$_{30}$-D_{5h} isomer.

	$\rho(r)$	$\nabla^2\rho(r)$	G(r)	|V(r)|	|V(r)|/G(r)
Gd1-C18	0.072	0.061	0.079	0.096	1.22
Gd1-C21	0.092	0.069	0.100	0.130	1.30
Gd1-C22	0.073	0.062	0.079	0.097	1.23
Gd1-C25	0.092	0.069	0.100	0.130	1.30
Gd1-C27	0.108	0.071	0.115	0.160	1.39
Gd1-C24	0.092	0.069	0.100	0.131	1.31
Gd1-C28	0.108	0.071	0.115	0.160	1.39
Gd1-C26	0.108	0.071	0.116	0.160	1.38
Gd1-C29	0.108	0.071	0.116	0.160	1.38
Gd1-C30	0.108	0.071	0.116	0.161	1.39
Gd1-C16	0.092	0.069	0.100	0.131	1.31
Gd1-C11	0.093	0.069	0.100	0.132	1.32
Gd1-C8	0.073	0.062	0.080	0.098	1.23
Gd2-C23	0.073	0.062	0.080	0.097	1.22
Gd2-C4	0.073	0.061	0.079	0.096	1.22
Gd2-C2	0.092	0.069	0.100	0.131	1.31
Gd2-C20	0.093	0.069	0.100	0.131	1.31
Gd2-C17	0.108	0.071	0.115	0.160	1.39
Gd2-C1	0.108	0.071	0.115	0.160	1.39
Gd2-C5	0.108	0.071	0.115	0.159	1.38
Gd2-C6	0.092	0.069	0.100	0.130	1.30
Gd2-C9	0.073	0.061	0.079	0.096	1.22
Gd2-C10	0.092	0.069	0.100	0.130	1.30
Gd2-C7	0.108	0.071	0.115	0.159	1.38
Gd2-C14	0.073	0.062	0.079	0.097	1.23
Gd2-C19	0.073	0.062	0.080	0.098	1.23

Table S4: The electron density ($\rho(r)$ in eÅ^{-3}), Laplacian of electron density ($\nabla^2\rho(r)$ in eÅ^{-5}), kinetic energy (G(r) in a.u.), potential energy (|V(r)| in a.u.) of the Gd-C BCPs in Gd$_2$@C$_{30}$-C_{2v} isomer.

	$\rho(r)$	$\nabla^2\rho(r)$	G(r)	|V(r)|	|V(r)|/G(r)
Gd1-C6	0.093	0.067	0.099	0.131	1.32
Gd1-C3	0.108	0.072	0.116	0.161	1.39
Gd1-C1	0.111	0.070	0.117	0.164	1.40
Gd1-C14	0.114	0.073	0.122	0.172	1.41
Gd1-C2	0.087	0.068	0.095	0.122	1.28
Gd1-C15	0.083	0.064	0.088	0.112	1.27
Gd1-C10	0.071	0.059	0.076	0.093	1.22
Gd1-C11	0.086	0.068	0.094	0.120	1.28
Gd1-C5	0.072	0.06	0.077	0.094	1.22
Gd1-C16	0.082	0.063	0.087	0.111	1.28
Gd1-C13	0.114	0.072	0.122	0.171	1.40
Gd1-C8	0.110	0.070	0.116	0.163	1.41
Gd2-C21	0.087	0.068	0.094	0.121	1.29
Gd2-C9	0.071	0.059	0.076	0.092	1.21
Gd2-C28	0.111	0.070	0.117	0.164	1.40
Gd2-C12	0.092	0.067	0.098	0.129	1.32
Gd2-C29	0.107	0.072	0.116	0.160	1.38

Gd2-C25	0.084	0.064	0.089	0.114	1.28
Gd2-C26	0.115	0.073	0.123	0.173	1.41
Gd2-C24	0.083	0.063	0.088	0.112	1.27
Gd2-C27	0.115	0.073	0.122	0.172	1.41
Gd2-C30	0.110	0.070	0.116	0.163	1.41
Gd2-C29	0.107	0.072	0.116	0.160	1.38
Gd2-C4	0.070	0.058	0.075	0.091	1.21
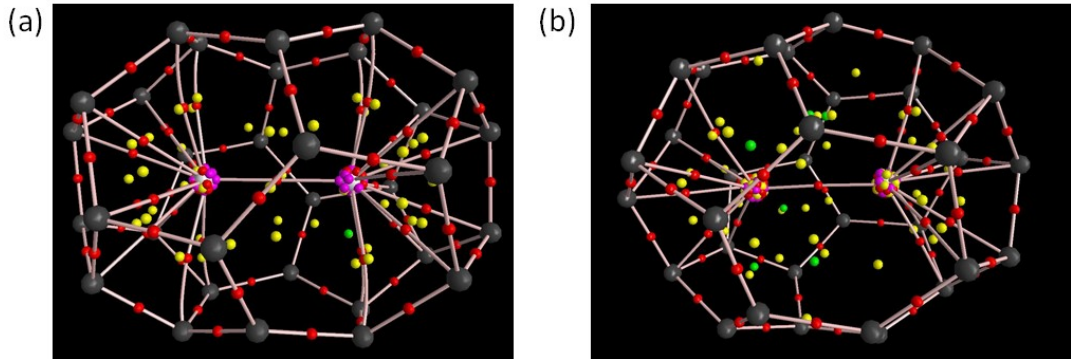
Figure S3: (a) Molecular graph of $Gd_2@C_{32}$-D_3. (b) Molecular graph of $Gd_2@C_{32}$-C_2. Colour Code: Gd-pink, C-grey.
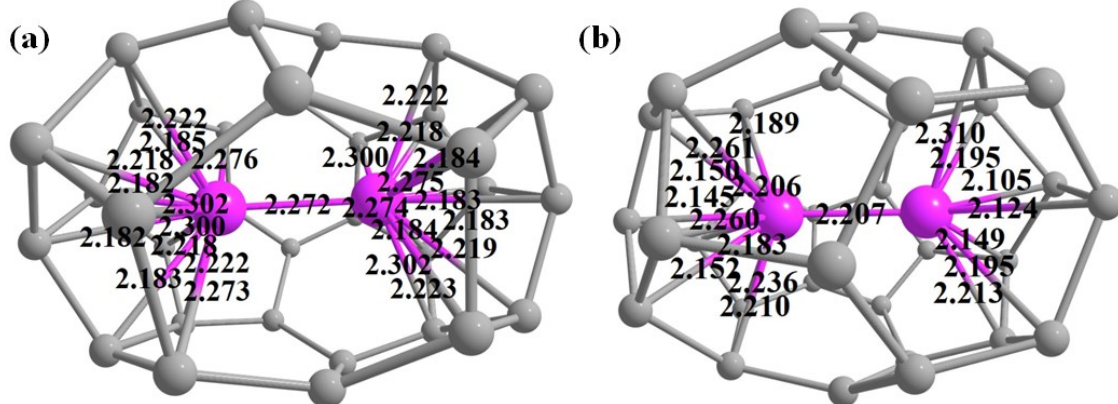
Figure S4: (a) The DFT optimised structure of $Gd_2@C_{32}$-D_3 isomer. (b) The DFT optimised structure of $Gd_2@C_{32}$-C_2 isomer. The Gd-C bonding interactions are obtained from AIM analysis. The Gd-C bond lengths are shown in the angstrom unit.

Table S5: The electron density ($\rho(r)$ in eÅ^{-3}), Laplacian of electron density ($\nabla^2\rho(r)$ in eÅ^{-5}), kinetic energy (G(r) in a.u.), potential energy ($|V(r)|$ in a.u.) of the Gd-C BCPs in $Gd_2@C_{32}$-C_2 isomer.

	$\rho(r)$	$\nabla^2\rho(r)$	G(r)	$|V(r)|$	$|V(r)|/G(r)$
Gd1-C2	0.078	0.063	0.084	0.105	1.25
Gd1-C7	0.111	0.070	0.116	0.163	1.40
Gd1-C8	0.097	0.067	0.102	0.137	1.34
Gd1-C17	0.115	0.073	0.123	0.174	1.41
Gd1-C18	0.097	0.063	0.099	0.134	1.35
Gd1-C16	0.106	0.070	0.112	0.154	1.37
Gd1-C12	0.095	0.065	0.099	0.133	1.34
Gd2-C29	0.086	0.063	0.089	0.115	1.29
Gd2-C4	0.084	0.065	0.090	0.115	1.28

	$\rho(r)$	$\nabla^2\rho(r)$	$G(r)$	$|V(r)|$	$|V(r)|/G(r)$
Gd2-C5	0.106	0.069	0.111	0.153	1.38
Gd2-C30	0.105	0.069	0.111	0.153	1.38
Gd2-C32	0.109	0.072	0.117	0.162	1.38
Gd2-C22	0.094	0.067	0.100	0.133	1.33
Gd2-C27	0.089	0.065	0.094	0.123	1.31
Gd2-C31	0.093	0.066	0.097	0.128	1.32
Gd2-C26	0.102	0.068	0.108	0.147	1.36
Gd2-C23	0.097	0.066	0.100	0.134	1.34

Table S6: The electron density ($\rho(r)$ in eÅ^{-3}), Laplacian of electron density ($\nabla^2\rho(r)$ in eÅ^{-5}), kinetic energy ($G(r)$ in a.u.), potential energy ($|V(r)|$ in a.u.) of the Gd-C BCPs in Gd$_2$@C$_{32}$-D_3 isomer.

	$\rho(r)$	$\nabla^2\rho(r)$	$G(r)$	$|V(r)|$	$|V(r)|/G(r)$
Gd1-C1	0.079	0.063	0.085	0.106	1.25
Gd1-C8	0.089	0.069	0.098	0.126	1.29
Gd1-C11	0.101	0.066	0.104	0.142	1.37
Gd1-C7	0.100	0.065	0.103	0.141	1.37
Gd1-C32	0.089	0.069	0.097	0.126	1.30
Gd1-C6	0.101	0.069	0.108	0.148	1.37
Gd1-C29	0.094	0.066	0.100	0.133	1.33
Gd1-C14	0.102	0.069	0.109	0.148	1.36
Gd1-C12	0.079	0.065	0.085	0.106	1.25
Gd1-C28	0.079	0.063	0.085	0.107	1.26
Gd1-C5	0.094	0.066	0.100	0.139	1.39
Gd1-C4	0.079	0.064	0.085	0.106	1.25
Gd2-C19	0.079	0.064	0.085	0.106	1.25
Gd2-C2	0.079	0.063	0.085	0.107	1.26
Gd2-C18	0.100	0.065	0.103	0.141	1.37
Gd2-C15	0.089	0.069	0.097	0.126	1.30
Gd2-C23	0.094	0.066	0.100	0.133	1.33
Gd2-C21	0.101	0.069	0.108	0.148	1.37
Gd2-C16	0.094	0.066	0.099	0.133	1.34
Gd2-C22	0.101	0.069	0.108	0.148	1.37
Gd2-C17	0.079	0.063	0.085	0.106	1.25
Gd2-C27	0.100	0.066	0.104	0.142	1.37
Gd2-C26	0.079	0.064	0.085	0.106	1.25
Gd2-C24	0.089	0.069	0.098	0.127	1.30

Table S7: The electron density ($\rho(r)$ in eÅ^{-3}), Laplacian of electron density ($\nabla^2\rho(r)$ in eÅ^{-5}), kinetic energy ($G(r)$ in a.u.), potential energy ($|V(r)|$ in a.u.) of the Gd-C BCPs in Gd$_2$@C$_{34}$-C_2 isomer.

Gd2C34 (C_2)	$\rho(r)$	$\nabla^2\rho(r)$	$G(r)$	$|V(r)|$	$|V(r)|/G(r)$
Gd1-C14	0.092	0.064	0.095	0.126	1.33
Gd1-C17	0.078	0.060	0.082	0.105	1.28
Gd1-C12	0.096	0.067	0.101	0.135	1.34
Gd1-C11	0.106	0.069	0.111	0.153	1.38
Gd1-C7	0.101	0.067	0.106	0.145	1.37
Gd1-C6	0.084	0.063	0.089	0.115	1.29
Gd1-C1	0.096	0.066	0.101	0.136	1.35
Gd2-C34	0.093	0.063	0.095	0.128	1.35
Gd2-C33	0.097	0.066	0.102	0.137	1.34
Gd2-C25	0.101	0.067	0.106	0.145	1.37

Gd2-C27	0.095	0.067	0.100	0.134	1.34
Gd2-C28	0.105	0.068	0.110	0.152	1.38
Gd2-C23	0.079	0.060	0.082	0.105	1.28
Gd2-C26	0.085	0.063	0.090	0.116	1.29
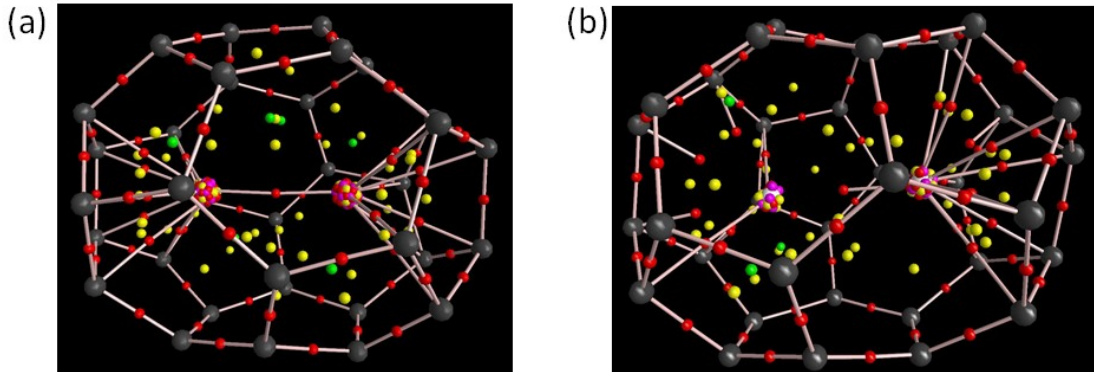
Figure S5: (a) Molecular graph of $Gd_2@C_{34}$-C_2. (b) Molecular graph of $Gd_2@C_{34}$-C_s.
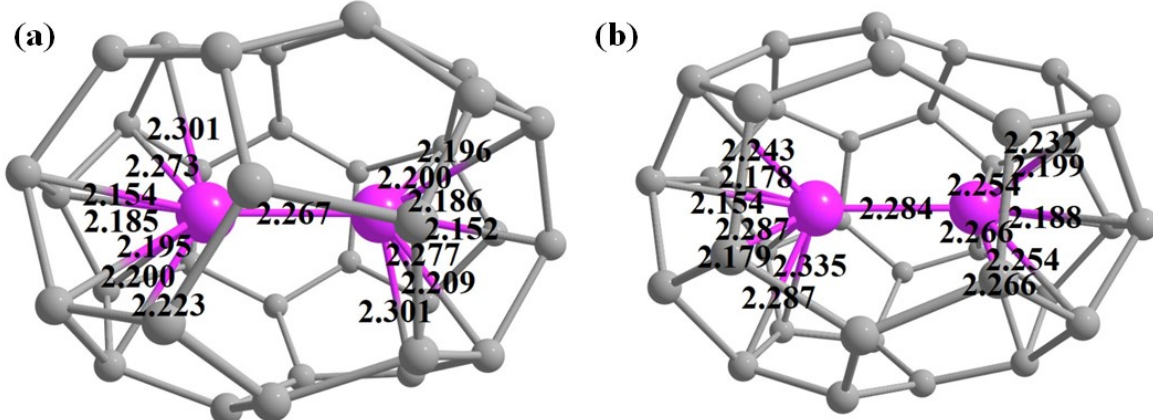
Figure S6: (a) The DFT optimised structure of $Gd_2@C_{34}$-C_2 isomer. (b) The DFT optimised structure of $Gd_2@C_{34}$-C_s isomer. The Gd-C bonding interactions are obtained from AIM analysis. The Gd-C bond lengths are shown in the angstrom unit. Colour Code: Gd-pink, C-grey.

Table S8: The electron density (ρ(r) in eÅ^{-3}), Laplacian of electron density ($\nabla^2\rho$(r) in eÅ^{-5}), kinetic energy (G(r) in a.u.), potential energy (|V(r)| in a.u.) of the Gd-C BCPs in $Gd_2@C_{34}$-C_s isomer.

	ρ(r)	$\nabla^2\rho$(r)	G(r)	|V(r)|	V(r)/G(r)
Gd1-C32	0.080	0.059	0.082	0.105	1.28
Gd1-C7	0.101	0.064	0.102	0.141	1.38
Gd1-C8	0.104	0.071	0.112	0.152	1.36
Gd1-C15	0.101	0.064	0.102	0.141	1.38
Gd1-C34	0.080	0.059	0.082	0.105	1.28
Gd1-C33	0.071	0.057	0.074	0.091	1.23
Gd1-C6	0.091	0.061	0.092	0.124	1.35
Gd2-C24	0.080	0.065	0.087	0.109	1.25
Gd2-C25	0.087	0.063	0.091	0.119	1.31
Gd2-C22	0.099	0.065	0.102	0.139	1.36
Gd2-C23	0.100	0.070	0.108	0.146	1.35
Gd2-C17	0.099	0.065	0.102	0.139	1.36

Gd2-C18	0.087	0.063	0.091	0.118	1.30
Gd2-C16	0.090	0.064	0.094	0.125	1.33
Gd2-C29	0.080	0.065	0.087	0.109	1.25

Table S9: The electron density ($\rho(r)$ in eÅ^{-3}), Laplacian of electron density ($\nabla^2\rho(r)$ in eÅ^{-5}), kinetic energy (G(r) in a.u.), potential energy (|V(r)| in a.u.) of the Gd-C BCPs in Gd$_2$@C$_{36}$-C_s isomer.

	$\rho(r)$	$\nabla^2\rho(r)$	G(r)	|V(r)|	|V(r)|/G(r)
Gd1-C31	0.092	0.062	0.094	0.126	1.34
Gd1-C33	0.092	0.062	0.094	0.126	1.34
Gd1-C30	0.091	0.064	0.095	0.126	1.33
Gd1-C34	0.092	0.064	0.095	0.127	1.34
Gd1-C20	0.085	0.060	0.087	0.115	1.32
Gd1-C26	0.080	0.058	0.080	0.102	1.28
Gd2-C25	0.076	0.063	0.083	0.102	1.23
Gd2-C5	0.076	0.063	0.082	0.102	1.24
Gd2-C2	0.090	0.060	0.090	0.120	1.33
Gd2-C23	0.083	0.060	0.085	0.110	1.29
Gd2-C1	0.089	0.063	0.093	0.123	1.32
Gd2-C22	0.089	0.061	0.091	0.121	1.33
Gd2-C3	0.088	0.061	0.091	0.121	1.33
Gd2-C6	0.082	0.060	0.085	0.110	1.29
Gd2-C9	0.084	0.061	0.087	0.113	1.30
Gd2-C18	0.084	0.061	0.087	0.113	1.30
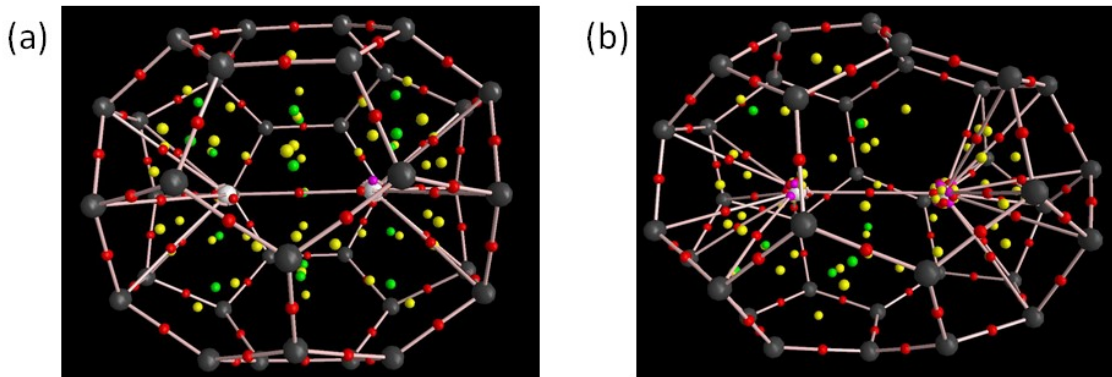
Figure S7: (a) Molecular graph of Gd$_2$@C$_{36}$-D_{2d}. (b) Molecular graph of Gd$_2$@C$_{36}$-C_s.
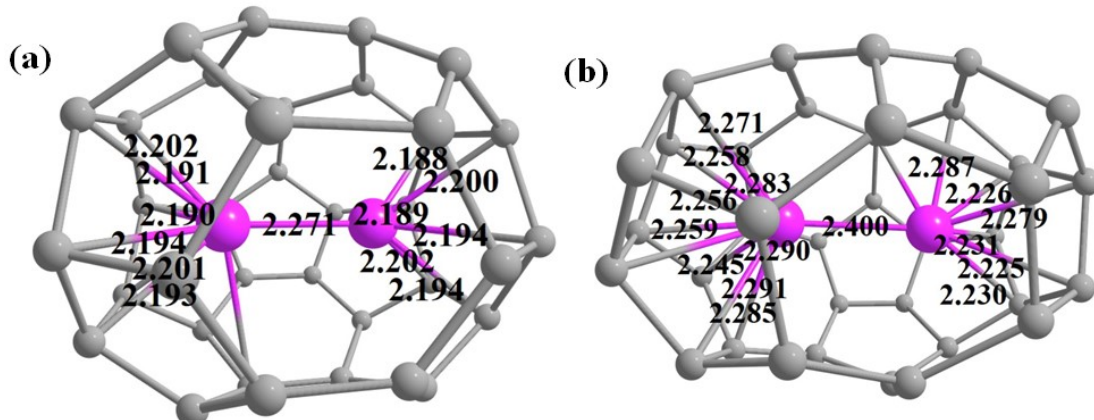
Figure S8: (a) The DFT optimised structure of Gd$_2$@C$_{36}$-D_{2d} isomer. (b) The DFT optimised structure of Gd$_2$@C$_{36}$-C_s isomer. The Gd-C bonding interactions are obtained from AIM analysis. The Gd-C bond lengths are shown in the angstrom unit. Colour Code: Gd-pink, C-grey.

Table S10: The electron density (ρ(r) in eÅ^{-3}), Laplacian of electron density ($\nabla^2\rho$(r) in eÅ^{-5}), kinetic energy (G(r) in a.u.), potential energy (|V(r)| in a.u.) of the Gd-C BCPs in Gd$_2$@C$_{36}$-D_{2d} isomer.

	ρ(r)	$\nabla^2\rho$(r)	G(r)	|V(r)|	|V(r)|/G(r)
Gd1-C26	0.097	0.060	0.096	0.131	1.36
Gd1-C24	0.098	0.064	0.100	0.136	1.36
Gd1-C18	0.096	0.063	0.098	0.131	1.34
Gd1-C17	0.096	0.063	0.097	0.131	1.35
Gd1-C25	0.097	0.060	0.095	0.131	1.38
Gd1-C23	0.098	0.064	0.100	0.136	1.36
Gd2-C33	0.097	0.060	0.095	0.131	1.38
Gd2-C12	0.096	0.063	0.098	0.132	1.35
Gd2-C15	0.098	0.060	0.096	0.131	1.36
Gd2-C31	0.098	0.064	0.100	0.136	1.36
Gd2-C14	0.096	0.063	0.098	0.132	1.35
Gd2-C32	0.097	0.064	0.100	0.136	1.36
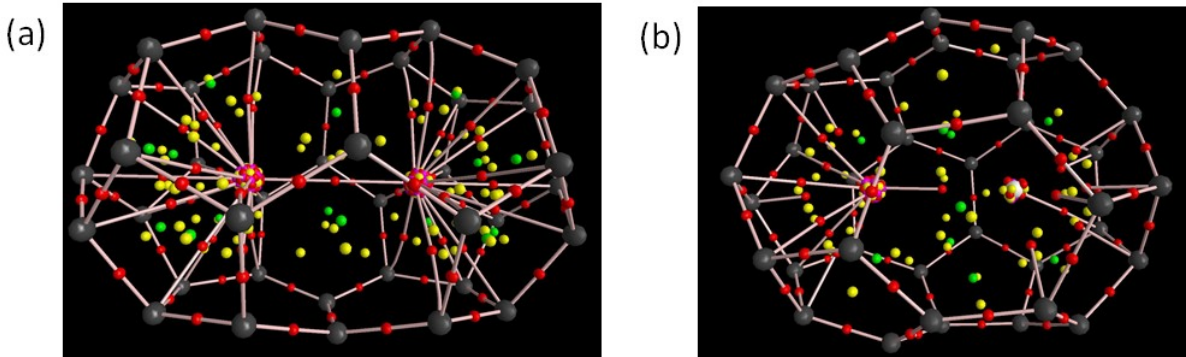
Figure S9: (a) Molecular graph of Gd$_2$@C$_{38}$-D_{3h}. (b) Molecular graph of Gd$_2$@C$_{38}$-C_1.

Figure S10: (a) The DFT optimised structure of Gd$_2$@C$_{38}$-D_{3h} isomer. (b) The DFT optimised structure of
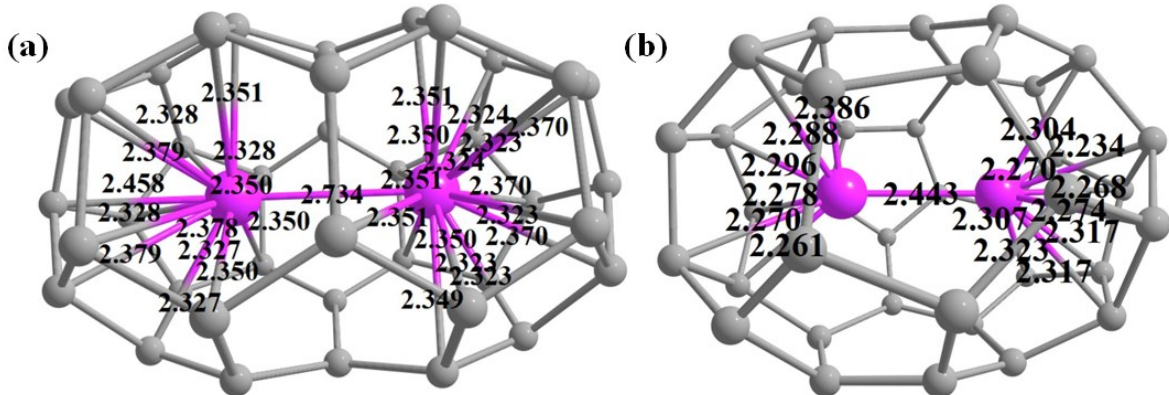
Gd$_2$@C$_{38}$-C_1 isomer. The Gd-C bonding interactions are obtained from AIM analysis. The Gd-C bond lengths are shown in the angstrom unit. Colour Code: Gd-pink, C-grey.

Table S11: The electron density (ρ(r) in eÅ^{-3}), Laplacian of electron density ($\nabla^2\rho$(r) in eÅ^{-5}), kinetic energy (G(r) in a.u.), potential energy (|V(r)| in a.u.) of the Gd-C BCPs in Gd$_2$@C$_{38}$-C_1 isomer.

	ρ(r)	$\nabla^2\rho$(r)	G(r)	|V(r)|	|V(r)|/G(r)
Gd1-C3	0.077	0.056	0.078	0.100	1.28
Gd1-C4	0.082	0.060	0.084	0.108	1.29
Gd1-C1	0.079	0.059	0.082	0.107	1.30
Gd1-C2	0.076	0.057	0.078	0.098	1.26
Gd1-C28	0.088	0.059	0.089	0.118	1.33
Gd1-C31	0.077	0.059	0.079	0.100	1.27
Gd1-C29	0.085	0.060	0.087	0.113	1.30
Gd1-C16	0.090	0.062	0.092	0.112	1.22
Gd1-C14	0.079	0.058	0.081	0.103	1.27
Gd2-C38	0.087	0.058	0.086	0.115	1.34
Gd2-C37	0.082	0.061	0.085	0.110	1.29
Gd2-C34	0.084	0.060	0.086	0.112	1.30
Gd2-C32	0.084	0.057	0.083	0.110	1.33
Gd2-C20	0.066	0.052	0.067	0.082	1.22
Gd2-C21	0.078	0.058	0.080	0.102	1.28

Table S12: The electron density (ρ(r) in eÅ^{-3}), Laplacian of electron density ($\nabla^2\rho$(r) in eÅ^{-5}), kinetic energy (G(r) in a.u.), potential energy (|V(r)| in a.u.) of the Gd-C BCPs in Gd$_2$@C$_{38}$-D_{3h} isomer.

	ρ(r)	$\nabla^2\rho$(r)	G(r)	|V(r)|	|V(r)|/G(r)
Gd1-C1	0.070	0.055	0.071	0.088	1.24
Gd1-C6	0.070	0.055	0.071	0.087	1.23
Gd1-C2	0.074	0.058	0.077	0.097	1.26
Gd1-C19	0.074	0.058	0.077	0.097	1.26
Gd1-C22	0.070	0.055	0.071	0.088	1.24
Gd1-C28	0.069	0.055	0.071	0.087	1.23
Gd1-C18	0.074	0.058	0.077	0.096	1.25
Gd1-C16	0.070	0.052	0.071	0.090	1.27
Gd1-C33	0.069	0.055	0.071	0.087	1.23
Gd1-C17	0.074	0.058	0.077	0.096	1.25
Gd1-C10	0.074	0.058	0.077	0.096	1.25
Gd1-C15	0.070	0.052	0.071	0.089	1.25
Gd1-C9	0.074	0.058	0.077	0.096	1.25
Gd1-C14	0.062	0.049	0.063	0.078	1.24
Gd1-C8	0.071	0.052	0.071	0.090	1.27
Gd2-C27	0.070	0.055	0.071	0.088	1.24
Gd2-C23	0.070	0.055	0.071	0.088	1.24
Gd2-C35	0.074	0.059	0.079	0.098	1.24
Gd2-C25	0.074	0.059	0.078	0.098	1.26
Gd2-C32	0.072	0.053	0.072	0.092	1.28
Gd2-C12	0.069	0.055	0.071	0.087	1.23
Gd2-C37	0.070	0.055	0.071	0.088	1.24
Gd2-C36	0.074	0.059	0.078	0.098	1.26
Gd2-C38	0.072	0.053	0.072	0.092	1.28

Gd2-C7	0.074	0.059	0.078	0.097	1.24
Gd2-C4	0.069	0.055	0.071	0.087	1.23
Gd2-C21	0.069	0.055	0.071	0.087	1.23
Gd2-C26	0.074	0.059	0.078	0.098	1.26
Gd2-C30	0.072	0.053	0.072	0.092	1.28
Gd2-C3	0.074	0.059	0.078	0.098	1.26
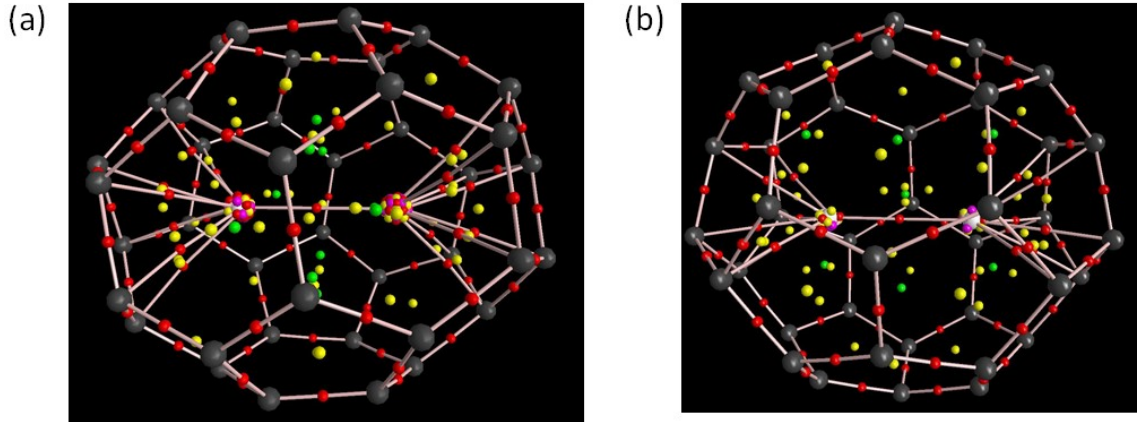
Figure S11: (a) Molecular graph of $Gd_2@C_{40}$-D_3. (b) Molecular graph of $Gd_2@C_{40}$-C_{2v}.
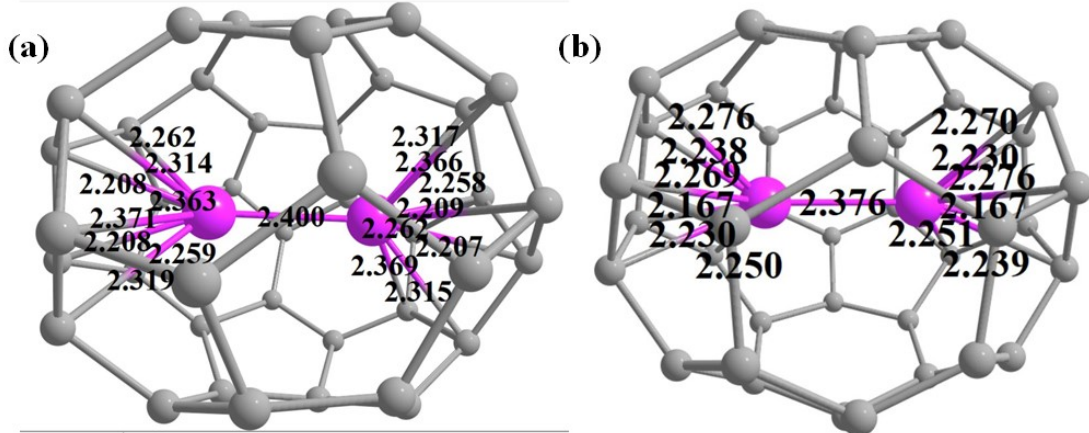
Figure S12: (a) The DFT optimised structure of $Gd_2@C_{40}$-D_3 isomer. (b) The DFT optimised structure of $Gd_2@C_{40}$-C_{2v} isomer. The Gd-C bonding interactions are obtained from AIM analysis. The Gd-C bond lengths are shown in the angstrom unit. Colour Code: Gd-pink, C-grey.

Table S13: The electron density ($\rho(r)$ in e$Å^{-3}$), Laplacian of electron density ($\nabla^2\rho(r)$ in e$Å^{-5}$), kinetic energy (G(r) in a.u.), potential energy (|V(r)| in a.u.) of the Gd-C BCPs in $Gd_2@C_{40}$-D_3 isomer.

	$\rho(r)$	$\nabla^2\rho(r)$	G(r)	|V(r)|	|V(r)|/G(r)
Gd1-C5	0.078	0.057	0.077	0.101	1.31
Gd1-C40	0.071	0.052	0.070	0.088	1.26
Gd1-C4	0.097	0.061	0.097	0.133	1.37
Gd1-C38	0.084	0.059	0.084	0.109	1.30
Gd1-C36	0.097	0.061	0.097	0.132	1.36
Gd1-C30	0.084	0.060	0.085	0.111	1.31
Gd1-C31	0.072	0.052	0.070	0.089	1.27

Gd1-C35	0.078	0.057	0.078	0.100	1.28
Gd2-C15	0.072	0.052	0.070	0.089	1.27
Gd2-C9	0.084	0.060	0.084	0.110	1.31
Gd2-C7	0.097	0.061	0.097	0.132	1.36
Gd2-C14	0.078	0.057	0.079	0.101	1.28
Gd2-C21	0.084	0.059	0.084	0.109	1.30
Gd2-C13	0.097	0.061	0.097	0.133	1.37
Gd2-C26	0.071	0.052	0.070	0.087	1.24
Gd2-C6	0.077	0.057	0.078	0.100	1.28

Table S14: The electron density ($\rho(r)$ in e$\mathrm{Å}^{-3}$), Laplacian of electron density ($\nabla^2\rho(r)$ in e$\mathrm{Å}^{-5}$), kinetic energy (G(r) in a.u.), potential energy (|V(r)| in a.u.) of the Gd-C BCPs in Gd$_2$@C$_{40}$-C_{2v} isomer.

|	$\rho(r)$	$\nabla^2\rho(r)$	G(r)	|V(r)|	|V(r)|/G(r)
Gd1-C32	0.085	0.060	0.087	0.114	1.31
Gd1-C22	0.093	0.058	0.091	0.124	1.36
Gd1-C23	0.100	0.067	0.105	0.142	1.35
Gd1-C31	0.084	0.060	0.086	0.113	1.31
Gd1-C27	0.092	0.056	0.090	0.121	1.34
Gd1-C25	0.086	0.056	0.082	0.109	1.33
Gd2-C10	0.084	0.060	0.086	0.112	1.30
Gd2-C7	0.092	0.058	0.089	0.121	1.36
Gd2-C9	0.085	0.060	0.087	0.114	1.31
Gd2-C36	0.093	0.058	0.091	0.124	1.36
Gd2-C21	0.086	0.055	0.082	0.109	1.33
Gd2-C20	0.100	0.067	0.104	0.142	1.37
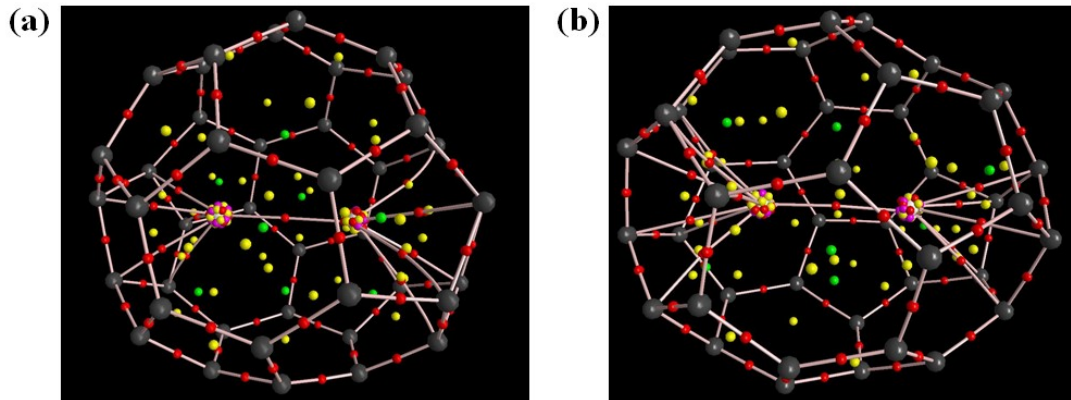
Figure S13: (a) Molecular graph of Gd$_2$@C$_{42}$-C_2. (b) Molecular graph of Gd$_2$@C$_{42}$-C_s.
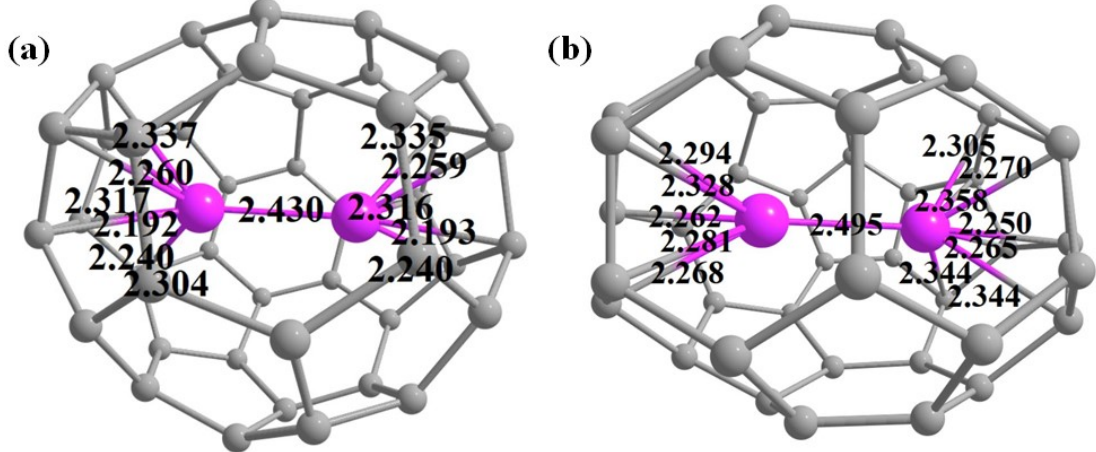
Figure S14: (a) The DFT optimised structure of $Gd_2@C_{42}$-C_2 isomer. (b) The DFT optimised structure of $Gd_2@C_{42}$-C_s isomer. The Gd-C bonding interactions are obtained from AIM analysis. The Gd-C bond lengths are shown in the angstrom unit. Colour Code: Gd-pink, C-grey.

Table S15: The electron density (ρ(r) in eÅ^{-3}), Laplacian of electron density ($\nabla^2\rho$(r) in eÅ^{-5}), kinetic energy (G(r) in a.u.), potential energy (|V(r)| in a.u.) of the Gd-C BCPs in $Gd_2@C_{42}$-C_1 isomer.

	ρ(r)	$\nabla^2\rho$(r)	G(r)	|V(r)|	|V(r)|/G(r)
Gd1-C42	0.072	0.053	0.071	0.090	1.27
Gd1-C36	0.076	0.057	0.078	0.098	1.26
Gd1-C5	0.072	0.052	0.070	0.087	1.24
Gd1-C8	0.087	0.057	0.085	0.113	1.33
Gd1-C30	0.090	0.060	0.090	0.120	1.33
Gd1-C27	0.087	0.055	0.084	0.113	1.35
Gd1-C31	0.074	0.054	0.073	0.092	1.26
Gd2-C21	0.088	0.058	0.086	0.115	1.34
Gd2-C10	0.087	0.057	0.085	0.113	1.33
Gd2-C22	0.082	0.057	0.082	0.106	1.29
Gd2-C9	0.081	0.057	0.081	0.104	1.28
Gd2-C20	0.078	0.053	0.075	0.097	1.29

Table S16: The electron density (ρ(r) in eÅ^{-3}), Laplacian of electron density ($\nabla^2\rho$(r) in eÅ^{-5}), kinetic energy (G(r) in a.u.), potential energy (|V(r)| in a.u.) of the Gd-C BCPs in $Gd_2@C_{42}$-D_3 isomer.

|	ρ(r)	$\nabla^2\rho$(r)	G(r)	|V(r)|	|V(r)|/G(r)
Gd1-C33	0.092	0.055	0.087	0.119	1.37
Gd1-C25	0.095	0.066	0.099	0.132	1.33
Gd1-C29	0.078	0.058	0.080	0.102	1.28
Gd1-C24	0.089	0.056	0.085	0.114	1.34
Gd1-C30	0.076	0.055	0.076	0.097	1.28
Gd2-C37	0.079	0.055	0.076	0.096	1.26
Gd2-C23	0.092	0.055	0.087	0.119	1.37
Gd2-C36	0.095	0.065	0.099	0.132	1.33
Gd2-C10	0.078	0.058	0.080	0.101	1.26
Gd2-C12	0.076	0.055	0.075	0.096	1.28
Gd2-C14	0.088	0.056	0.085	0.114	1.34
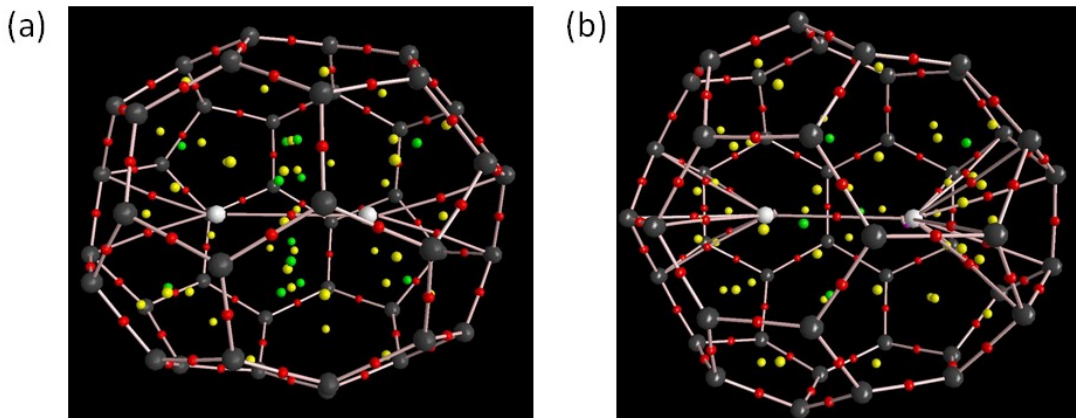
Figure S15: (a) Molecular graph of $Gd_2@C_{44}$-D_2. (b) Molecular graph of $Gd_2@C_{44}$-C_s.
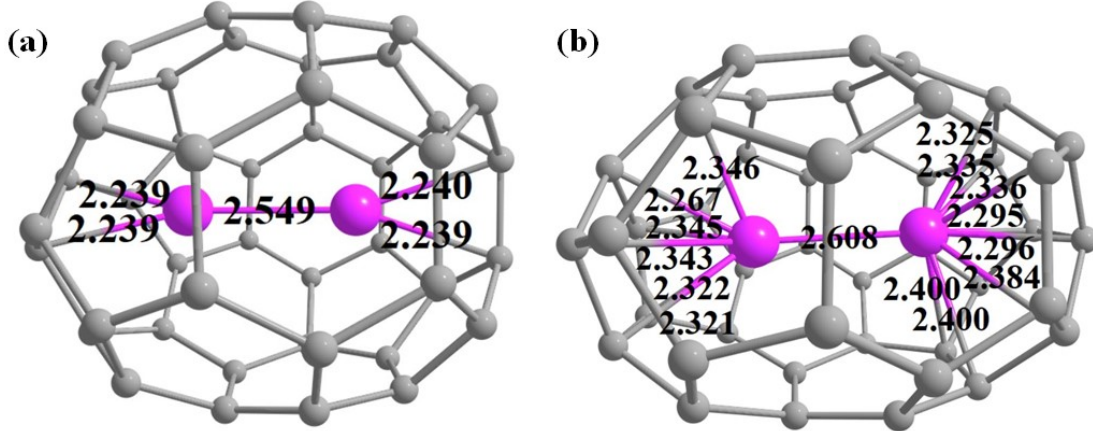

Figure S16: (a) The DFT optimised structure of $Gd_2@C_{44}$-D_2 isomer. (b) The DFT optimised structure of $Gd_2@C_{44}$-C_s isomer. The Gd-C bonding interactions are obtained from AIM analysis. The Gd-C bond lengths are shown in the angstrom unit. Colour Code: Gd-pink, C-grey.

Table S17: The electron density (ρ(r) in eÅ^{-3}), Laplacian of electron density ($\nabla^2\rho$(r) in eÅ^{-5}), kinetic energy (G(r) in a.u.), potential energy (|V(r)| in a.u.) of the Gd-C BCPs in $Gd_2@C_{44}$-D_2 isomer.

	ρ(r)	$\nabla^2\rho$(r)	G(r)	|V(r)|	|V(r)|/G(r)
Gd1-C33	0.089	0.059	0.087	0.116	1.33
Gd1-C32	0.089	0.059	0.087	0.116	1.33
Gd2-C7	0.089	0.059	0.087	0.116	1.33
Gd2-C6	0.089	0.059	0.087	0.116	1.33

Table S18: The electron density (ρ(r) in eÅ^{-3}), Laplacian of electron density ($\nabla^2\rho$(r) in eÅ^{-5}), kinetic energy (G(r) in a.u.), potential energy (|V(r)| in a.u.) of the Gd-C BCPs in $Gd_2@C_{44}$-C_s isomer.

Gd2C44(Cs)	ρ(r)	$\nabla^2\rho$(r)	|V(r)|	G(r)	|V(r)|/G(r)
Gd1-C43	0.075	0.051	0.072	0.093	1.29
Gd1-C36	0.075	0.051	0.072	0.093	1.29

|					
Gd1-C40	0.078	0.054	0.076	0.099	1.30
Gd1-C32	0.069	0.052	0.067	0.082	1.22
Gd1-C37	0.084	0.055	0.081	0.107	1.32
Gd1-C41	0.078	0.054	0.076	0.098	1.29
Gd2-C10	0.063	0.049	0.062	0.074	1.19
Gd2-C7	0.068	0.049	0.066	0.082	1.24
Gd2-C23	0.076	0.053	0.074	0.095	1.28
Gd2-C6	0.082	0.055	0.080	0.105	1.31
Gd2-C9	0.063	0.049	0.062	0.075	1.21
Gd2-C5	0.082	0.055	0.080	0.105	1.31
Gd2-C3	0.076	0.053	0.074	0.095	1.28
Gd2-C28	0.073	0.055	0.074	0.093	1.26
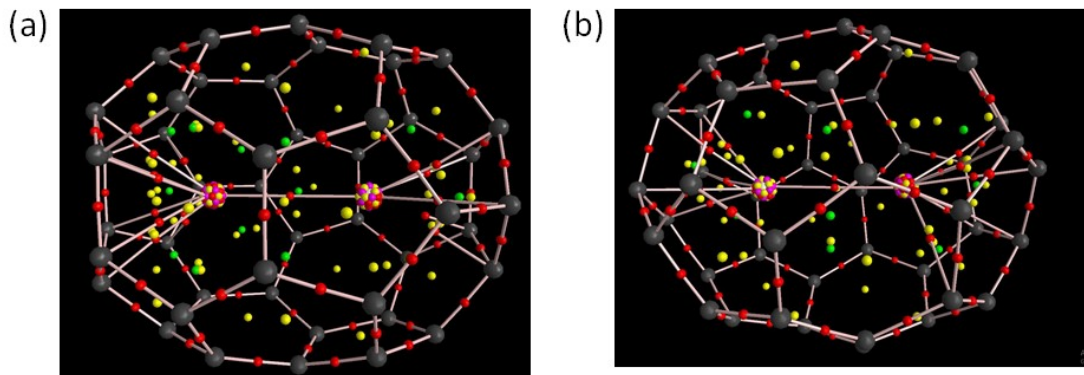
Figure S17: (a) Molecular graph of $Gd_2@C_{46}$-C_s. (b) Molecular graph of $Gd_2@C_{46}$-C_1.
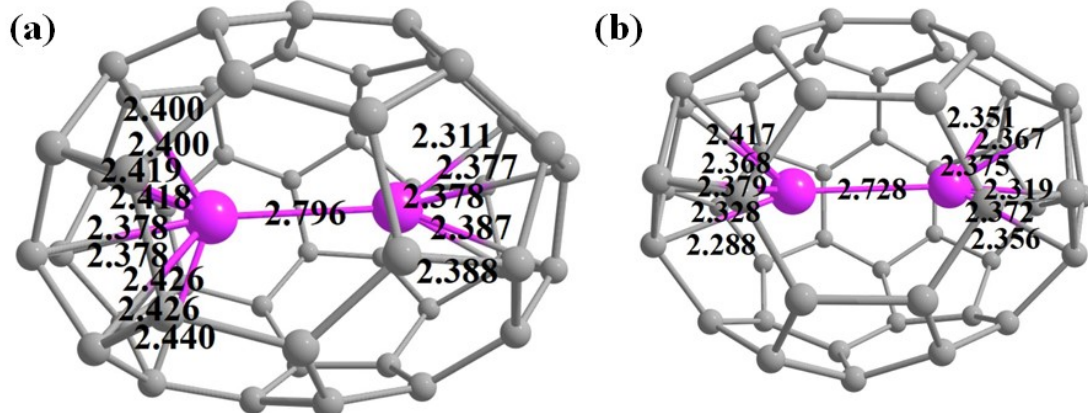

Figure S18: (a) The DFT optimised structure of $Gd_2@C_{46}$-C_s isomer. (b) The DFT optimised structure of $Gd_2@C_{46}$-C_1 isomer. The Gd-C bonding interactions are obtained from AIM analysis. The Gd-C bond lengths are shown in the angstrom unit. Colour Code: Gd-pink, C-grey.

Table S19: The electron density (ρ(r) in eÅ^{-3}), Laplacian of electron density ($\nabla^2\rho$(r) in eÅ^{-5}), kinetic energy (G(r) in a.u.), potential energy (|V(r)| in a.u.) of the Gd-C BCPs in $Gd_2@C_{46}$-C_s isomer.

	ρ(r)	$\nabla^2\rho$(r)	|V(r)|	G(r)	|V(r)|/G(r)
Gd1-C39	0.065	0.045	0.060	0.075	1.25
Gd1-C45	0.063	0.047	0.061	0.076	1.25
Gd1-C44	0.058	0.047	0.058	0.069	1.19
Gd1-C40	0.063	0.047	0.060	0.073	1.22

Gd1-C42	0.070	0.049	0.067	0.085	1.27
Gd1-C38	0.070	0.049	0.067	0.085	1.27
Gd1-C41	0.063	0.047	0.060	0.073	1.22
Gd1-C37	0.065	0.045	0.060	0.075	1.25
Gd1-C46	0.063	0.047	0.061	0.076	1.25
Gd2-C2	0.069	0.049	0.066	0.084	1.27
Gd2-C10	0.070	0.048	0.067	0.085	1.27
Gd2-C15	0.076	0.053	0.074	0.095	1.28
Gd2-C28	0.071	0.048	0.067	0.085	1.27
Gd2-C1	0.069	0.049	0.066	0.084	1.27

Table S20: The electron density ($\rho(r)$ in eÅ^{-3}), Laplacian of electron density ($\nabla^2\rho(r)$ in eÅ^{-5}), kinetic energy (G(r) in a.u.), potential energy (|V(r)| in a.u.) of the Gd-C BCPs in Gd$_2$@C$_{46}$-C_1 isomer.

	$\rho(r)$	$\nabla^2\rho(r)$	$|V(r)|$	$G(r)$	$|V(r)|/G(r)$
Gd1-C3	0.071	0.047	0.066	0.084	1.27
Gd1-C9	0.064	0.050	0.064	0.078	1.22
Gd1-C2	0.079	0.056	0.078	0.101	1.29
Gd1-C8	0.071	0.050	0.069	0.088	1.28
Gd1-C5	0.078	0.050	0.073	0.096	1.32
Gd2-C38	0.071	0.048	0.067	0.085	1.27
Gd2-C35	0.071	0.051	0.069	0.088	1.28
Gd2-C34	0.079	0.051	0.074	0.098	1.32
Gd2-C39	0.070	0.053	0.070	0.087	1.24
Gd2-C30	0.070	0.050	0.067	0.084	1.25
Gd2-C24	0.072	0.049	0.069	0.088	1.28
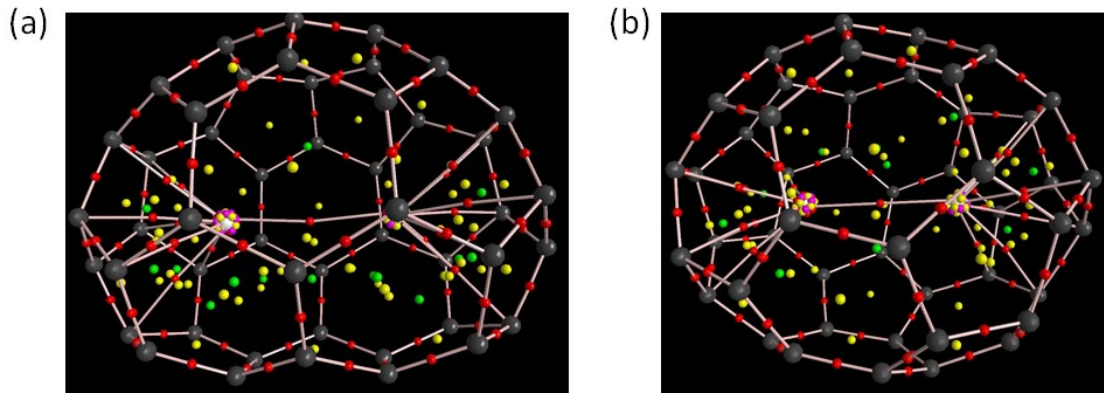
Figure S19: (a) Molecular graph of Gd$_2$@C$_{48}$-C_{2v}. (b) Molecular graph of Gd$_2$@C$_{48}$-C_1.

.

S19
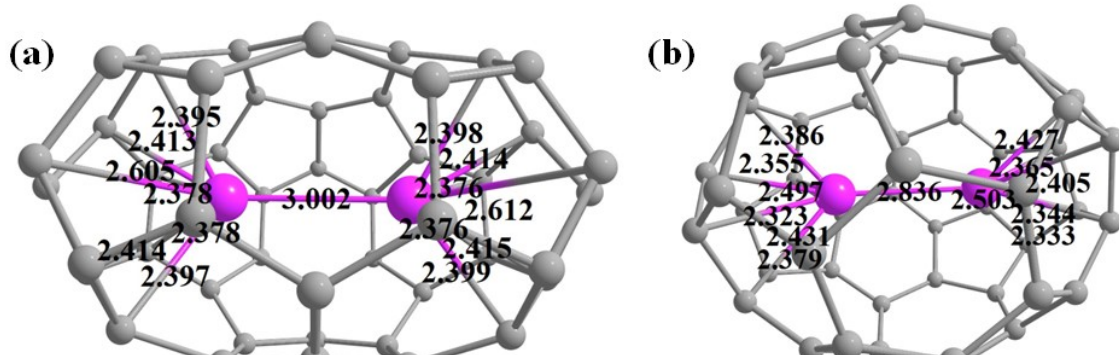
Figure S20: (a) The DFT optimised structure of $Gd_2@C_{48}$-C_{2v} isomer. (b) The DFT optimised structure of $Gd_2@C_{48}$-C_1 isomer. The Gd-C bonding interactions are obtained from AIM analysis. The Gd-C bond lengths are shown in the angstrom unit. Colour Code: Gd-pink, C-grey.

Table S21: The electron density ($\rho(r)$ in eÅ^{-3}), Laplacian of electron density ($\nabla^2\rho(r)$ in eÅ^{-5}), kinetic energy (G(r) in a.u.), potential energy (|V(r)| in a.u.) of the Gd-C BCPs in $Gd_2@C_{48}$-C_1 isomer.

	$\rho(r)$	$\nabla^2\rho(r)$	G(r)	|V(r)|	|V(r)|/G(r)
Gd1-C22	0.054	0.043	0.053	0.062	1.17
Gd1-C23	0.076	0.048	0.070	0.092	1.31
Gd1-C14	0.073	0.049	0.069	0.089	1.29
Gd1-C17	0.066	0.047	0.063	0.079	1.25
Gd1-C16	0.063	0.047	0.062	0.076	1.23
Gd1-C40	0.073	0.052	0.071	0.090	1.27
Gd2-C48	0.063	0.045	0.059	0.074	1.25
Gd2-C31	0.055	0.043	0.053	0.064	1.21
Gd2-C44	0.067	0.049	0.065	0.080	1.23
Gd2-C45	0.076	0.051	0.072	0.093	1.29
Gd2-C5	0.075	0.046	0.068	0.090	1.32
Gd2-C4	0.066	0.048	0.063	0.078	1.24

Table S22: The electron density ($\rho(r)$ in eÅ^{-3}), Laplacian of electron density ($\nabla^2\rho(r)$ in eÅ^{-5}), kinetic energy (G(r) in a.u.), potential energy (|V(r)| in a.u.) of the Gd-C BCPs in $Gd_2@C_{48}$-C_{2v} isomer.

|	$\rho(r)$	$\nabla^2\rho(r)$	G(r)	|V(r)|	|V(r)|/G(r)
Gd1-C34	0.068	0.049	0.065	0.081	1.25
Gd1-C33	0.068	0.049	0.065	0.081	1.25
Gd1-C31	0.065	0.046	0.061	0.077	1.26
Gd1-C37	0.065	0.046	0.061	0.077	1.26
Gd1-C43	0.063	0.048	0.061	0.074	1.21
Gd1-C24	0.063	0.048	0.061	0.074	1.21
Gd1-C21	0.045	0.037	0.045	0.053	1.18
Gd2-C4	0.067	0.049	0.065	0.081	1.25
Gd2-C45	0.067	0.049	0.064	0.080	1.25
Gd2-C5	0.065	0.046	0.061	0.077	1.26
Gd2-C16	0.065	0.046	0.061	0.077	1.26
Gd2-C17	0.063	0.048	0.061	0.074	1.21
Gd2-C1	0.063	0.048	0.061	0.074	1.21
Gd2-C9	0.046	0.037	0.045	0.053	1.18
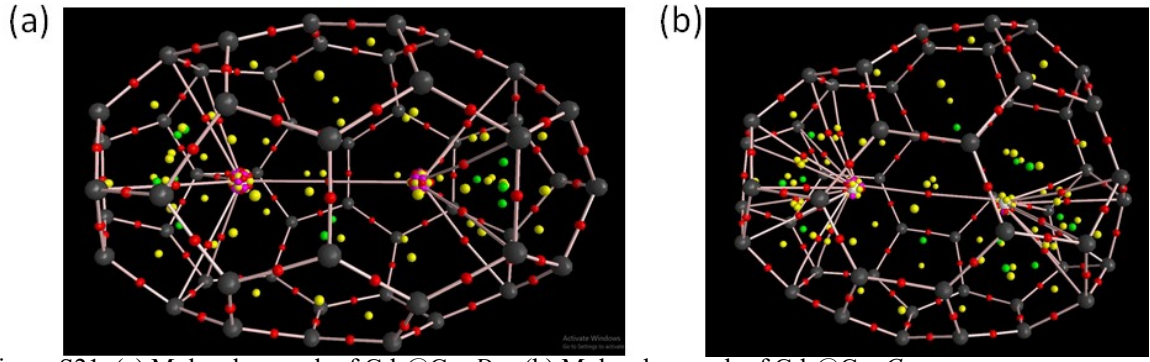
Figure S21: (a) Molecular graph of $Gd_2@C_{52}\text{-}D_{2d}$. (b) Molecular graph of $Gd_2@C_{52}\text{-}C_s$.
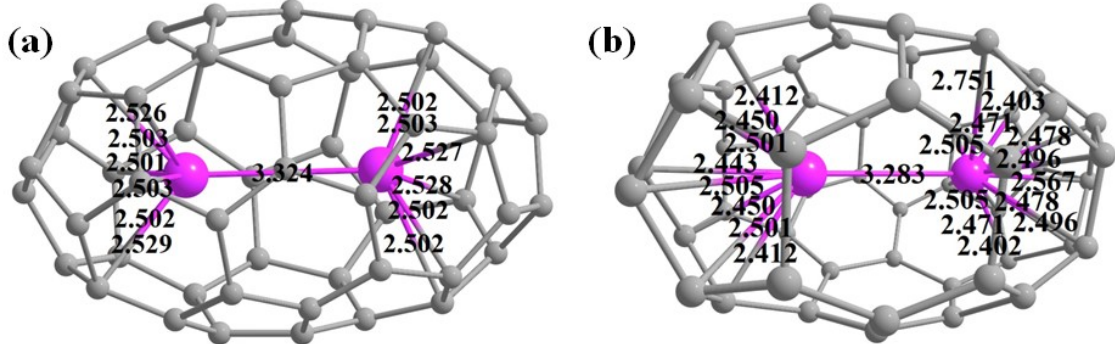
Figure S22: (a) The DFT optimised structure of $Gd_2@C_{52}\text{-}D_{2d}$ isomer. (b) The DFT optimised structure of $Gd_2@C_{52}\text{-}C_s$ isomer. The Gd-C bonding interactions are obtained from AIM analysis. The Gd-C bond lengths are shown in the angstrom unit. Colour Code: Gd-pink, C-grey.

Table S23: The electron density ($\rho(r)$ in eÅ^{-3}), Laplacian of electron density ($\nabla^2\rho(r)$ in eÅ^{-5}), kinetic energy (G(r) in a.u.), potential energy (|V(r)| in a.u.) of the Gd-C BCPs in $Gd_2@C_{52}\text{-}C_s$ isomer.

	$\rho(r)$	$\nabla^2\rho(r)$	G(r)	|V(r)|	|V(r)|/G(r)
Gd1-C22	0.052	0.041	0.050	0.059	1.18
Gd1-C5	0.052	0.041	0.050	0.059	1.18
Gd1-C21	0.057	0.044	0.056	0.067	1.20
Gd1-C6	0.057	0.044	0.056	0.067	1.20
Gd1-C19	0.063	0.047	0.060	0.074	1.23
Gd1-C10	0.052	0.039	0.049	0.060	1.22
Gd1-C24	0.063	0.047	0.060	0.074	1.23
Gd1-C11	0.050	0.040	0.049	0.059	1.20
Gd1-C12	0.057	0.043	0.054	0.065	1.20
Gd1-C31	0.053	0.041	0.050	0.059	1.18
Gd1-C14	0.053	0.041	0.050	0.059	1.18
Gd1-C32	0.057	0.043	0.054	0.065	1.20
Gd2-C49	0.063	0.045	0.058	0.072	1.24
Gd2-C48	0.058	0.045	0.056	0.067	1.20
Gd2-C52	0.062	0.041	0.056	0.070	1.25
Gd2-C45	0.054	0.042	0.052	0.063	1.21
Gd2-C40	0.054	0.042	0.052	0.063	1.21
Gd2-C37	0.063	0.045	0.058	0.072	1.24
Gd2-C38	0.058	0.045	0.056	0.067	1.20
Gd2-C41	0.057	0.041	0.054	0.066	1.22

Table S24: The electron density (ρ(r) in eÅ^{-3}), Laplacian of electron density ($\nabla^2\rho$(r) in eÅ^{-5}), kinetic energy (G(r) in a.u.), potential energy (|V(r)| in a.u.) of the Gd-C BCPs in Gd$_2$@C$_{52}$-D_{2d} isomer.

|	ρ(r)	$\nabla^2\rho$(r)	G(r)	|V(r)|	|V(r)|/G(r)
Gd1-C47	0.051	0.039	0.047	0.056	1.19
Gd1-C43	0.051	0.039	0.047	0.056	1.19
Gd1-C27	0.049	0.038	0.046	0.053	1.15
Gd1-C52	0.049	0.038	0.045	0.053	1.18
Gd1-C12	0.052	0.039	0.047	0.056	1.19
Gd1-C16	0.051	0.039	0.047	0.056	1.19
Gd2-C26	0.049	0.038	0.045	0.053	1.18
Gd2-C20	0.052	0.039	0.047	0.056	1.19
Gd2-C9	0.051	0.039	0.047	0.056	1.19
Gd2-C40	0.052	0.039	0.047	0.056	1.19
Gd2-C36	0.052	0.039	0.047	0.056	1.19
Gd2-C1	0.049	0.038	0.045	0.053	1.18
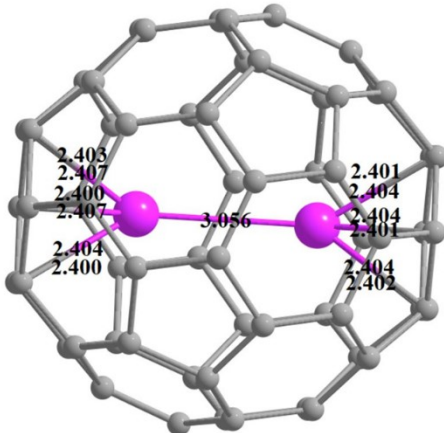
Figure S23: The DFT optimised structure of Gd$_2$@C$_{60}$-I_h isomer. The Gd-C bonding interactions are obtained from AIM analysis. The Gd-C bond lengths are shown in the angstrom unit. Colour Code: Gd-pink, C-grey.
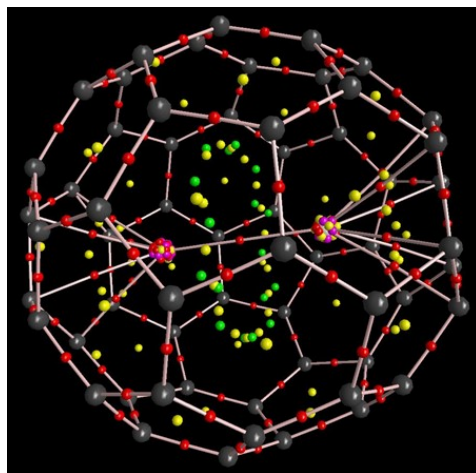

Figure S24: Molecular graph of Gd$_2$@C$_{60}$-I_h.

Table S25: The electron density (ρ(r) in eÅ^{-3}), Laplacian of electron density ($\nabla^2\rho$(r) in eÅ^{-5}), kinetic energy (G(r) in a.u.), potential energy (|V(r)| in a.u.) of the Gd-C BCPs in Gd$_2$@C$_{60}$-I_h isomer.

	ρ(r)	$\nabla^2\rho$(r)	G(r)	|V(r)|	|V(r)|/G(r)
Gd1-C23	0.065	0.045	0.060	0.074	1.23
Gd1-C22	0.064	0.045	0.059	0.073	1.24
Gd1-C46	0.065	0.045	0.060	0.075	1.25
Gd1-C47	0.065	0.045	0.060	0.074	1.23
Gd1-C29	0.064	0.045	0.059	0.073	1.24
Gd1-C32	0.064	0.045	0.060	0.074	1.23
Gd2-C6	0.064	0.045	0.060	0.074	1.23
Gd2-C7	0.064	0.045	0.060	0.074	1.23
Gd2-C2	0.065	0.045	0.060	0.074	1.23
Gd2-C8	0.064	0.045	0.060	0.074	1.23
Gd2-C4	0.065	0.045	0.060	0.074	1.23
Gd2-C5	0.065	0.045	0.060	0.074	1.23

Table S26: The electron density (ρ(r) in eÅ^{-3}), Laplacian of electron density ($\nabla^2\rho$(r) in eÅ^{-5}), kinetic energy (G(r) in a.u.), potential energy (|V(r)| in a.u.) of the Gd-C BCPs in Gd$_2$@C$_{80}$-C_{2v} isomer.

	ρ(r)	$\nabla^2\rho$(r)	G(r)	|V(r)|	|V(r)|/G(r)
Gd1-C1	0.057	-0.041	0.051	0.061	1.20
Gd1-C3	0.057	-0.041	0.051	0.061	1.20
Gd2-C68	0.059	-0.042	0.053	0.063	1.19
Gd2-C69	0.059	-0.042	0.053	0.063	1.19

Table S27: The electron density (ρ(r) in eÅ^{-3}), Laplacian of electron density ($\nabla^2\rho$(r) in eÅ^{-5}), kinetic energy (G(r) in a.u.), potential energy (|V(r)| in a.u.) of the Gd-C BCPs in Gd$_2$@C$_{80}$-D_{5h} isomer.

	ρ(r)	$\nabla^2\rho$(r)	G(r)	|V(r)|	|V(r)|/G(r)
Gd1-C67	0.049	0.041	0.046	0.051	1.11
Gd1-C66	0.056	0.039	0.048	0.057	1.19
Gd1-C70	0.057	0.039	0.049	0.059	1.20
Gd1-C71	0.051	0.042	0.048	0.054	1.13
Gd1-C72	0.053	0.037	0.044	0.052	1.18
Gd1-C65	0.052	0.036	0.043	0.050	1.16
Gd2-C8	0.053	0.036	0.044	0.052	1.18
Gd2-C9	0.051	0.042	0.048	0.054	1.13
Gd2-C4	0.051	0.036	0.043	0.050	1.16
Gd2-C10	0.057	0.039	0.049	0.059	1.20
Gd2-C2	0.049	0.041	0.046	0.051	1.11
Gd2-C3	0.056	0.039	0.048	0.057	1.19
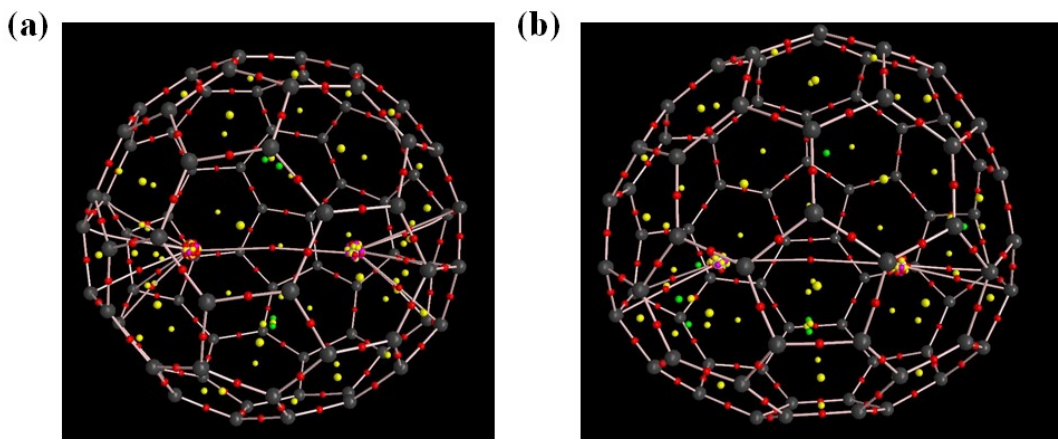
Figure S25: (a) The DFT optimised structure of $Gd_2@C_{80}$-C_{2v} isomer. (b) The DFT optimised structure of $Gd_2@C_{80}$-D_{5h} isomer. The Gd-C bonding interactions are obtained from AIM analysis. The Gd-C bond lengths are shown in the angstrom unit.
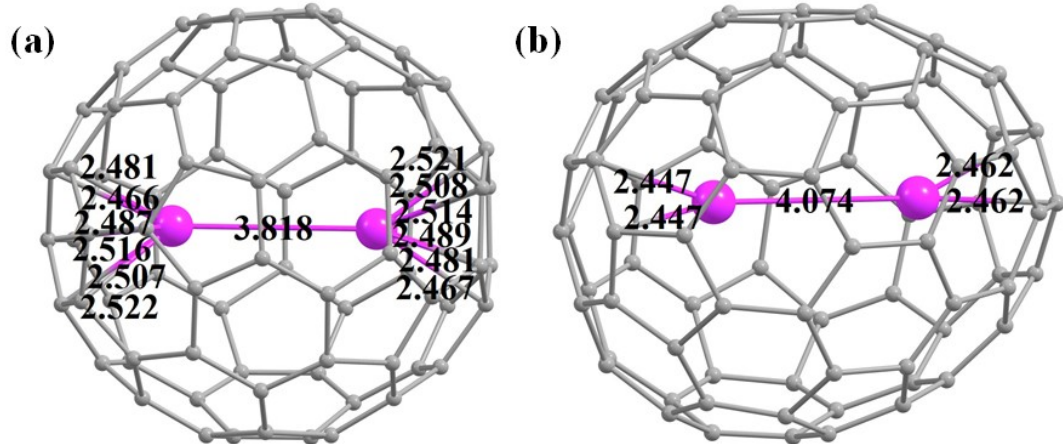

Figure S26: (a) The DFT optimised structure of $Gd_2@C_{80}$-D_{5h} isomer. (b) The DFT optimised structure of $Gd_2@C_{80}$-C_{2v} isomer. The Gd-C bonding interactions are obtained from AIM analysis. The Gd-C bond lengths are shown in the angstrom unit. Colour Code: Gd-pink, C-grey.
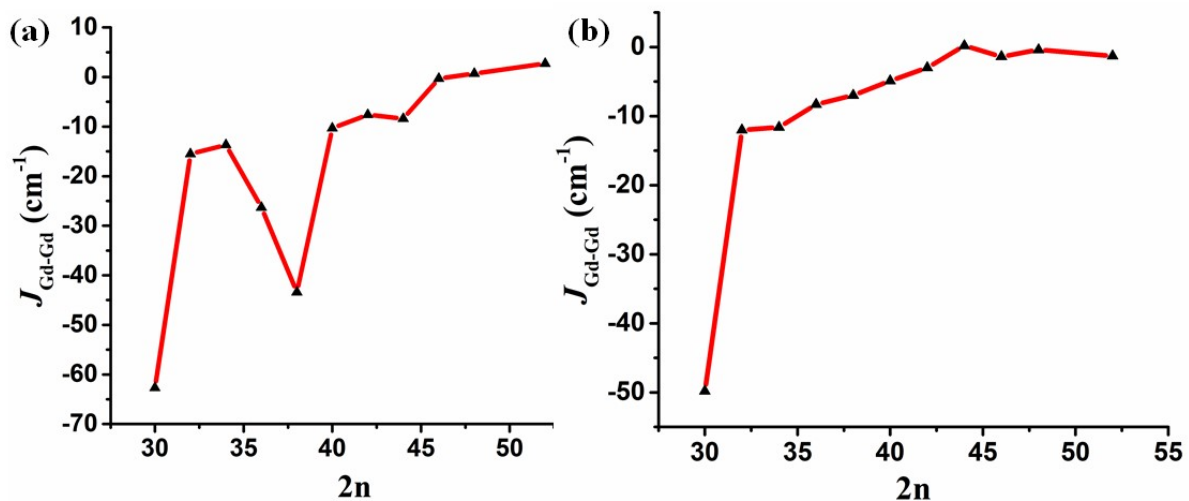
Figure S27: (a) The plot of $J_{Gd\text{-}Gd}$ with cage size for higher symmetry isomers such as $Gd_2@C_{30}$-D_{5h}, $Gd_2@C_{32}$-D_3, $Gd_2@C_{34}$-C_2, $Gd_2@C_{36}$-D_{2d}, $Gd_2@C_{38}$-D_{3h}, $Gd_2@C_{40}$-D_3, $Gd_2@C_{42}$-C_2, $Gd_2@C_{44}$-D_2, $Gd_2@C_{46}$-C_s, $Gd_2@C_{48}$-C_{2v}, $Gd_2@C_{52}$-D_{2d} (b) The plot of $J_{Gd\text{-}Gd}$ with cage size for lower symmetry isomers such as $Gd_2@C_{30}$-C_{2v}, $Gd_2@C_{32}$-C_2, $Gd_2@C_{34}$-C_s, $Gd_2@C_{36}$-C_s, $Gd_2@C_{38}$-C_1, $Gd_2@C_{40}$-C_{2v}, $Gd_2@C_{42}$-C_s, $Gd_2@C_{44}$-C_s, $Gd_2@C_{46}$-C_1, $Gd_2@C_{48}$-C_1, $Gd_2@C_{52}$-C_s, $Gd_2@C_{80}$-C_{2v}.
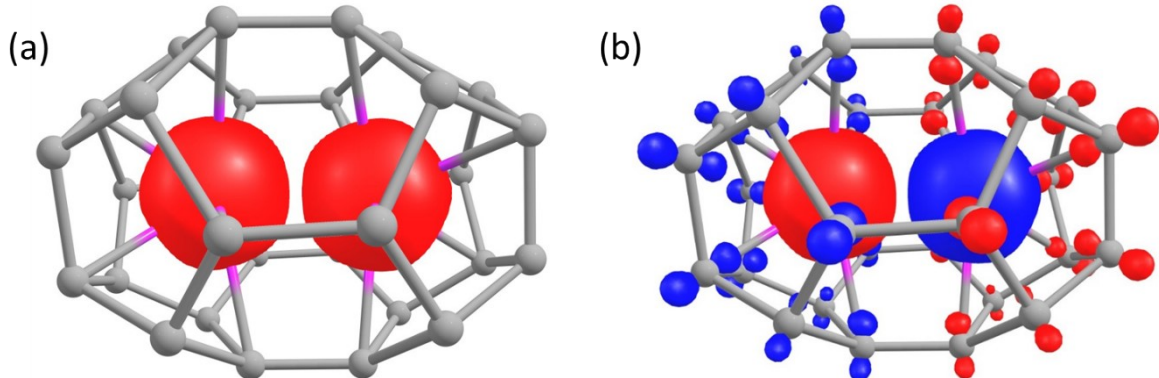
Figure S28: (a) The spin density of $Gd_2@C_{30}$-D_{5h} in the high spin (HS) conformation (b) The spin density of $Gd_2@C_{30}$-D_{5h} in the broken symmetry (BS) conformation. The spin density is shown here with an isosurface value of 0.006 e$^-$/bohr^3. Colour Code: Gd-pink, C-grey.
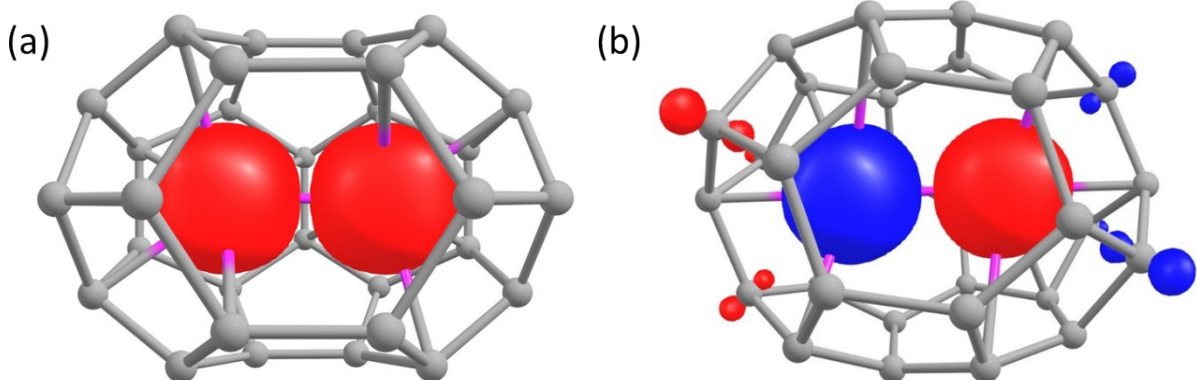
Figure S29: (a) The spin density of $Gd_2@C_{30}$-C_{2v} in the HS conformation (b) The spin density of $Gd_2@C_{30}$-C_{2V} in the BS conformation. The spin density is shown here with an isosurface value of 0.006 e$^-$/bohr^3. Colour Code: Gd-pink, C-grey.

Table S28: The overlap integral values between the SOMOs of two Gd^{+3} ions in $Gd_2@C_{30}$-D_{5h}.

Gd2 → Gd1 ↓	59	60	61	62	63	64	65
59	-0.519	-0.163	0.244	0.000	-0.002	0.000	-0.271
60	0.021	-0.160	-0.192	0.004	0.003	-0.000	-0.053
61	0.292	-0.192	0.158	0.004	-0.004	-0.000	-0.066
62	-0.001	0.004	0.003	0.164	0.070	0.001	0.001
63	0.002	-0.002	0.004	-0.070	0.163	-0.000	-0.001
64	-0.000	0.000	-0.000	0.001	0.001	-0.098	-0.000
65	-0.080	-0.038	-0.077	0.001	0.001	-0.000	0.044

Table S29: The overlap integral values between the SOMOs of two Gd^{+3} ions in Gd$_2$@C$_{30}$-C$_{2v}$.

Gd2 → Gd1 ↓	59	60	61	62	63	64	65
59	-0.614	-0.002	-0.003	-0.034	0.001	0.002	0.023
60	-0.001	-0.291	0.096	0.004	-0.028	-0.022	-0.001
61	0.003	-0.086	0.051	-0.001	-0.013	0.069	-0.000
62	-0.034	0.004	0.001	0.123	-0.001	0.001	-0.032
63	0.001	-0.029	0.016	-0.001	-0.130	-0.091	-0.003
64	0.002	-0.023	-0.068	0.001	-0.086	-0.014	-0.003
65	-0.039	0.001	-0.000	0.035	0.003	0.003	-0.213

(a) (b)
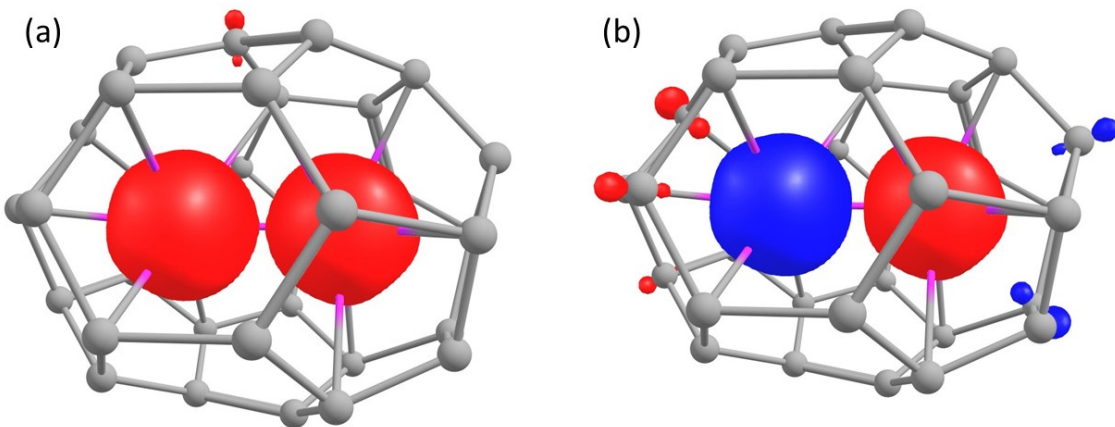
Figure S30: (a) The spin density of Gd$_2$@C$_{32}$-C_2 in the HS conformation (b) The spin density of Gd$_2$@C$_{32}$-C$_2$ in the BS conformation. The spin density is shown here with an isosurface value of 0.006 e$^-$/bohr^3. Colour Code: Gd-pink, C-grey.

(a) (b)
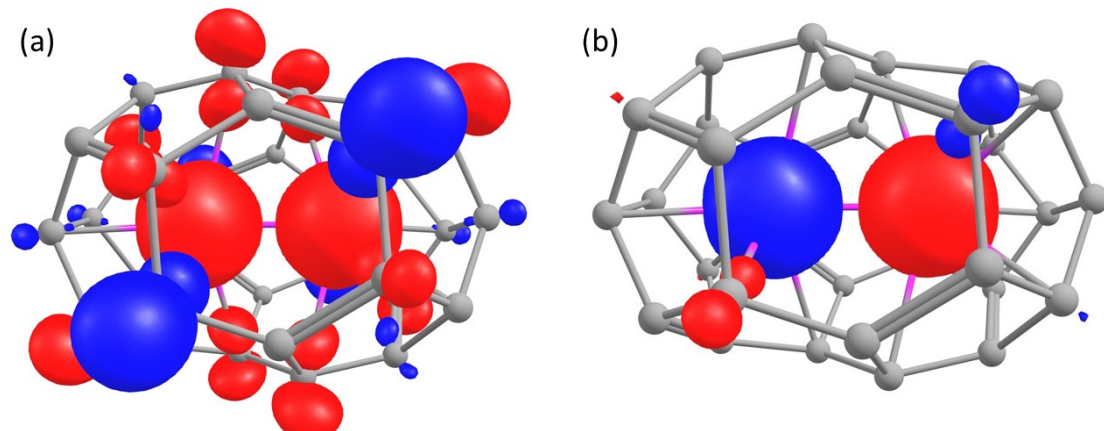
Figure S31: (a) The spin density of Gd$_2$@C$_{32}$-D_3 in the HS conformation (b) The spin density of Gd$_2$@C$_{32}$-D_3 in the BS conformation. The spin density is shown here with an isosurface value of 0.006 e$^-$/bohr^3. Colour Code: Gd-pink, C-grey.
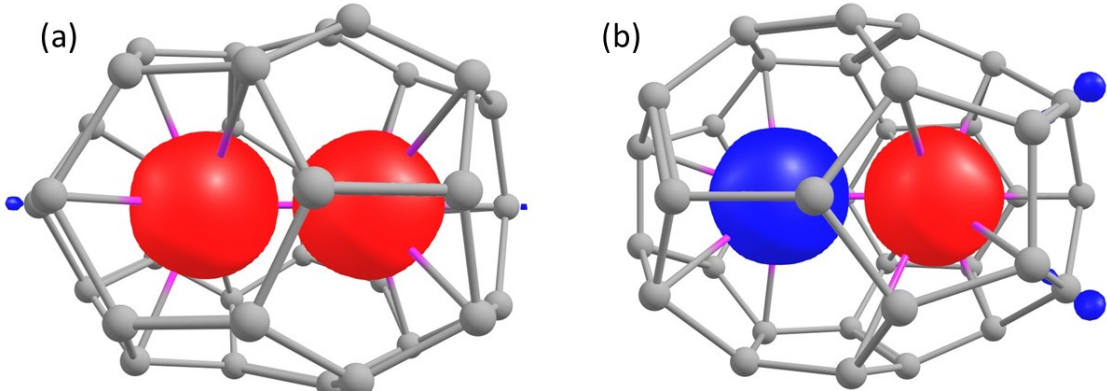
Figure S32: (a) The spin density of $Gd_2@C_{34}$-C_s in the HS conformation (b) The spin density of $Gd_2@C_{34}$-C_s in the BS conformation. The spin density is shown here with an isosurface value of 0.006 e⁻/bohr³. Colour Code: Gd-pink, C-grey.
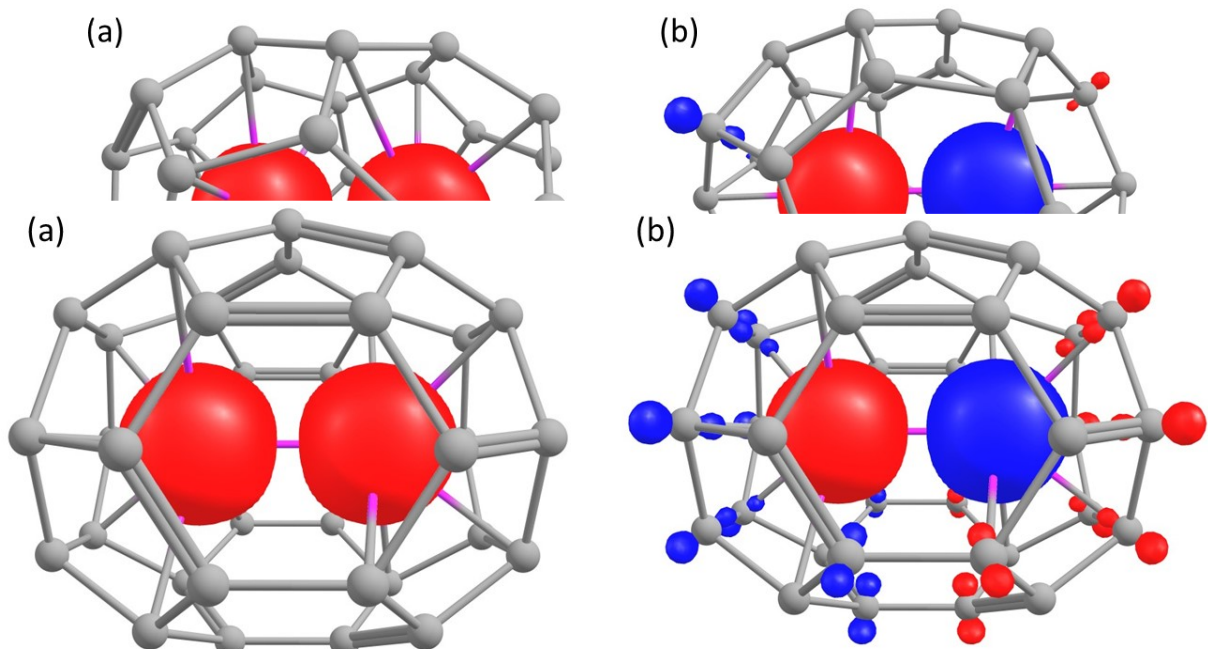
Figure S33: (a) The spin density of $Gd_2@C_{34}$-C_2 in the HS conformation (b) The spin density of $Gd_2@C_{34}$-C_2 in the BS conformation. The spin density is shown here with an isosurface value of 0.006 e⁻/bohr³. Colour Code: Gd-pink, C-grey.

Figure S34: (a) The spin density of $Gd_2@C_{36}$-D_{2d} in the HS conformation (b) The spin density of $Gd_2@C_{36}$-D_{2d} in the BS conformation. The spin density is shown here with an isosurface value of 0.006 e⁻/bohr³. Colour Code: Gd-pink, C-grey.

Table S30: The overlap integral values between the SOMOs of two Gd^{+3} ions in $Gd_2@C_{32}$-C_2.

Gd2 → Gd1 ↓	63	64	65	66	67	68	70
63	-0.145	-0.153	-0.055	-0.119	-0.111	0.025	0.077
64	0.097	0.061	-0.110	0.026	0.106	-0.022	-0.030
65	-0.070	0.003	-0.040	-0.015	0.032	-0.030	-0.022
66	0.036	0.179	0.093	0.046	0.109	-0.075	-0.106
67	-0.082	-0.264	-0.168	-0.031	-0.224	0.158	0.124
68	-0.013	0.107	0.171	-0.040	-0.174	0.038	-0.015

| 70 | -0.014 | 0.101 | -0.117 | 0.032 | 0.081 | -0.034 | -0.278 |

Table S31: The overlap integral values between the SOMOs of two Gd^{+3} ions in Gd$_2$@C$_{32}$-D_3.

Gd2 $\rightarrow$ Gd1 $\downarrow$	63	64	65	66	67	68	69
63	-0.264	0.000	-0.102	-0.000	-0.000	0.086	-0.043
64	-0.000	0.188	0.000	-0.014	-0.065	0.000	0.001
65	0.167	-0.000	-0.012	0.000	0.000	-0.057	0.021
66	-0.001	-0.000	0.000	0.018	-0.008	0.000	0.000
67	-0.002	-0.000	0.000	0.000	0.089	0.000	0.001
68	-0.128	-0.000	-0.018	0.000	-0.000	-0.055	0.010
69	0.054	-0.001	0.045	-0.000	0.000	0.146	-0.218

Table S32: The overlap integral values between the SOMOs of two Gd^{+3} ions in Gd$_2$@C$_{34}$-C_2.

Gd2 $\rightarrow$ Gd1 $\downarrow$	67	68	69	70	71	72	73
67	0.135	0.023	0.008	0.014	-0.061	0.005	0.089
68	-0.031	-0.071	-0.050	-0.002	0.027	0.072	0.098
69	0.009	0.050	-0.015	0.044	-0.050	0.112	0.021
70	-0.013	0.001	-0.041	0.022	-0.010	0.198	-0.024
71	0.062	0.029	0.043	0.006	-0.042	-0.144	-0.087
72	-0.011	0.072	-0.110	0.206	-0.144	0.146	-0.093
73	0.091	-0.102	0.026	0.019	0.076	0.104	-0.397

Table S33: The overlap integral values between the SOMOs of two Gd^{+3} ions in Gd$_2$@C$_{34}$-C_s.

Gd2 $\rightarrow$ Gd1 $\downarrow$	65	66	67	68	69	70	71
65	0.469	0.060	0.000	0.109	-0.000	-0.068	0.000
66	0.000	0.001	0.073	0.000	0.046	0.000	-0.041
67	-0.037	0.073	-0.001	0.008	-0.000	0.055	-0.000
68	0.056	0.128	-0.001	0.040	0.001	-0.101	-0.001
69	0.001	0.003	0.048	0.001	-0.048	-0.002	0.047
70	-0.080	-0.029	0.000	0.006	-0.000	-0.028	0.000
71	-0.000	-0.000	-0.028	-0.000	0.015	0.000	-0.019

Table S34: The overlap integral values between the SOMOs of two Gd^{+3} ions in Gd$_2$@C$_{36}$-D_{2d}.

Gd2 $\rightarrow$ Gd1 $\downarrow$	68	69	70	71	72	73	74
68	0.120	-0.100	0.001	0.006	0.001	-0.027	-0.001
69	-0.017	-0.282	0.001	-0.091	-0.000	0.093	-0.004
70	-0.001	0.001	0.023	0.000	-0.005	-0.000	0.016
71	0.033	0.090	-0.000	0.018	0.001	0.021	0.001
72	0.001	-0.000	0.004	0.001	-0.120	-0.001	0.190
73	-0.054	-0.085	0.000	0.020	-0.000	-0.065	-0.003
74	-0.001	-0.009	0.014	-0.003	-0.189	0.004	0.230

Table S35: The overlap integral values between the SOMOs of two Gd^{+3} ions in Gd$_2$@C$_{36}$-C$_s$.

Gd2 → Gd1 ↓	68	69	70	71	72	73	74
68	-0.001	0.139	-0.000	-0.015	-0.001	0.112	-0.001
69	0.150	0.001	-0.017	-0.000	0.046	0.001	-0.056
70	0.096	0.001	0.039	-0.000	-0.010	-0.001	-0.009
71	0.002	-0.006	0.000	0.014	-0.001	0.078	0.000
72	0.010	-0.000	-0.020	-0.000	-0.032	0.001	0.085
73	-0.001	0.022	0.000	0.031	0.001	-0.098	-0.001
74	-0.314	-0.001	0.067	-0.000	0.089	0.000	-0.463
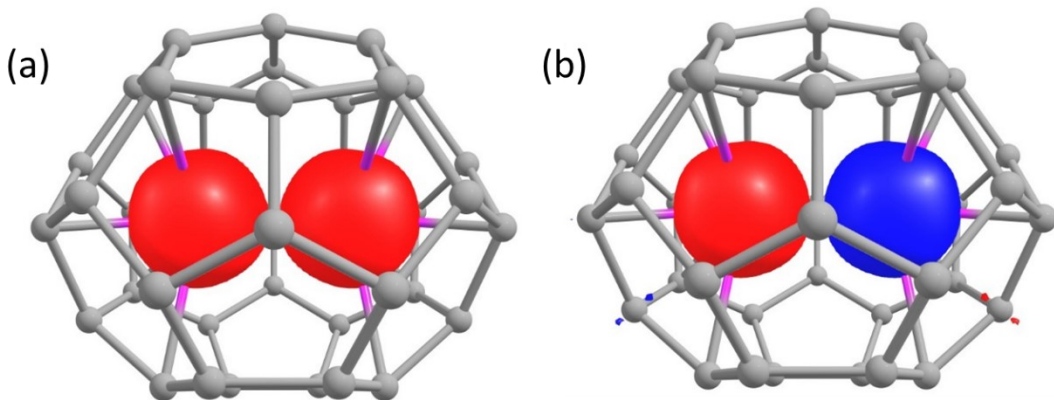
Figure S35: (a) The spin density of Gd$_2$@C$_{36}$-C$_s$ in the HS conformation (b) The spin density of Gd$_2$@C$_{36}$-C$_s$ in the BS conformation. The spin density is shown here with an isosurface value of 0.006 e$^-$/bohr^3. Colour Code: Gd-pink, C-grey.
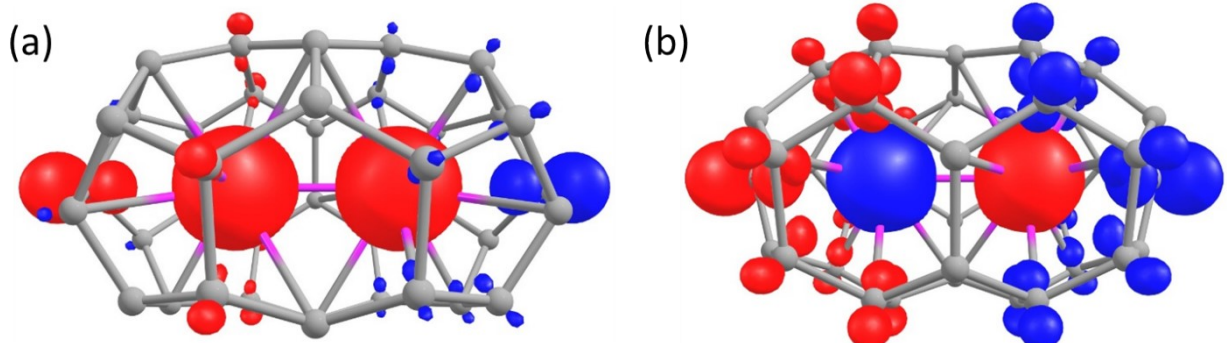
Figure S36: (a) The spin density of Gd$_2$@C$_{38}$-D$_{3h}$ in the HS conformation (b) The spin density of Gd$_2$@C$_{38}$-D$_{3h}$ in the BS conformation. The spin density is shown here with an isosurface value of 0.006 e$^-$/bohr^3. Colour Code: Gd-pink, C-grey.
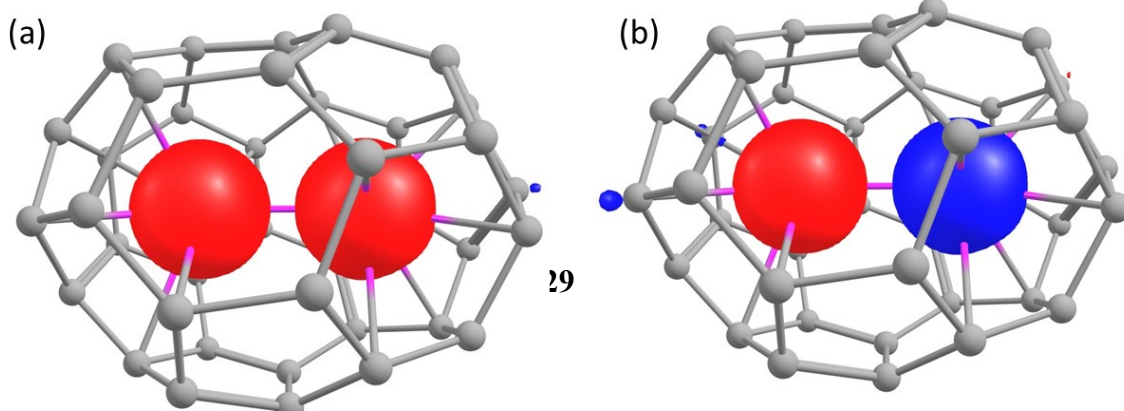
Figure S37: (a) The spin density of $Gd_2@C_{38}$-C_1 in the HS conformation (b) The spin density of $Gd_2@C_{38}$-C_1 in the BS conformation. The spin density is shown here with an isosurface value of 0.06 e⁻/bohr³. Colour Code: Gd-pink, C-grey.

Table S36: The overlap integral values between the SOMOs of two Gd^{+3} ions in $Gd_2@C_{38}$-D_{3h}.

Gd2 → Gd1 ↓	72	73	74	75	76	77	78
72	0.219	0.332	-0.001	-0.001	-0.000	0.005	-0.001
73	-0.332	0.219	0.002	0.000	0.000	0.001	0.005
74	0.005	0.003	0.573	-0.000	0.000	-0.000	-0.001
75	-0.000	-0.001	0.000	-0.103	0.046	0.000	0.000
76	-0.001	-0.000	-0.000	-0.041	0.056	-0.003	-0.003
77	-0.004	-0.005	0.000	-0.001	-0.000	0.162	-0.057
78	0.006	-0.005	-0.002	-0.001	0.001	0.058	0.163

Table S37: The overlap integral values between the SOMOs of two Gd^{+3} ions in $Gd_2@C_{38}$-C_1.

Gd2 → Gd1 ↓	70	71	72	73	74	75	76
70	-0.406	-0.264	-0.026	0.009	-0.095	-0.323	-0.106
71	-0.180	0.167	0.079	-0.025	-0.005	-0.062	0.001
72	0.113	0.040	-0.153	0.004	0.040	0.092	0.011
73	-0.052	-0.023	0.043	0.062	0.040	-0.091	-0.030
74	-0.186	0.069	0.049	0.110	-0.014	-0.102	-0.023
75	-0.054	-0.039	-0.015	-0.069	-0.044	-0.062	-0.036
76	-0.030	0.101	0.010	0.059	0.027	0.051	-0.011
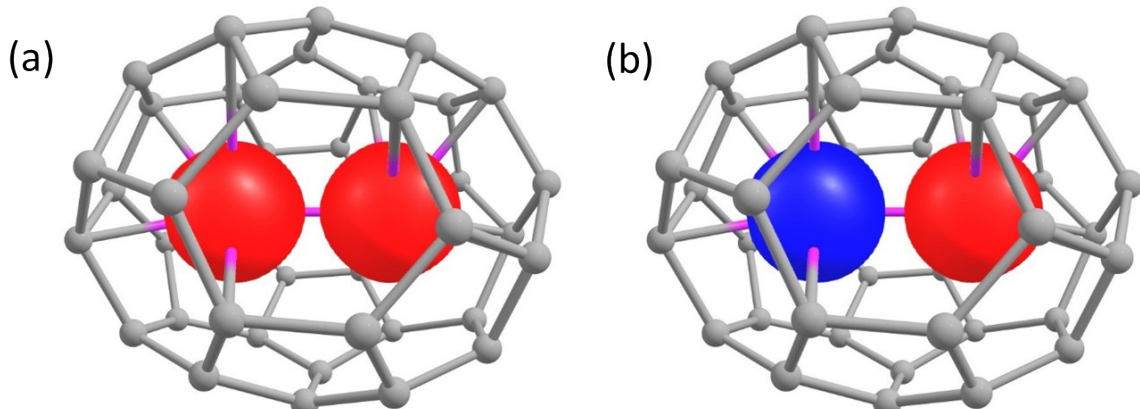
Figure S38: (a) The spin density of $Gd_2@C_{40}$-D_2 in the HS conformation (b) The spin density of $Gd_2@C_{40}$-D_2 in the BS conformation. The spin density is shown here with an isosurface value of 0.006 e⁻/bohr³. Colour Code: Gd-pink, C-grey.
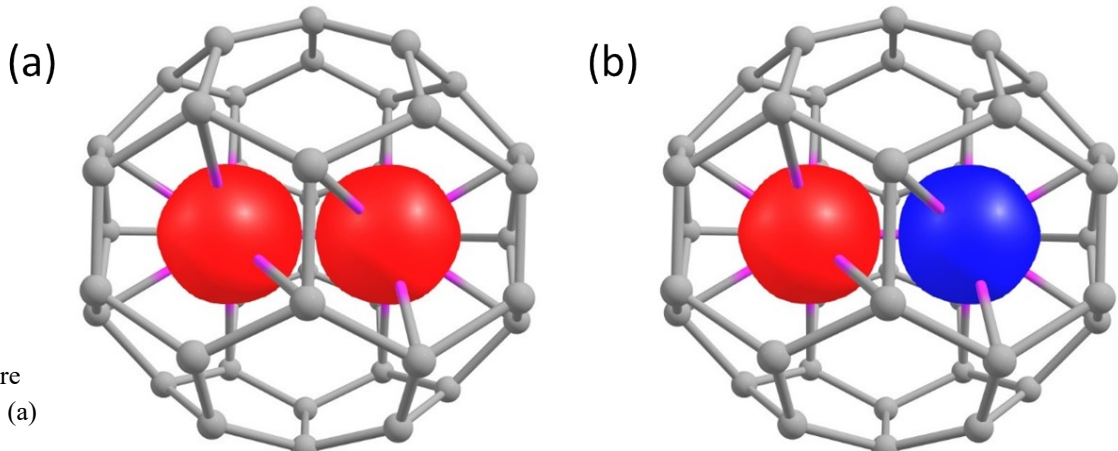
Figure S39: (a) The spin density of $Gd_2@C_{40}$-C_{2V} in the HS conformation (b) The spin density of $Gd_2@C_{40}$-C_{2V} in the BS conformation. The spin density is shown here with an isosurface value of 0.006 e⁻/bohr³. Colour Code: Gd-pink, C-grey.

Table S38: The overlap integral values between the SOMOs of two Gd^{+3} ions in $Gd_2@C_{40}$-C_{2V}.

Gd2 → Gd1 ↓	74	75	76	77	78	79	80
74	0.116	0.008	0.001	-0.007	-0.011	0.020	0.003
75	-0.008	0.157	-0.083	0.012	-0.169	0.088	0.240
76	0.000	0.083	0.050	0.005	-0.029	0.044	0.114
77	-0.007	-0.012	0.006	0.032	0.019	-0.082	0.015
78	0.011	-0.167	0.029	-0.019	0.180	-0.073	-0.230
79	-0.020	0.084	-0.043	0.083	-0.070	-0.139	0.066
80	-0.003	0.242	-0.115	-0.014	-0.232	0.065	0.041

Table S39: The overlap integral values between the SOMOs of two Gd^{+3} ions in $Gd_2@C_{40}$-D_2.

| Gd2 → Gd1 ↓	72	73	74	75	76	77	78
72	-0.224	-0.001	-0.002	-0.064	0.001	-0.100	0.014
73	0.003	-0.364	-0.154	0.004	0.081	-0.004	-0.002
74	0.002	-0.153	-0.008	-0.001	0.066	-0.003	-0.000
75	0.063	0.010	0.004	0.041	-0.002	-0.030	-0.010
76	0.001	-0.081	-0.066	0.003	0.017	-0.001	-0.001
77	-0.100	-0.002	0.000	0.030	0.001	-0.032	0.003
78	-0.014	-0.006	-0.003	-0.011	0.001	-0.003	0.006
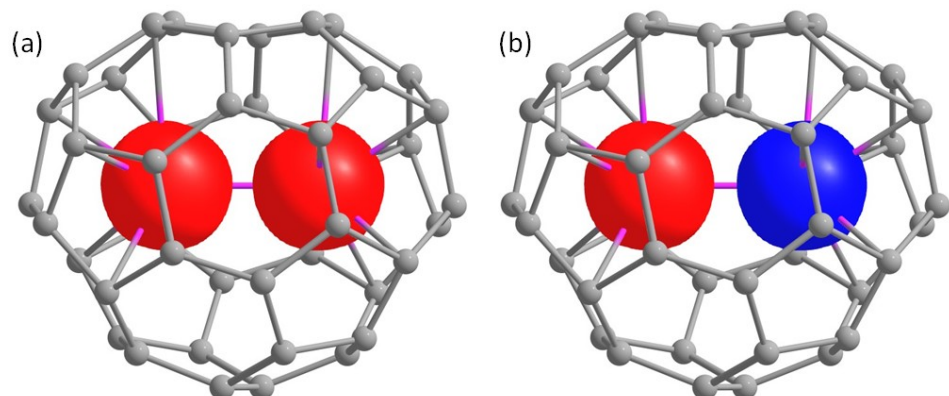
Figure S40: (a) The spin density of $Gd_2@C_{42}$-D_3 in the HS conformation (b) The spin density of $Gd_2@C_{42}$-D_3 in the BS conformation. The spin density is shown here with an isosurface value of 0.006 e⁻/bohr³. Colour Code: Gd-pink, C-grey.
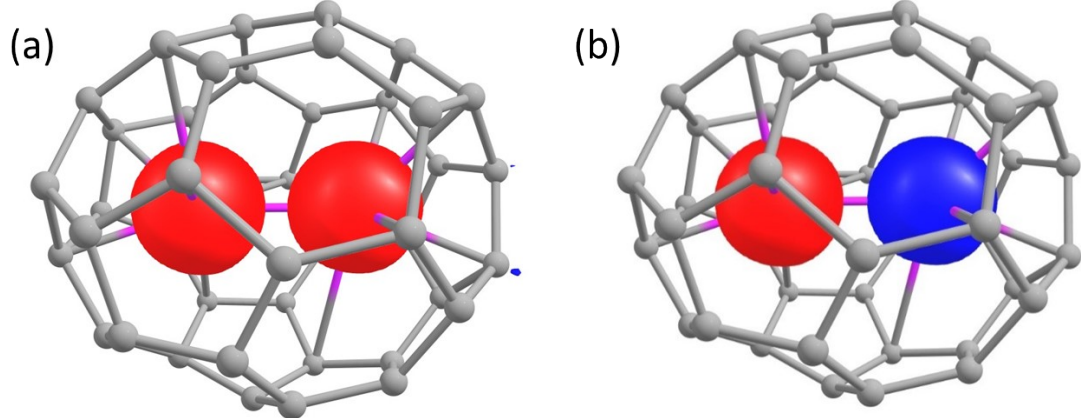
Figure S41: (a) The spin density of $Gd_2@C_{42}$-C_1 in the HS conformation (b) The spin density of $Gd_2@C_{42}$-C_1 in the BS conformation. The spin density is shown here with an isosurface value of 0.006 e⁻/bohr³. Colour Code: Gd-pink, C-grey.

Table S40: The overlap integral values between the SOMOs of two Gd^{+3} ions in $Gd_2@C_{42}$-C_1.

Gd2 → Gd1 ↓	75	76	77	78	79	80	81
75	-0.404	0.024	0.021	-0.039	0.068	-0.085	0.000
76	-0.021	0.042	-0.008	-0.097	0.026	-0.025	0.022
77	0.140	0.063	-0.033	0.046	0.005	0.039	0.009
78	-0.067	-0.013	-0.030	0.036	0.044	-0.003	0.021
79	-0.038	-0.010	0.037	0.007	0.013	0.008	-0.002
80	-0.068	-0.006	0.010	-0.035	0.007	-0.021	0.006
81	0.034	-0.007	0.018	0.018	-0.018	0.005	-0.051

Table S41: The overlap integral values between the SOMOs of two Gd^{+3} ions in $Gd_2@C_{42}$-D_3.

| Gd2 → Gd1 ↓	75	76	77	78	79	80	81
75	0.069	-0.078	-0.020	0.000	0.024	-0.012	-0.021
76	-0.078	-0.009	0.042	0.023	0.033	-0.009	0.011
77	0.019	-0.041	0.028	-0.004	-0.023	-0.009	0.003
78	0.000	-0.023	-0.004	0.029	0.005	0.004	0.002
79	0.025	0.033	0.023	-0.005	-0.014	-0.001	0.009
80	-0.012	-0.008	0.009	-0.003	-0.001	0.003	0.000
81	0.021	-0.011	0.003	0.002	-0.009	-0.000	-0.008

S32
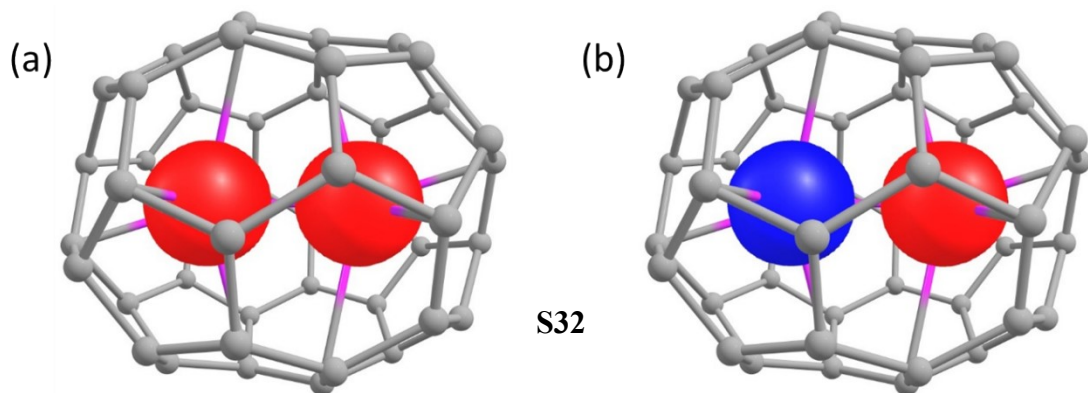
Figure S42: (a) The spin density of Gd$_2$@C$_{44}$-D_2 in the HS conformation (b) The spin density of Gd$_2$@C$_{44}$-D_2 in the BS conformation. The spin density is shown here with an isosurface value of 0.006 e$^-$/bohr^3. Colour Code: Gd-pink, C-grey.

Table S42: The overlap integral values between the SOMOs of two Gd^{+3} ions in Gd$_2$@C$_{44}$-C_s.

Gd2 → Gd1 ↓	79	80	81	82	83	84	85
79	-0.122	0.000	0.018	-0.007	0.000	0.007	-0.000
80	-0.031	0.000	0.026	0.006	0.000	0.002	-0.000
81	-0.000	0.046	0.000	-0.000	0.007	0.001	-0.044
82	-0.034	0.000	0.017	-0.034	-0.000	0.088	-0.000
83	0.000	0.009	0.000	0.000	-0.010	0.000	-0.117
84	-0.052	0.001	-0.003	-0.051	0.000	0.199	0.001
85	0.000	0.003	-0.000	0.000	-0.030	-0.001	0.240

Table S43: The overlap integral values between the SOMOs of two Gd^{+3} ions in Gd$_2$@C$_{44}$-D_2.

| Gd2 → Gd1 ↓	78	79	80	81	82	83	84
78	0.095	-0.029	0.004	-0.000	-0.000	-0.007	-0.011
79	0.028	-0.017	0.018	-0.013	-0.007	-0.007	0.007
80	-0.009	0.013	0.046	-0.041	-0.021	0.002	-0.003
81	0.000	0.006	0.042	-0.034	-0.022	0.000	-0.000
82	-0.000	-0.003	-0.022	0.022	0.013	0.000	0.000
83	0.007	-0.075	0.001	0.000	0.000	0.009	0.004
84	-0.011	-0.007	0.001	0.000	-0.000	-0.004	0.022
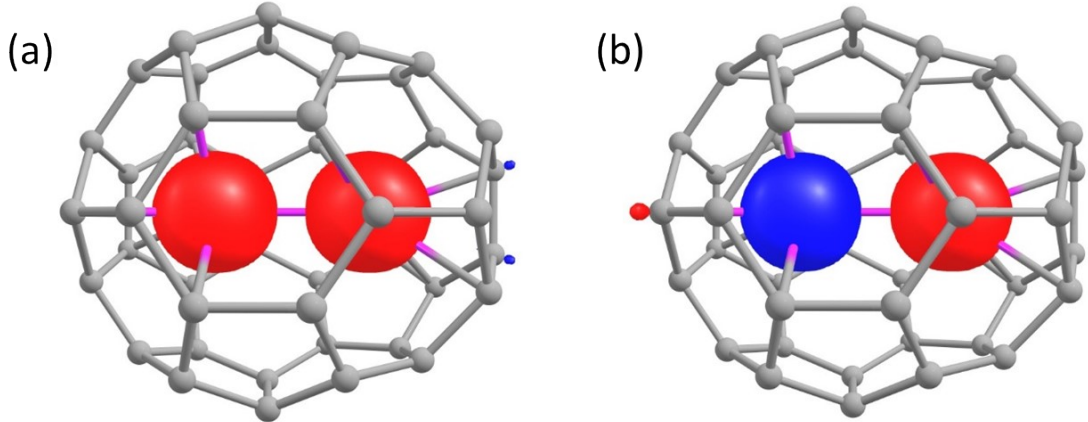
Figure S43: (a) The spin density of Gd$_2$@C$_{44}$-C_s in the HS conformation (b) The spin density of Gd$_2$@C$_{44}$-C_s in the BS conformation. The spin density is shown here with an isosurface value of 0.006 e$^-$/bohr^3. Colour Code: Gd-pink, C-grey.

Table S44: The overlap integral values between the SOMOs of two Gd^{+3} ions in Gd$_2$@C$_{46}$-C_1.

Gd2 → Gd1 ↓	81	82	83	84	85	86	87
81	0.190	-0.001	-0.008	0.008	0.015	-0.030	-0.010
82	0.021	0.057	-0.018	-0.026	-0.004	0.026	-0.053

83	-0.050	0.055	0.052	-0.009	-0.011	0.059	-0.020
84	0.021	0.008	0.010	0.008	0.013	0.004	-0.062
85	-0.019	-0.016	-0.031	0.014	-0.002	-0.037	-0.005
86	0.043	-0.055	-0.069	0.034	0.016	-0.089	0.062
87	-0.030	-0.001	0.101	-0.041	-0.042	0.057	0.458

Table S45: The overlap integral values between the SOMOs of two Gd^{+3} ions in $Gd_2@C_{46}$-C_s.

Gd2 → Gd1 ↓	81	82	83	84	85	86	87
81	0.071	-0.052	0.021	0.033	0.001	0.000	0.000
82	0.050	0.041	0.000	0.037	0.010	-0.000	0.000
83	-0.000	0.000	0.050	-0.000	-0.000	-0.027	0.018
84	0.014	0.031	-0.000	-0.079	0.056	-0.000	-0.000
85	0.007	-0.018	0.000	0.061	-0.008	0.000	-0.000
86	-0.000	0.000	0.006	0.000	0.000	-0.006	-0.100
87	0.000	0.000	-0.005	-0.000	-0.000	-0.024	0.229
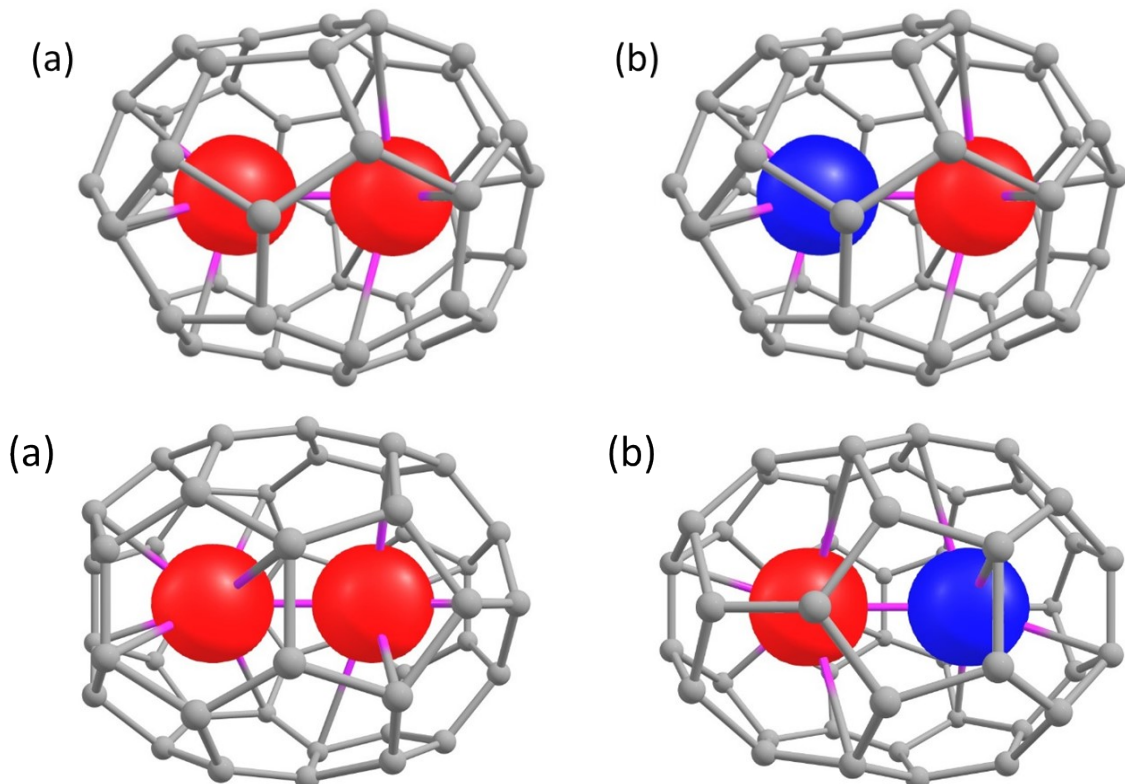
Figure S44: (a) The spin density of $Gd_2@C_{46}$-C_1 in the HS conformation (b) The spin density of $Gd_2@C_{46}$-C_1 in the BS conformation. The spin density is shown here with an isosurface value of 0.006 e$^-$/bohr^3. Colour Code: Gd-pink, C-grey.

Figure S45: (a) The spin density of Gd$_2$@C$_{46}$-C_s in the HS conformation (b) The spin density of Gd$_2$@C$_{46}$-C_s in the BS conformation. The spin density is shown here with an isosurface value of 0.006 e$^-$/bohr^3. Colour Code: Gd-pink, C-grey.

Table S46: The overlap integral values between the SOMOs of two Gd^{+3} ions in Gd$_2$@C$_{48}$-C_{2V}.

| Gd2 → Gd1 ↓	86	87	88	89	90	91	92
86	0.031	0.000	0.007	0.002	-0.000	0.012	0.000
87	-0.000	0.042	0.000	-0.000	-0.049	-0.000	-0.032
88	0.007	0.000	0.025	-0.007	-0.000	0.037	-0.000
89	-0.001	-0.000	0.010	0.068	0.000	-0.005	-0.000
90	-0.000	-0.051	0.000	0.000	0.187	0.000	-0.056
91	-0.013	-0.001	-0.040	-0.006	-0.001	0.298	0.000
92	0.000	0.034	0.000	-0.000	-0.056	-0.000	0.494

(a)

(b)
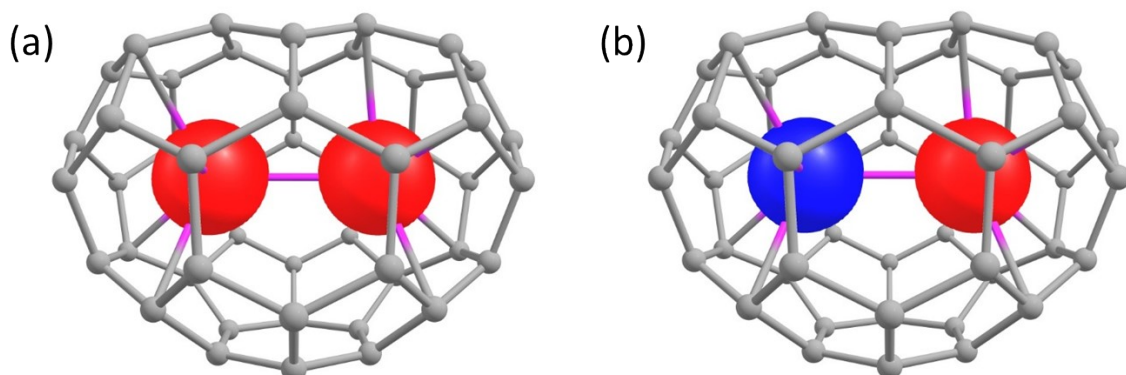
Figure S46: (a) The spin density of Gd$_2$@C$_{48}$-C_{2V} in the HS conformation (b) The spin density of Gd$_2$@C$_{48}$-C_{2V} in the BS conformation. The spin density is shown here with an isosurface value of 0.006 e$^-$/bohr^3. Colour Code: Gd-pink, C-grey.


(a)

(b)
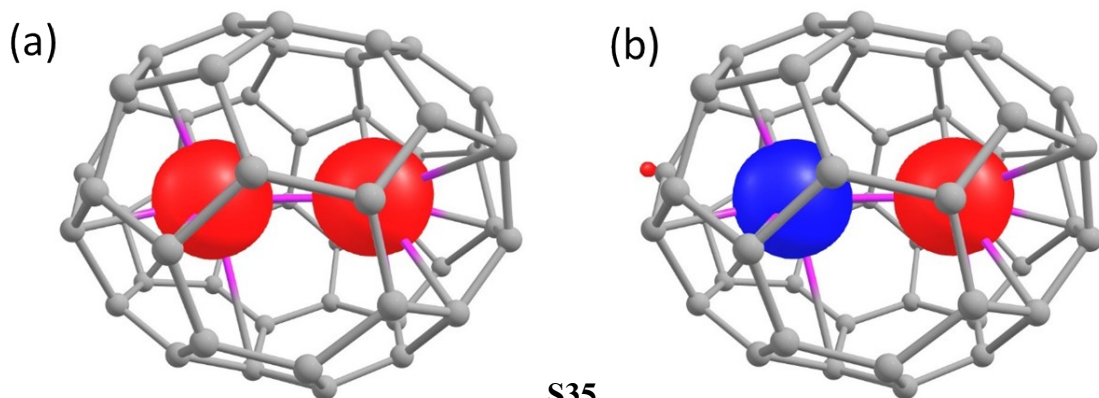
Figure S47: (a) The spin density of $Gd_2@C_{48}$-C_1 in the HS conformation (b) The spin density of $Gd_2@C_{48}$-C_1 in the BS conformation. The spin density is shown here with an isosurface value of 0.006 e⁻/bohr³. Colour Code: Gd-pink, C-grey.

Table S47: The overlap integral values between the SOMOs of two Gd^{+3} ions in $Gd_2@C_{48}$-C_1.

Gd2 → Gd1 ↓	84	85	86	87	88	89	90
84	-0.119	-0.034	0.014	0.002	-0.019	0.012	-0.028
85	-0.052	0.079	-0.017	-0.015	-0.017	-0.024	-0.032
86	-0.018	0.025	0.037	0.000	-0.029	-0.034	-0.041
87	0.046	0.001	-0.012	-0.016	0.016	0.037	0.072
88	-0.013	-0.010	0.023	0.017	-0.018	-0.062	0.012
89	-0.001	-0.031	0.018	-0.021	-0.033	0.298	0.199
90	-0.184	-0.031	0.069	0.035	-0.071	0.129	-0.527

Table S48: The overlap integral values between the SOMOs of two Gd^{+3} ions in $Gd_2@C_{52}$-D_{2d}.

Gd2 → Gd1 ↓	90	91	92	93	94	95	96
90	0.115	0.000	0.000	0.063	0.000	-0.000	-0.000
91	0.000	0.000	0.014	0.000	0.000	-0.006	0.000
92	0.000	0.014	-0.000	0.000	-0.021	0.000	-0.000
93	0.064	-0.000	0.000	0.055	0.001	-0.000	-0.000
94	0.001	-0.000	-0.021	0.001	0.000	0.019	0.000
95	-0.001	-0.006	-0.000	-0.001	0.020	0.000	-0.000
96	-0.000	-0.000	0.000	-0.000	-0.000	0.000	0.078

Table S49: The overlap integral values between the SOMOs of two Gd^{+3} ions in $Gd_2@C_{52}$-C_s.

Gd2 → Gd1 ↓	90	91	92	93	94	95	96
90	0.270	0.008	0.000	-0.000	-0.022	-0.000	-0.028
91	-0.007	0.213	0.018	0.002	-0.000	0.031	0.000
92	-0.002	0.068	-0.015	0.004	0.000	0.012	-0.000
93	0.000	-0.023	-0.010	0.001	-0.000	0.008	0.000
94	0.012	0.001	-0.000	0.000	0.046	0.000	0.014
95	-0.047	-0.002	-0.000	-0.000	-0.041	-0.000	0.196
96	0.001	-0.032	0.009	-0.010	0.000	0.081	-0.000

(a)

(b)
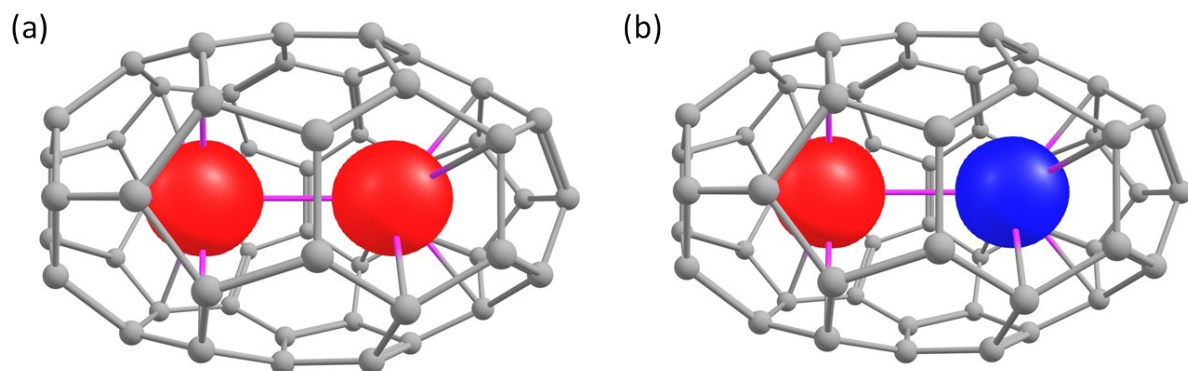
Figure S48: (a) The spin density of $Gd_2@C_{52}$-D_{2d} in the HS conformation (b) The spin density of $Gd_2@C_{52}$-D_{2d} in the BS conformation. The spin density is shown here with an isosurface value of 0.006 e^-/bohr^3. Colour Code: Gd-pink, C-grey.
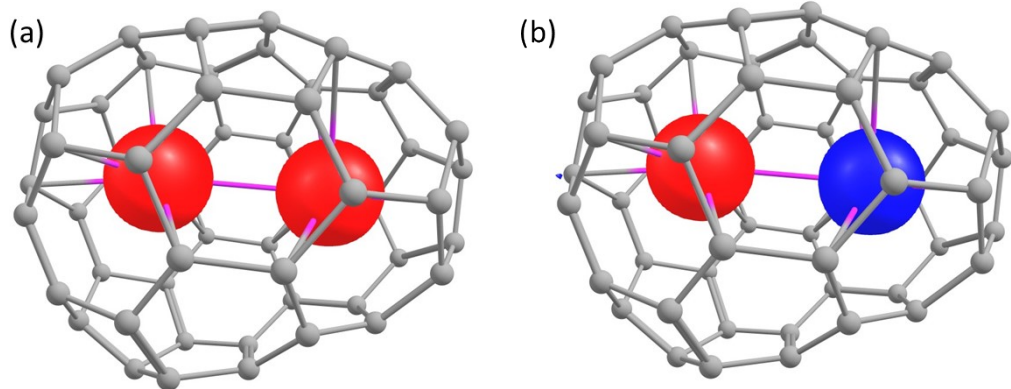

Figure S49: (a) The spin density of $Gd_2@C_{52}$-C_s in the HS conformation (b) The spin density of $Gd_2@C_{52}$-C_s in the BS conformation. The spin density is shown here with an isosurface value of 0.006 e^-/bohr^3. Colour Code: Gd-pink, C-grey.
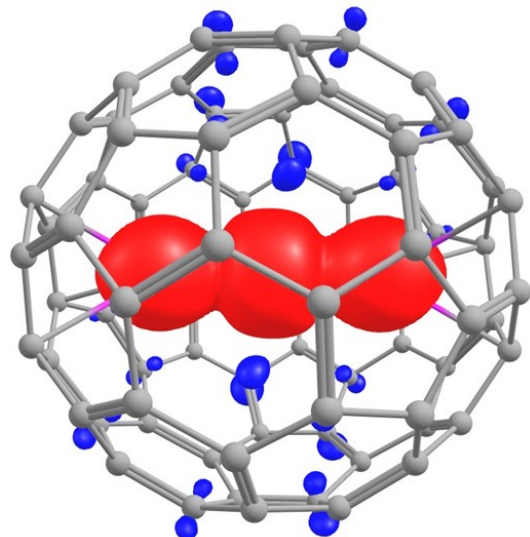
Figure S50: The spin density of $Gd_2@C_{80}$-D_{5h} in the HS conformation. The spin density is shown here with an isosurface value of 0.006 e^-/bohr^3. Colour Code: Gd-pink, C-grey.
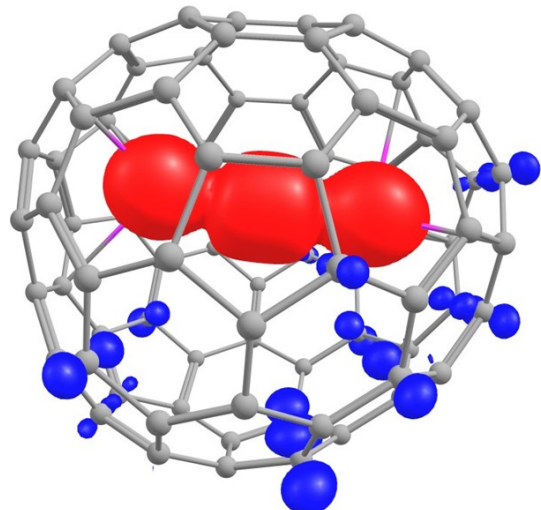
Figure S51: (a) The spin density of $Gd_2@C_{80}$-C_{2V} in the HS conformation. The spin density is shown here with an isosurface value of 0.006 e$^-$/bohr^3. Colour Code: Gd-pink, C-grey.
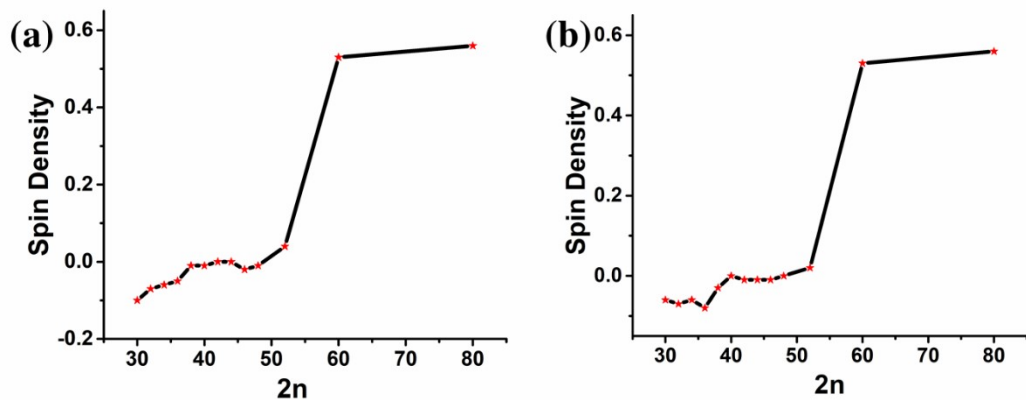

Figure S52: (a) The residual spin density of the Gd1 centre (DFT computed spin density-7) in the higher symmetry isomers of $Gd_2@C_{2n}$. (b) The residual spin density of the Gd1 centre (DFT computed spin density-7) in the lower symmetry isomers of $Gd_2@C_{2n}$.

Table S50: The Mulliken spin density of Gd1, Gd2 and C_{2n} ring of $Gd_2@C_{2n}$-isomers.

$Gd_2@C_{2n}$	Gd1	Gd2	C_{2n}
$Gd_2@C_{30}$ (D_{5h})	6.90	6.90	0.20
$Gd_2@C_{30}$ (C_{2v})	6.94	6.94	0.12
$Gd_2@C_{32}$ (C_2)	6.93	6.95	0.12
$Gd_2@C_{32}$ (D_3)	6.93	6.93	0.14
$Gd_2@C_{34}$ (C_s)	6.94	6.94	0.12
$Gd_2@C_{34}$ (C_2)	6.94	6.94	0.12
$Gd_2@C_{36}$ (C_s)	6.92	6.97	0.11
$Gd_2@C_{36}$ (D_{2d})	6.96	6.95	0.09
$Gd_2@C_{38}$ (C_1)	6.97	6.93	0.10
$Gd_2@C_{38}$ (D_{3h})	6.99	6.99	0.02
$Gd_2@C_{40}$ (D_3)	6.99	6.99	0.02
$Gd_2@C_{40}$ (C_{2v})	7.00	7.00	-0.01
$Gd_2@C_{42}$ (C_2)	6.99	6.99	0.02
$Gd_2@C_{42}$ (D_3)	7.00	7.00	-0.00
$Gd_2@C_{44}$ (C_s)	6.99	7.02	-0.01
$Gd_2@C_{44}$ (D_2)	7.00	7.00	-0.00
$Gd_2@C_{46}$ (C_s)	6.98	6.98	0.04
$Gd_2@C_{46}$ (C_1)	6.99	7.00	0.01
$Gd_2@C_{48}$ (C_{2v})	6.99	6.99	0.02
$Gd_2@C_{48}$ (C_1)	7.00	7.00	-0.00
$Gd_2@C_{52}$ (C_s)	7.02	6.99	-0.01
$Gd_2@C_{52}$ (D_{2d})	7.04	7.04	-0.08
$Gd_2@C_{60}$ (I_h)	7.53	7.53	-1.06
$Gd_2@C_{80}$ (C_{2v})	7.55	7.56	-1.11
$Gd_2@C_{80}$ (D_{5h})	7.56	7.56	-1.12

Table S51: The electron density ($\rho(r)$ in eÅ^{-3}), Laplacian of electron density ($\nabla^2\rho(r)$ in eÅ^{-5}), kinetic energy (G(r) in a.u.), potential energy (|V(r)| in he^{-1}) of the Gd-Gd BCP in Gd$_2$@C$_{2n}$ isomer. The presence of (3, -1) critical points in AIM analysis suggests bonding interaction between two atoms. We have found the (3, -1) bond critical points (BCPs) between two Gd^{3+} ions in all Gd$_2$@C$_{2n}$ isomers, which suggests sizeable bonding interaction between two Gd^{3+} ions. The Laplacian of electron density between two Gd^{3+} ions (Gd$_2$@C$_{2n}$, $30 \leq 2n \leq 48$) is found to increase with the decrease in the ring size. This is due to the increase in the overlap between the 4f orbitals with a decrease in the ring size.

Gd$_2$@C$_{2n}$	$\rho(r)$	$\nabla^2\rho(r)$	G(r)	|V(r)|	|V(r)|/G(r)
Gd$_2$@C$_{30}$-D_{5h}	0.135	0.159	0.209	0.259	1.24
Gd$_2$@C$_{30}$-C_{2v}	0.146	0.172	0.231	0.291	1.26
Gd$_2$@C$_{32}$-C_2	0.139	0.162	0.215	0.269	1.25
Gd$_2$@C$_{32}$-D_3	0.118	0.140	0.177	0.213	1.20
Gd$_2$@C$_{34}$-C_s	0.115	0.136	0.171	0.206	1.20
Gd$_2$@C$_{34}$-C_2	0.120	0.141	0.179	0.217	1.21
Gd$_2$@C$_{36}$-C_s	0.089	0.100	0.119	0.138	1.16
Gd$_2$@C$_{36}$-D_{2d}	0.116	0.142	0.177	0.211	1.19
Gd$_2$@C$_{38}$-C_1	0.079	0.090	0.105	0.119	1.13
Gd$_2$@C$_{38}$-D_{3h}	0.041	0.043	0.046	0.049	1.06
Gd$_2$@C$_{40}$-D_3	0.090	0.099	0.119	0.140	1.18
Gd$_2$@C$_{40}$-C_{2v}	0.095	0.105	0.128	0.152	1.19
Gd$_2$@C$_{42}$-C_1	0.072	0.077	0.089	0.101	1.13
Gd$_2$@C$_{42}$-D_3	0.084	0.090	0.109	0.127	1.17
Gd$_2$@C$_{44}$-C_s	0.055	0.058	0.064	0.070	1.09
Gd$_2$@C$_{44}$-D_2	0.064	0.067	0.076	0.085	1.12
Gd$_2$@C$_{46}$-C_s	0.036	0.035	0.037	0.039	1.05
Gd$_2$@C$_{46}$-C_1	0.042	0.042	0.045	0.048	1.07
Gd$_2$@C$_{48}$-C_{2v}	0.025	0.020	0.021	0.022	1.05
Gd$_2$@C$_{48}$-C_1	0.033	0.032	0.033	0.035	1.06
Gd$_2$@C$_{52}$-C_s	0.011	0.011	0.010	0.009	0.90
Gd$_2$@C$_{52}$-D_{2d}	0.018	0.006	0.008	0.010	1.25
Gd$_2$@C$_{60}$-I_h	0.042	0.003	0.016	0.029	1.81
Gd$_2$@C$_{80}$-C_{2v}	0.016	0.002	0.001	0.003	3
Gd$_2$@C$_{80}$-D_{5h}	0.019	0.002	0.002	0.006	3
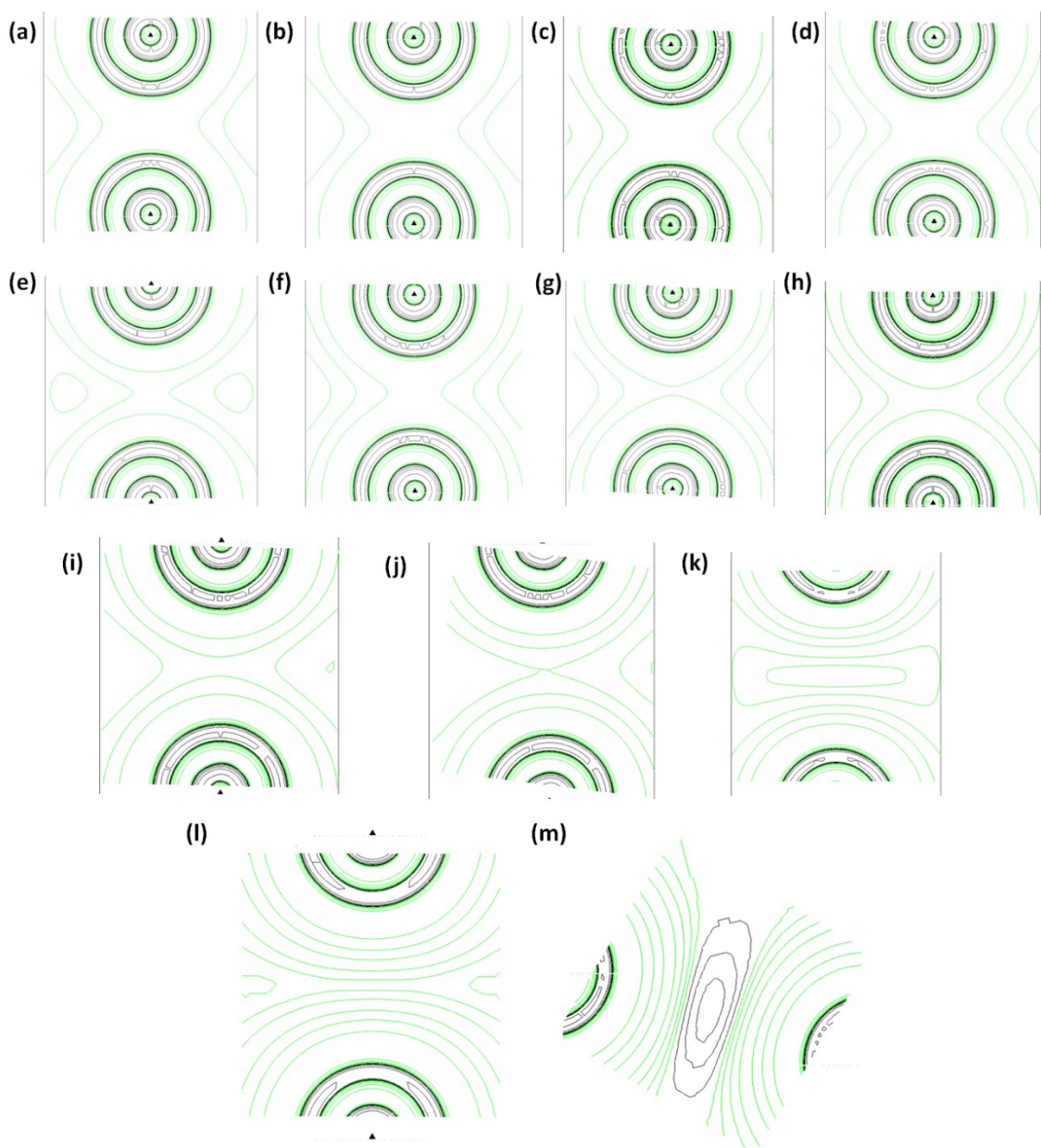
Figure S53: The contour plot of Laplacian of electron density between two Gd^{+3} ions in (a) $Gd_2@C_{30}$-D_{5h} (b) $Gd_2@C_{32}$-D_3 (c) $Gd_2@C_{34}$-C_2 (d) $Gd_2@C_{36}$-D_{2d} (e) $Gd_2@C_{38}$-D_{3h} (f) $Gd_2@C_{40}$-D_3 (g) $Gd_2@C_{42}$-C_2 (h) $Gd_2@C_{44}$-D_2 (i) $Gd_2@C_{46}$-C_s (j) $Gd_2@C_{48}$-C_{2v} (k) $Gd_2@C_{52}$-D_{2d} (l) $Gd_2@C_{60}$-I_h (m) $Gd_2@C_{80}$-D_{5h}.
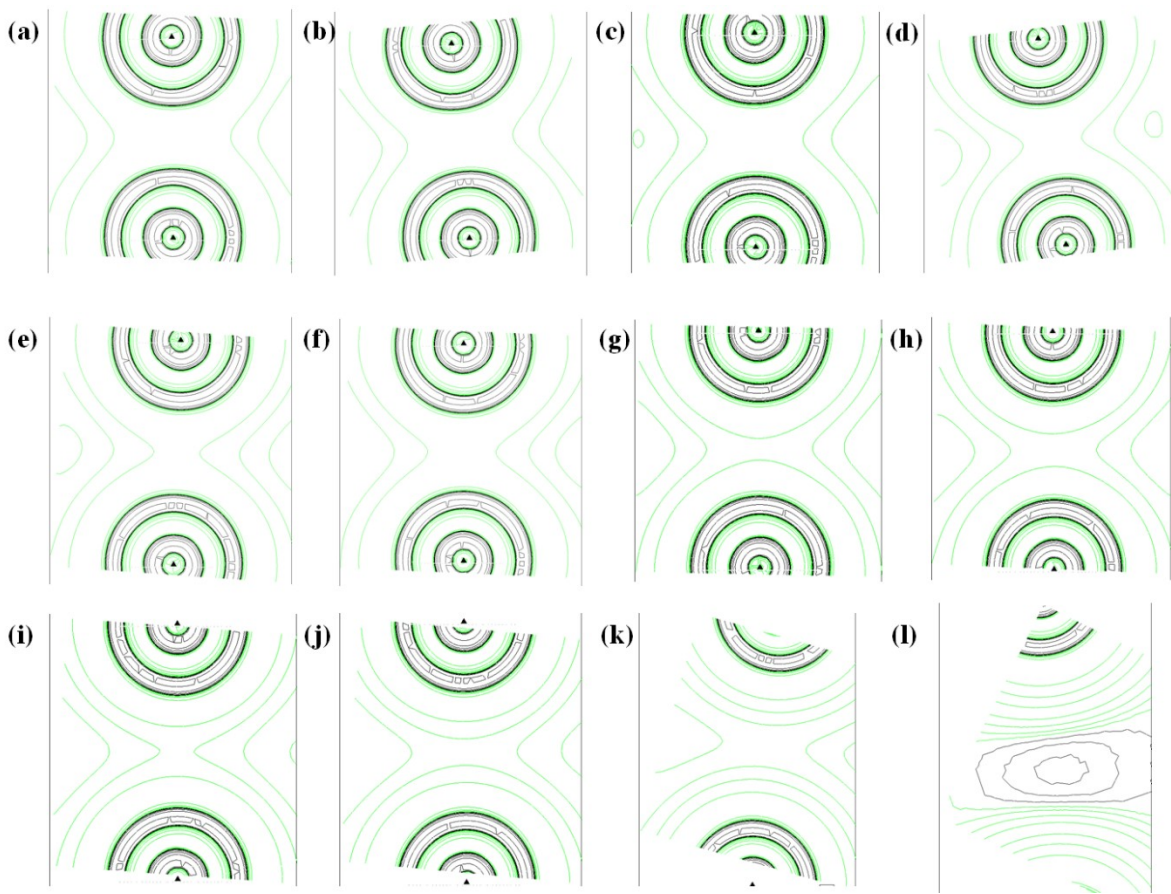
Figure S54: The contour plot of Laplacian of electron density between two Gd^{+3} ions in (a) $Gd_2@C_{30}$-C_{2v} (b) $Gd_2@C_{32}$-C_2 (c) $Gd_2@C_{34}$-C_s (d) $Gd_2@C_{36}$-C_s (e) $Gd_2@C_{38}$-C_1 (f) $Gd_2@C_{40}$-C_{2v} (g) $Gd_2@C_{42}$-C_s (h) $Gd_2@C_{44}$-C_s (i) $Gd_2@C_{46}$-C_1 (j) $Gd_2@C_{48}$-C_1 (k) $Gd_2@C_{52}$-C_s (l) $Gd_2@C_{80}$-C_{2v}.
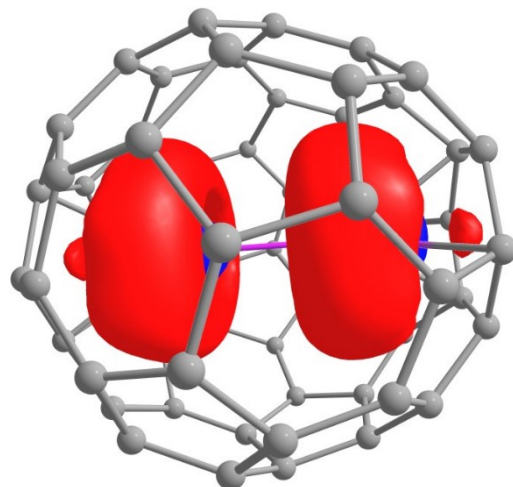
Figure S55: The orbital (from NBO analysis) constituting the unpaired electron between Gd1 and Gd2 centre in Gd$_2$@C$_{60}$-I_h. Colour Code: Gd-pink, C-grey.

It should be noted that, although the bonding of Gd$_2$ in Gd$_2$@C$_{52}$-D_{2d} and Gd$_2$@C$_{48}$-C_{2v} is found to be $\sigma_g^2\pi_u^3\sigma_u^1$ (ignoring the 4f orbitals) due to the smaller ring size, the energy of the empty orbitals of C$_{52}$-D_{2d} and C$_{48}$-C_{2v} is lower compared to the occupied frontier orbitals of Gd$_2$. Therefore, a transfer of six electrons takes place from Gd$_2$ to the fullerene ring (Figure S56-57).
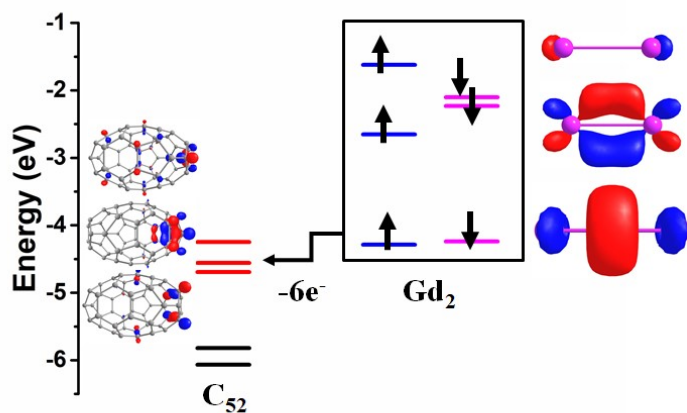
Figure S56: The MO diagram for the formation of Gd$_2$@C$_{52}$-D_{2d}. The three black and red horizontal lines correspond to the energy of the three highest occupied and three lowest unoccupied orbitals of the C$_{2n}$ fullerene ring, respectively. The blue and pink horizontal lines correspond to the energy of α and β orbitals of Gd$_2$. We have shown the three lowest unoccupied α orbitals of the C$_{52}$ fullerene ring with an isosurface value of 0.065 e$^-$/bohr^3. The three highest occupied β orbitals of Gd$_2$ in the C$_{52}$ ring also has been shown with an isosurface value of 0.065 e$^-$/bohr^3.
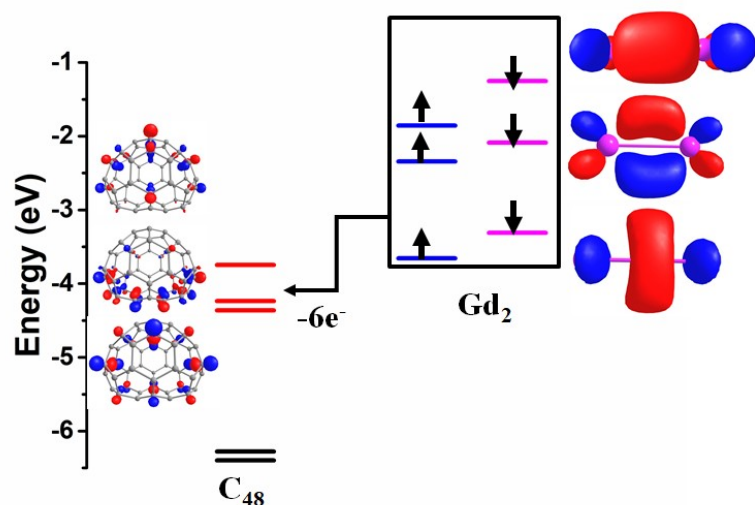
Figure S57: The MO diagram for the formation of $Gd_2@C_{48}$-C_{2v}. The three black and red horizontal lines correspond to the energy of the three highest occupied and three lowest unoccupied orbitals of the C_{2n} fullerene ring, respectively. The blue and pink horizontal lines correspond to the energy of α and β orbitals of Gd_2. We have shown the three lowest unoccupied α orbitals of the C_{48} fullerene ring with an isosurface value of 0.065 e^-/bohr^3. The three highest occupied α orbitals of Gd_2 in the C_{48} ring also has been shown with an isosurface value of 0.06 e^-/bohr^3.
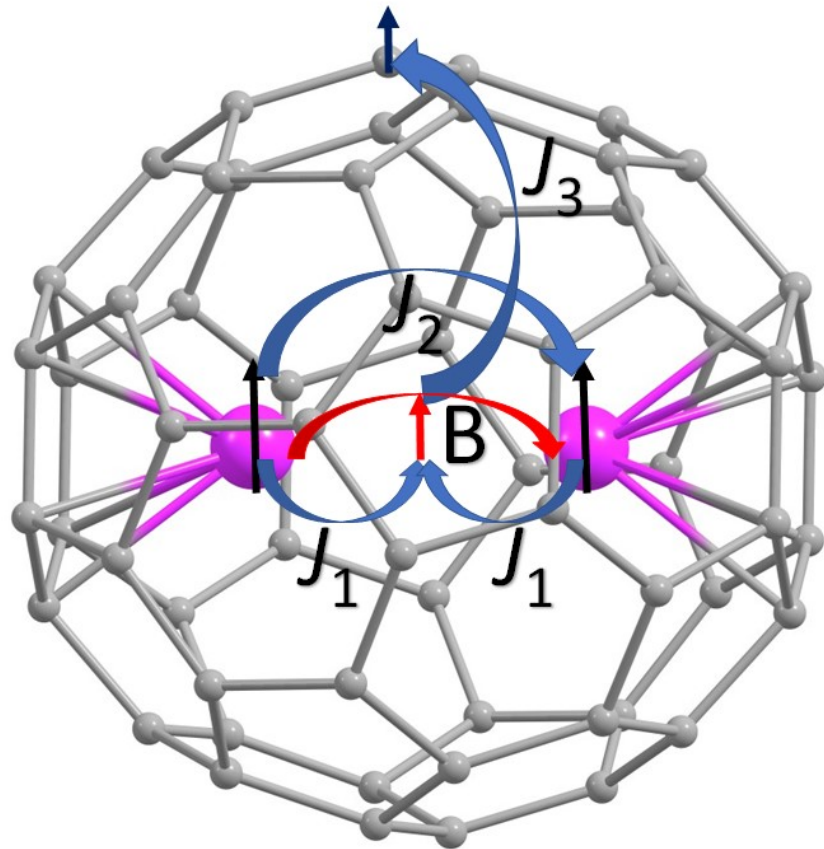
Scheme S2: Schematic representation of the several possible exchange pathways in $Gd_2@C_{60}$. Colour Code: Gd-pink, C-grey. The vertical black, red and blue arrow denotes the spin of the Gd, inner radical and outside radical on the cage, respectively.

Table S52: The energy of the all-possible spin states of $Gd_2@C_{59}N$-C_s.

Spin Multiplicity (2S+1)	Energy (a.u)	The difference in energy of the two roots divided by 2S+1 in cm^{-1} (B)

16	-24813.07549240	
14	-24813.07224845 -24813.04451009	434.8
12	-24813.07026195 -24813.04648094	434.9
10	-24813.06827167 -24813.04845903	434.8
8	-24813.06628537 -24813.05043575	434.8
6	-24813.06430031 -24813.05241370	438.8
4	-24813.06231672 -24813.05439234	434.8
2	-24813.06098645	

Table S53: The energy of the all-possible spin states of $Gd_2@C_{79}N$-C_s-1.

Spin Multiplicity (2S+1)	Energy (a.u)	The difference in energy of the two roots divided by 2S+1 in cm^{-1} (B)
16	-25571.29993837	
14	-25571.29836836 -25571.28547570	202.1
12	-25571.29744575 -25571.28639454	202.1
10	-25571.29652164 -25571.28731551	202.1
8	-25571.29560105 -25571.28823358	202.1
6	-25571.29467849 -25571.28915417	202.1
4	-25571.29375772 -25571.29007359	202.1
2	-25571.29310224	

Table S54: The energy of the all-possible spin states of $Gd_2@C_{79}N$-C_s-2.

Spin Multiplicity (2S+1)	Energy (a.u)	The difference in energy of the two roots divided by 2S+1 in cm^{-1} (B)
16	-25571.22579757	
14	-25571.22442487 -25571.21322082	175.6
12	-25571.22362290 -25571.21401937	175.6
10	-25571.22282085 -25571.21481861	175.6
8	-25571.22201987 -25571.21561734	175.6
6	-25571.22121873 -25571.21641676	175.6
4	-25571.22041843 -25571.21721585	175.7
2	-25571.21981407	

Table S55: The orbital occupation of the one unpaired electron in $Gd_2@C_{59}N$-I_h, $Gd_2@C_{79}N$-C_s-1 and $Gd_2@C_{79}N$-C_s-2. This has been computed for S = 15/2 state from *ab initio* calculation with CAS (15,15) active space.

Orbital	$Gd_2@C_{59}N$-Cs	$Gd_2@C_{79}N$-C_s-1	$Gd_2@C_{79}N$-C_s-2
6s	0.29	0.34	0.33
$5p_z$	0.18	0.12	0.10
$6p_z$	0.17	0.26	0.28
$5d_0$	0.36	0.28	0.29

Estimation of magnetic exchange in $Gd_2@C_{60}$-I_h, $Gd_2@C_{80}$-D_{5h}, $Gd_2@C_{80}$-C_{2v}

As all the spin Hamiltonian parameters are estimated using the azafullerene, we turn to the homofullerene cage to estimate the J_3 interaction. Here, we have used the DFT method to estimate this coupling between the inside cage radical and the radical on the cage (see scheme S2) using a broken symmetry approach which requires one high-spin (the spins of both radicals and Gd^{3+} ions are "up") and one broken-symmetry configuration (where all the spins are "up" except the one on the cage). These calculations yield a ferromagnetic J_3 value of +40.2 cm^{-1} for $Gd_2@C_{60}$-I_h and antiferromagnetic J_3 = -41.3 and -95.5 cm^{-1} for $Gd_2@C_{80}$-D_{5h} and $Gd_2@C_{80}$-C_{2v} cages, respectively (see Figure S58-60 for spin density). In the smaller cage ($Gd_2@C_{60}$), the inside cage radical is found to reside in the 5d orbitals (particularly $5dz^2$, along with 6s) of Gd, which is orthogonal to the SOMO of the cage radical (see Figure S58 and Table S56 in ESI). This leads to ferromagnetic J_3 interaction in $Gd_2@C_{60}$. Further, the radical on the cage is localised in few carbon atoms, restricting a strong overlap with $5dz^2$, leading to a ferromagnetic coupling.

On the other hand, for the $Gd_2@C_{80}$ cage, the inside cage radical has a diminished contribution from the 5d orbital (see Table S56) and enhanced contribution of 6s and 6p orbitals compared to $Gd_2@C_{60}$. The 6s orbital is spherical, and the cage radical, strongly delocalised to many atoms, favours a substantial overlap between these two radicals (inside and cage), leading to strong antiferromagnetic J_3 interactions (Figure S59). In the $Gd_2@C_{80}$-C_{2v} isomer, the 6s orbital contribution is even larger, and spin density is evenly distributed in the cage leading to a greater degree of overlap (Figure S60). Thus, a stronger antiferromagnetic J_3 exchange is attained in the $Gd_2@C_{80}$-C_{2v} isomer among the systems studied (Figure S60).

Table S56: The orbital composition of the inside cage electron in $Gd_2@C_{60}$-I_h, $Gd_2@C_{80}$-D_{5h} and $Gd_2@C_{80}$-C_{2v}.

Orbital	$Gd_2@C_{60}$-I_h	Orbital	$Gd_2@C_{80}$-D_{5h}	Orbital	$Gd_2@C_{79}N$-C_{2v}
6s	0.69	6s	0.55	6s	0.58
7p	0.08	6p	0.37	6p	0.39
5d	0.23	5d	0.08	5d	0.03
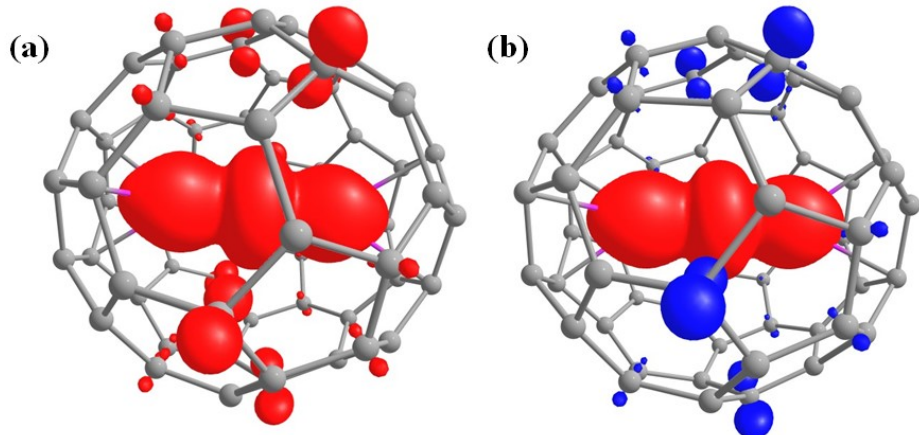
Figure S58: (a) The spin density of $Gd_2@C_{60}$-I_h in the HS configuration (b) The spin density of $Gd_2@C_{60}$-I_h in the BS configuration. Colour Code: Gd-pink, C-grey.
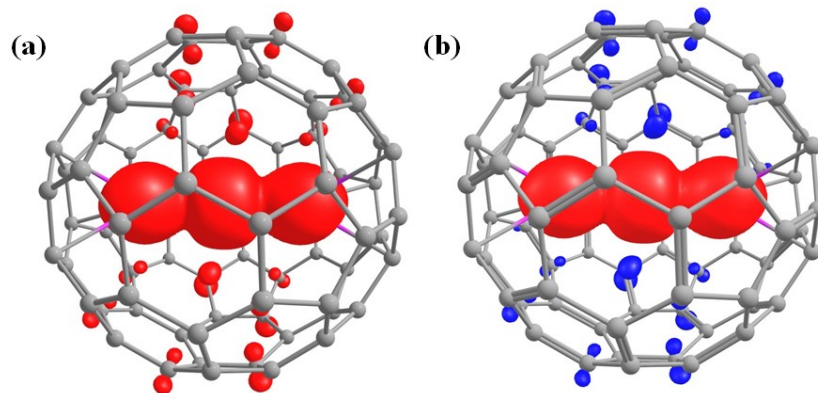
Figure S59: (a) The spin density of $Gd_2@C_{80}$-D_{5h} in the HS configuration (b) The spin density of $Gd_2@C_{80}$-D_{5h} in the BS configuration. Colour Code: Gd-pink, C-grey.
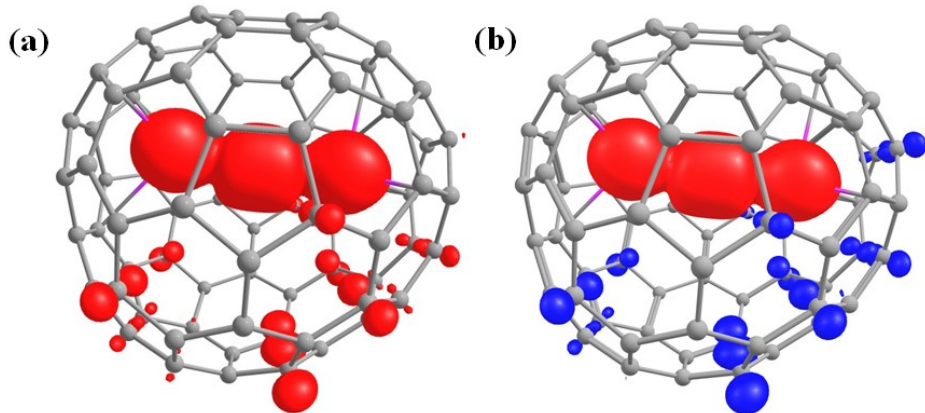
Figure S60: (a) The spin density of $Gd_2@C_{80}$-C_{2v} in the HS configuration (b) The spin density of $Gd_2@C_{80}$-C_{2v} in the BS configuration. Colour Code: Gd-pink, C-grey.

Magnetic anisotropy and mechanism of magnetic relaxation in selected $Ln_2@C_{2n}$ cages:

Studies on Dy$_2$@C$_{52}$-D$_{2d}$ and Er$_2$@C$_{52}$-D$_{2d}$: Among the studied Gd$_2$@C$_{2n}$ (30 ≤ 2n ≤ 52) isomers, the strongest J_{Gd-Gd} ferromagnetic exchange (2.7 cm^{-1}) was obtained in the Gd$_2$@C$_{52}$-D_{2d} isomer – a value relatively large for a 4f-4f ferromagnetic interaction. Utilising this J and the geometry, we have modelled Dy$_2$@C$_{52}$-D$_{2d}$ and Er$_2$@C$_{52}$-D$_{2d}$ isomers and performed *ab initio* CASSCF/RASSI-SO/SINGLE_ANISO calculations to probe their possible SMM characteristics. The single-ion relaxation mechanism developed for the Dy^{3+} and Er^{3+} centres is shown in Figure S61-62. The calculations reveal a very strong ground state QTM for both the ions (Dy^{3+} and Er^{3+}) due to significant mixing of m$_J$ = $|\pm15/2>$ with other states (Figure S61-62 and Table S57-60). This is essentially due to the η^2 + η^2 + η^1 + η^1 binding of the Ln^{3+} ions with three different rings of the C$_{52}$-D$_{2d}$ cage (see Figure S63-64 for anisotropy axis). This type of ligand field does not favour either prolate or oblate ions, and hence the ground state QTM is very strong for both models. The incorporation of the exchange interactions (see computational details) leading to a relaxation mechanism shown in Figure S65 for the Dy$_2$@C$_{52}$-D$_{2d}$ and Er$_2$@C$_{52}$-D$_{2d}$ isomers. The ferromagnetic exchange, while yielding a large magnetic moment for the ground state, the tunnel splitting is still very large (Table S61-62) as the exchange coupling is clearly not strong enough to suppress tunnelling in these systems.
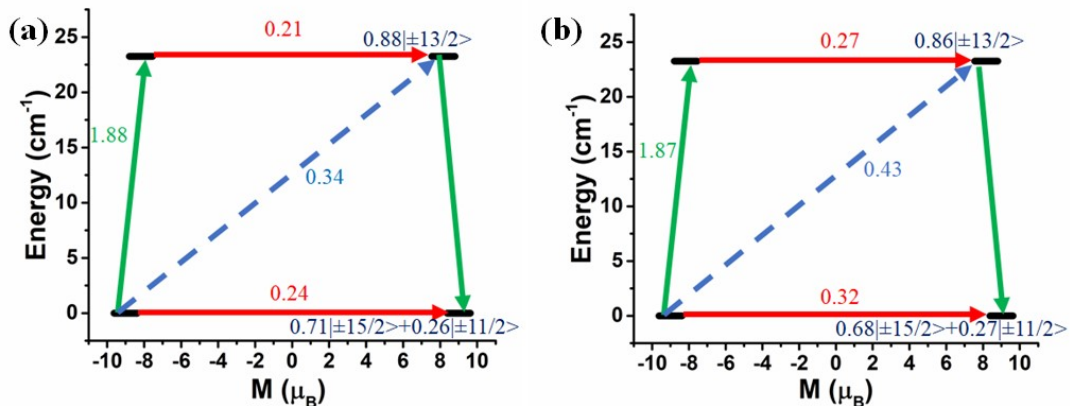
Figure S61: The mechanism of magnetisation relaxation of (a) Dy1 (b) Dy2 centre in Dy$_2$@C$_{52}$-D$_{2d}$. The thick black line represents the magnetic moment of KDs. Here the red arrows indicate QTM for the ground KD and TA-QTM for the excited KD; the sky dotted arrows indicate the Orbach pathway, and the green arrows indicate the pathway of magnetic relaxation. The blue characters signify the m$_J$ composition of a corresponding KD.

Table S57: The CASSCF/RASSI-SO/SINGLE_ANISO computed energy of the eight ground KDs along with the g tensor of the Dy1 centre in Dy$_2$@C$_{52}$-D$_{2d}$.

Energy (cm^{-1})	g$_x$	g$_y$	g$_z$
0.0	0.234	1.206	18.005
23.3	0.277	1.014	16.347
121.2	0.166	0.504	19.209
239.9	9.618	7.514	4.627
300.6	2.245	4.443	9.308
389.0	2.259	4.491	12.555
507.9	1.409	1.412	16.372
965.5	0.018	0.067	19.642

Table S58: The CASSCF/RASSI-SO/SINGLE_ANISO computed energy of the eight ground KDs along with the g tensor of the Dy2 centre in $Dy_2@C_{52}-D_{2d}$.

Energy (cm^{-1})	g_x	g_y	g_z
0.0	0.331	1.571	17.840
28.8	0.439	1.181	16.164
115.8	0.148	0.484	19.313
229.3	8.551	8.462	4.860
288.2	2.972	3.108	9.734
372.3	2.037	4.009	12.976
501.8	1.211	1.272	16.455
691.1	0.007	0.062	19.542
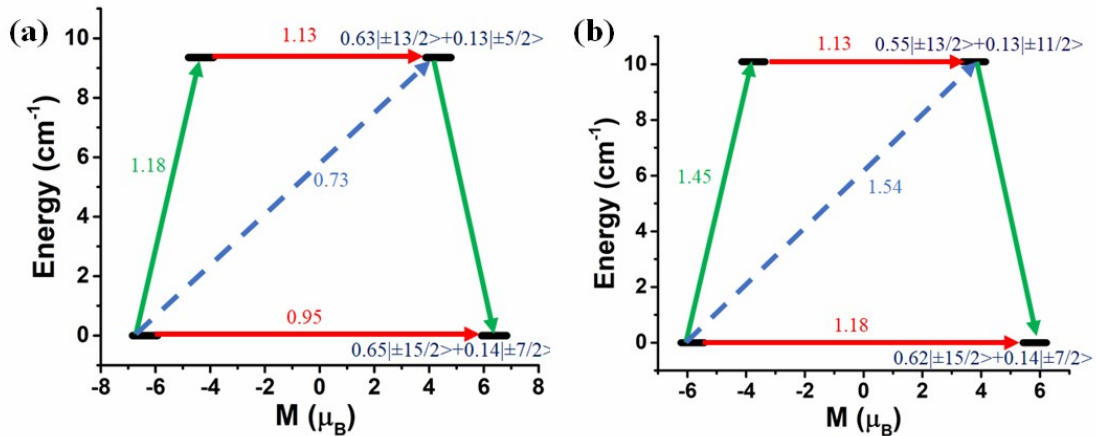
Figure S62: The mechanism of magnetisation relaxation of (a) Er1 (b) Er2 centre in $Er_2@C_{52}-D_{2d}$. The thick black line represents the magnetic moment of KDs. Here the red arrows indicate QTM for the ground KD and TA-QTM for the excited KD, the sky dotted arrows indicate the Orbach pathway, and the green arrows indicate the pathway of magnetic relaxation. The blue characters signify the m_J composition of a corresponding KD.

Table S59: The CASSCF/RASSI-SO/SINGLE_ANISO computed energy of the eight ground KDs along with the g tensor of the Er1 centre in $Er_2@C_{52}-D_{2d}$.

Energy (cm^{-1})	g_x	g_y	g_z
0.0	2.810	2.884	12.758
9.4	2.217	4.443	8.692
72.5	3.669	4.584	5.568
147.4	2.209	3.323	8.880
149.1	0.020	0.589	10.942
274.6	7.060	6.930	3.443
391.6	4.866	4.629	3.740
468.4	1.396	4.081	12.961

Table S60: The CASSCF/RASSI-SO/SINGLE_ANISO computed energy of the eight ground KDs along with the g tensor of the Er1 centre in $Er_2@C_{52}-D_{2d}$.

Energy (cm^{-1})	g_x	g_y	g_z
0.0	3.349	3.750	11.644
10.1	7.853	5.042	1.472
71.8	3.862	4.672	5.885
148.1	1.848	4.581	8.778
149.5	0.060	2.222	10.713

276.6	7.059	6.968	3.415
391.4	4.980	4.545	3.776
468.6	1.363	3.993	13.038
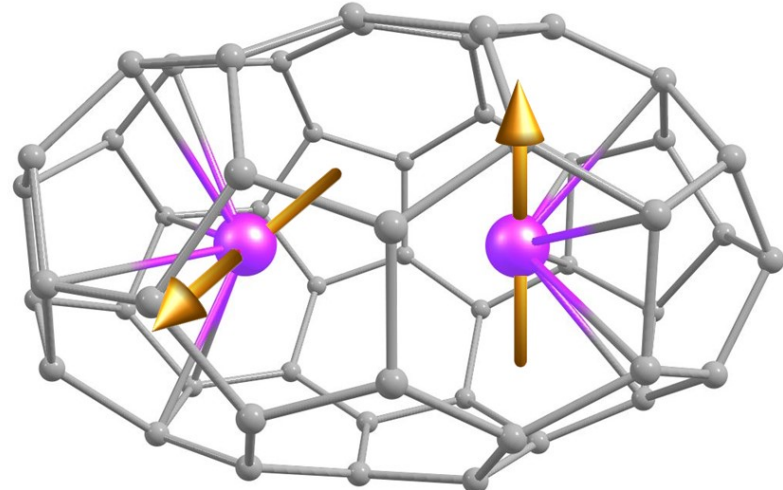
Figure S63: The ground state anisotropy axis of the metal centres in $Dy_2@C_{52}$-D_{2d}. Colour code: Dy-blue violet, C-grey.
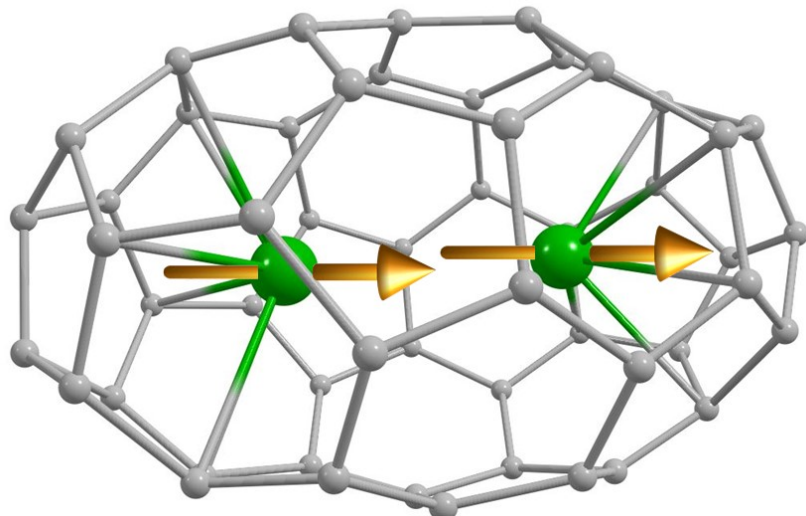
Figure S64: The ground state anisotropy axis of the metal centres in $Er_2@C_{52}$-D_{2d}. Colour code: Er-green, C-grey.
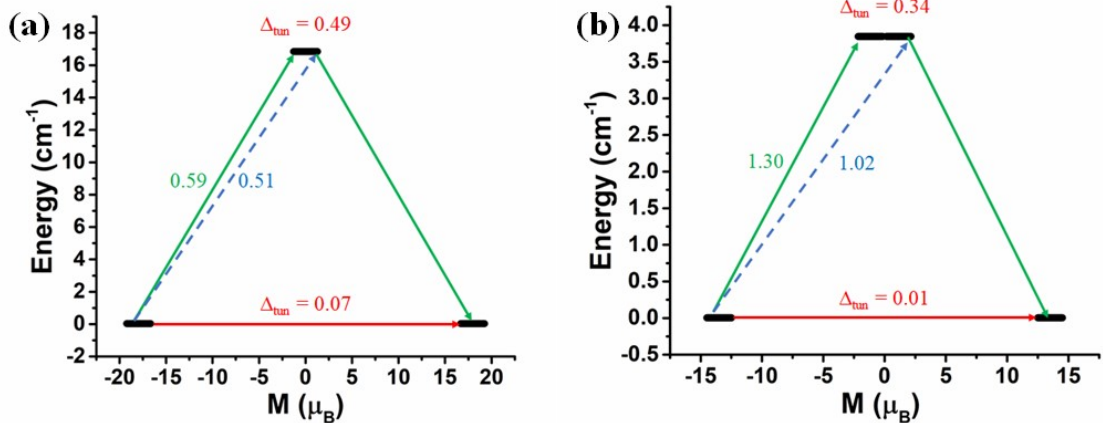
Figure S65: The POLY_ANISO computed relaxation mechanism of (a) $Dy_2@C_{52}$-D_{2d}. (b) $Er_2@C_{52}$-D_{2d}. The thick black line represents the magnetic moment of KDs. The red arrows imply tunnel splitting for the ground pKDs. The sky dotted arrows indicate a possible Orbach process. The green arrows represent the mechanism of magnetic relaxation.

Table S61: The computed energy and tunnel splitting of the eight lowest exchange coupled pKDs (pseudo-Kramers doublets) of $Dy_2@C_{52}$-D_{2d}.

State	Energy (cm^{-1})	Tunnel splitting (cm^{-1})
1	0.0	0.0665
2	0.1	
3	16.6	0.4949
4	17.1	
5	27.0	0.8371
6	27.8	
7	32.3	0.3041
8	32.6	

Table S62: The computed energy and tunnel splitting of eight lowest exchange coupled pKDs of $Er_2@C_{52}$-D_{2d}.

State	Energy (cm^{-1})	Tunnel splitting (cm^{-1})
1	0.0	0.0082
2	0.0	
3	3.7	0.3392
4	4.0	
5	9.6	0.3788
6	10.0	
7	11.9	0.0593
8	11.9	

Studies in $Dy_2@C_{38}$-D_{3h}, $Er_2@C_{38}$-D_{3h}, and $PrEr@C_{38}$-D_{3h}: Among the cages studied, the C_{38}-D_{3h} cage is the most attractive as it yields favourable exothermic binding energy (essential for experimental realisation) and strongest $Gd^{3+}\cdots Gd^{3+}$ interaction (-43.4 cm^{-1}), though the $J_{Gd\text{-}Gd}$ value is antiferromagnetic in nature. Here, we aim to utilise such a large magnetic exchange in search of the best SMM characteristics. To begin with, we have modelled $Dy_2@C_{38}$-D_{3h}, and the single-ion mechanism developed for the Dy^{3+} ion is shown in Figure 66a. The *ab initio*

calculation on both the Dy1 and Dy2 centre reveals large transverse anisotropy in the ground KD resulting in large QTM for magnetisation relaxation (see Figure 66a and Table S63-64). The geometry of $Ln_2@C_{38}$-D_{3h} unveils several Ln-C bonds, particularly with a six-member and the adjacent five-membered ring (see Figure S67-68 for anisotropy axis). The interactions of Ln^{3+} ions with such larger rings are known to offer a strong equatorial ligand field. This is witnessed in $[Dy(COT)_2]$ SMMs.[4, 5] Here, the computed QTM is much larger than that witnessed in the $[Dy(COT)_2]$ molecule (see Figure 66a).[4]

(a)   **(b)**   **(c)**
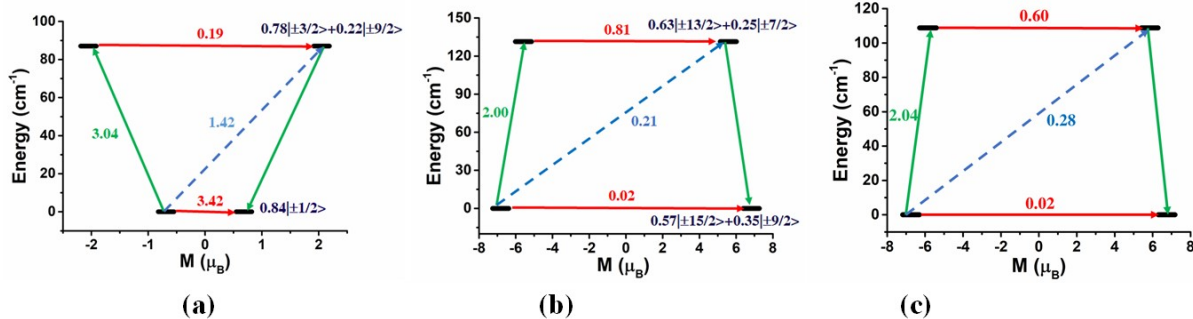
Figure S66: The mechanism of magnetisation relaxation of (a) Dy1 centre in $Dy_2@C_{38}$-D_{3h} (b) Er1 centre in $Er_2@C_{38}$-D_{3h}. (c) The exchange-coupled magnetic relaxation of $PrEr@C_{38}$-D_{3h}. Here the red arrows indicate QTM for the ground KD and TA-QTM for the excited KD. The sky-dotted arrows indicate the Orbach pathway, and the green arrows indicate the pathway of magnetic relaxation. The blue characters signify the m_J composition of a corresponding KD.

However, such ligand field could be favourable for prolate ions like Er^{3+}, as $[Er(COT)_2]^-$ is reported to possess a large U_{eff} value and blocking temperature.[6] Keeping this in mind, we have modelled $Er_2@C_{38}$-D_{3h}, and here as expected, the ground state QTM for Er^{3+} ion is found to be quenched (Figure 66b). This is also supported by the negligible g_x and g_y and very large g_z values (see Figure 66b and Table S65-66). The magnetisation relaxation occurs via the first excited KD due to the significant TA-QTM, and this leads to the U_{cal} value of 131.4 and 110.1 cm^{-1} for Er1 and Er2 centre in $Er_2@C_{38}$-D_{3h}. After computing the single-ion anisotropy of both the metal centres, they have been coupled using the POLY_ANISO routine to compute the exchange-coupled energy spectrum. However, a strong antiferromagnetic exchange leading to a diamagnetic ground state and SMM behaviour is not expected here (Figure S69, Table S67). Finally, to check the feasibility of stronger magnetic anisotropy in the C_{38}-D_{3h} fullerene cage with hetero dilanthanide EMF, we have modelled the $PrEr@C_{38}$-D_{3h} (see Figure S69 for anisotropy axis). The calculations on the Pr^{3+} ion reveals large tunnel splitting between the spin-orbit coupled states (see Table S68). Quite interestingly, the coupling of Er^{3+} with the Pr^{3+} ion quenches the QTM between the exchange-coupled KDs (see Table S69 and Figure 66c). However, a significant TA-QTM in the first excited KDs favours magnetisation relaxation, results in the U_{cal} value of 108.9 cm^{-1} in $PrEr@C_{38}$-D_{3h} isomer. These findings suggest that significant magnetic anisotropy is attainable with large antiferromagnetic interaction in hetero dilanthanide EMF.
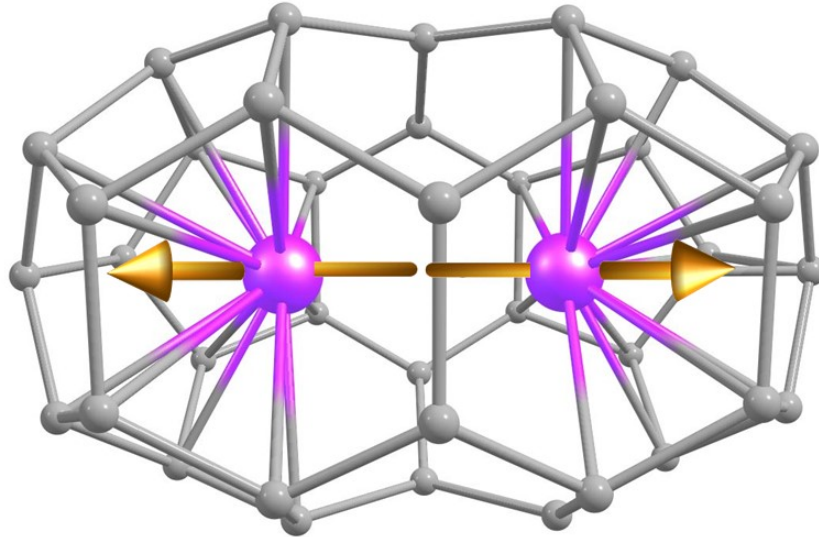
Figure S67: The ground state anisotropy axis of the metal centres in $Dy_2@C_{38}$-D_{3h}. Colour code: Dy-blue violet, C-grey.

Table S63: The computed energy of the eight ground KDs along with the g tensor of the Dy1 centre in $Dy_2@C_{38}$-D_{3h}.

Energy (cm^{-1})	g_x	g_y	g_z
0.0	10.707	9.832	1.370
87.1	0.035	0.816	4.100
188.1	0.528	8.774	0.982
642.2	1.215	3.562	13.325
646.0	3.403	5.000	11.812
780.0	1.543	1.574	13.338
1073.4	1.983	2.003	15.075
1589.0	0.001	0.002	18.451

Table S64: The computed energy of the eight ground KDs along with the g tensor of the Dy2 centre in $Dy_2@C_{38}$-D_{3h}.

Energy (cm^{-1})	g_x	g_y	g_z
0.0	10.477	10.142	1.370
94.3	0.092	0.158	4.049
203.4	9.175	9.050	1.006
633.4	9.040	8.006	4.661
640.0	0.260	0.520	10.441
785.0	1.700	1.710	13.280
1071.1	2.145	2.147	14.811
1578.1	0.001	0.001	18.328
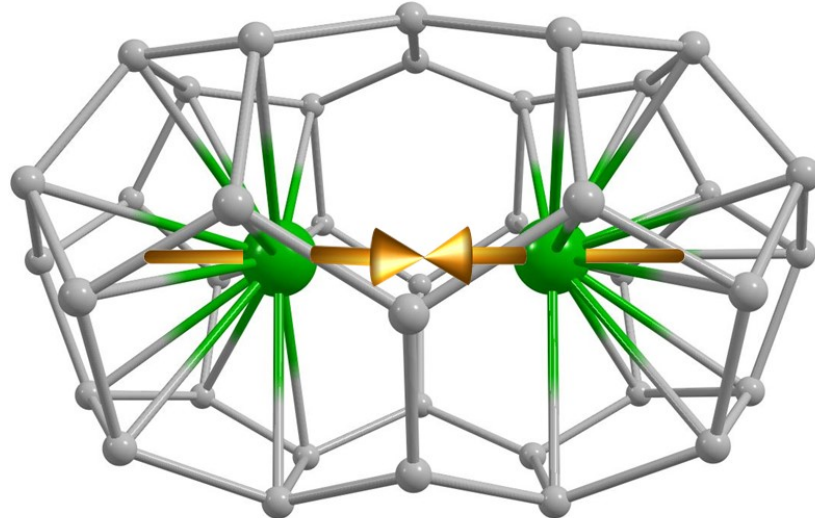
Figure S68: The ground state anisotropy axis of the metal centres in $Er_2@C_{38}$-D_{3h}. Colour code: Er-green, C-grey.

Table S65: The computed energy of the eight ground KDs along with the g tensor of the Er1 centre in $Er_2@C_{38}$-D_{3h}.

Energy (cm^{-1})	g_x	g_y	g_z
0.0	0.002	0.111	13.638
131.4	2.389	2.445	11.159
296.2	4.563	4.438	4.232
569.7	0.278	0.742	5.794
602.7	7.432	6.159	1.706
794.3	5.900	5.774	4.906
1317.0	0.033	0.122	7.229
1509.8	8.502	8.400	2.517

Table S66: The computed energy of the eight ground KDs along with the g tensor of the Er2 centre in $Er_2@C_{38}$-D_{3h}.

Energy (cm^{-1})	g_x	g_y	g_z
0.0	0.013	0.133	13.483
110.1	1.743	1.809	11.701
269.9	4.402	4.229	4.569
555.3	0.404	1.175	5.994
579.6	8.188	6.118	1.424
752.7	5.854	5.718	5.179
1296.7	0.034	0.128	7.495
1485.6	8.512	8.398	2.564
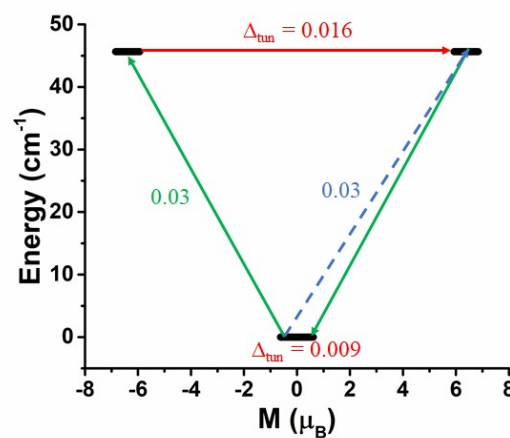
Figure S69: The POLY_ANISO computed relaxation mechanism of $Er_2@C_{38}$-D_{3h}. The thick black line represents the magnetic moment of KDs. The red arrows imply tunnel splitting. The sky dotted arrows indicate a possible Orbach process. The green arrows represent the mechanism of magnetic relaxation.

Table S67: The computed energy and tunnel splitting of ten lowest exchange coupled states of $Er_2@C_{38}$-D_{3h}.

State	Energy (cm^{-1})	Tunnel splitting (cm^{-1})
1	0.0	0.0087
2	0.0	
3	45.6	0.0161
4	45.6	
5	113.9	0.0595
6	114.0	
7	136.1	0.0611
8	136.2	
9	148.3	0.0294
10	148.4	
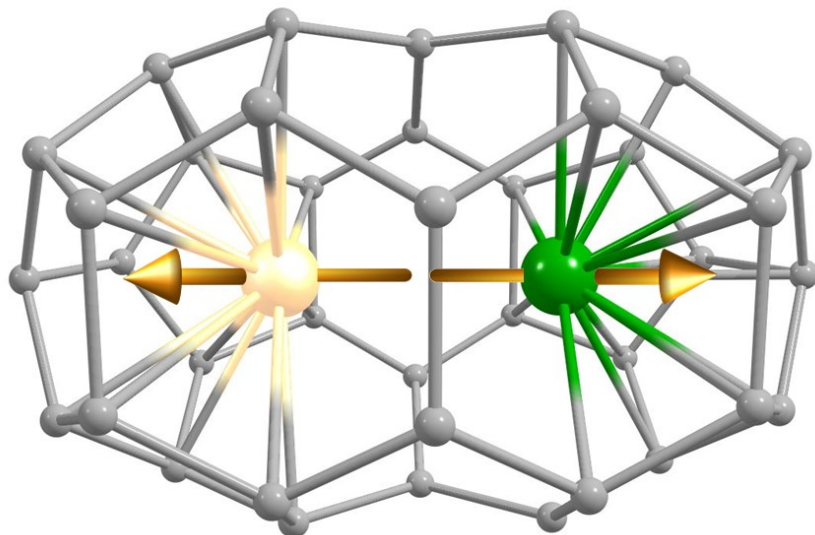
Figure S70: The ground state anisotropy axis of the metal centres in PrEr@C_{38}-D_{3h}. Colour code: Pr-yellow, Er-green, C-grey.

Table S68: The computed energy of the ten lowest spin-orbit states of PrLu@C_{38}-D_{3h}.

State	Energy (cm^{-1})
1	0.0
2	158.5
3	160.6
4	648.5
5	925.3
6	927.9
7	1169.9
8	1170.2

9	1373.2
10	3035.0

Table S69: The computed energy and g tensors of the eight low lying exchange-coupled states of PrEr@C$_{38}$-D_{3h}.

Energy (cm^{-1})	g_x	g_y	g_z
0.0	0.012	0.137	13.478
108.9	1.780	1.848	11.697
155.0	0.002	0.032	12.007
166.1	0.004	0.023	14.922
264.6	0.293	0.402	10.242
275.5	0.341	0.353	13.154
648.8	0.013	0.132	13.486
758.9	1.740	1.806	11.704

Table S70: The computed energy (cm^{-1}) and g tensor of the eight KDs of Dy1 centre in Dy$_2$@C$_{59}$N-C_s.

Energy	g_x	g_y	g_z	The angle of g_{zz} between ground and higher excited KDs (°)
0.0	0.001	0.001	19.976	
291.8	0.061	0.067	17.158	4.1
406.0	0.113	0.204	14.535	4.8
483.7	0.223	0.532	11.813	4.5
579.1	4.691	5.433	8.152	11.1
723.8	6.764	5.313	3.353	97.4
835.0	3.953	3.568	0.555	94.7
907.5	12.779	8.235	1.168	0.9

Table S71: The computed energy (cm^{-1}) and g tensor of the eight KDs of Dy2 centre in Dy$_2$@C$_{59}$N-C_s.

Energy	g_x	g_y	g_z	Angle of g_{zz} between ground and higher excited KDs (°)
0.0	0.002	0.002	19.968	
250.5	0.004	0.008	17.437	14.8
366.7	0.196	0.231	14.428	10.7
472.7	0.659	1.028	12.151	10.0
569.1	3.268	4.122	9.943	32.2
696.9	6.148	5.537	2.789	116.2
807.7	4.227	3.263	1.191	81.3
881.0	13.008	8.045	1.177	2.5
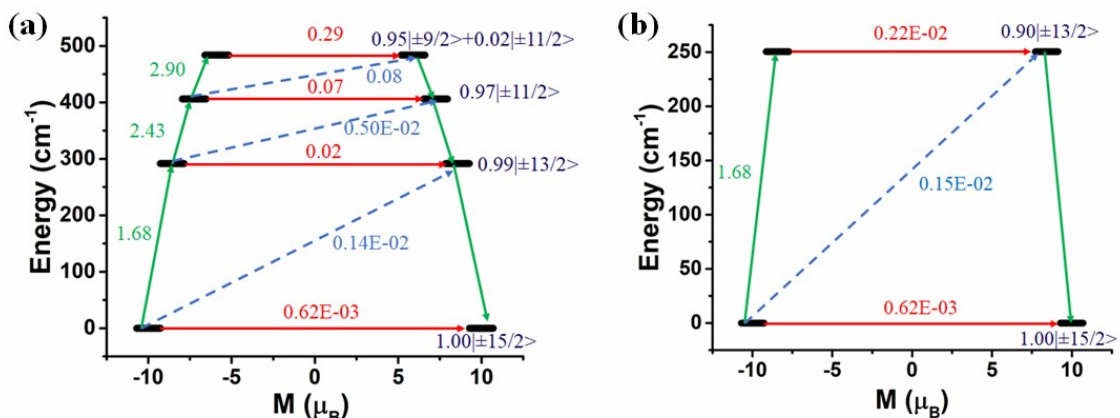
Figure S71: The mechanism of magnetic relaxation of Dy1 (a) Dy2 (b) centre of $Dy_2@C_{59}N$-C_s. The thick black line represents the magnetic moment of KDs. The red arrows imply the QTM for ground KD and TA-QTM for higher excited KDs. The blue dotted arrows indicate a possible Orbach process. The green arrows represent the mechanism of magnetic relaxation. The blue characters indicate the m_J composition of each KDs.

Figure S72: The POLY_ANISO computed relaxation mechanism of $Dy_2@C_{59}N$-C_s (left). The ground and fourth excited states anisotropy axis of metal and radical centres are shown in the right. Colour code: Dy-blue violet, C-grey, N-blue. (b) The thick black line represents the magnetic moment of KDs. The red arrows imply the QTM for ground KD and TA-QTM for higher excited KDs. The blue dotted arrows indicate a possible Orbach process. The green arrows represent the mechanism of magnetic relaxation.

Table S72: The CASSCF/RASSI-SO/SINGLE_ANISO computed crystal field parameter of the Dy1 and Dy2 centre of $Dy_2@C_{59}N$-C_s.

k	q	B_k^q	
		Dy1	Dy2
2	-2	-2.13E-03	1.16E-01
	-1	2.72E-01	-1.42E+00
	0	**-4.83E+00**	**-4.73E+00**
	1	4.64E-01	2.24E-01
	2	-3.83E-02	-2.76E-01
4	-4	7.62E-04	2.17E-03
	-3	3.65E-03	1.63E-02
	-2	-2.19E-03	4.14E-03
	-1	-3.03E-03	-2.39E-03
	0	1.44E-03	1.89E-03
	1	-8.47E-04	-1.95E-03
	2	-1.98E-03	-1.23E-03
	3	1.87E-02	1.91E-02
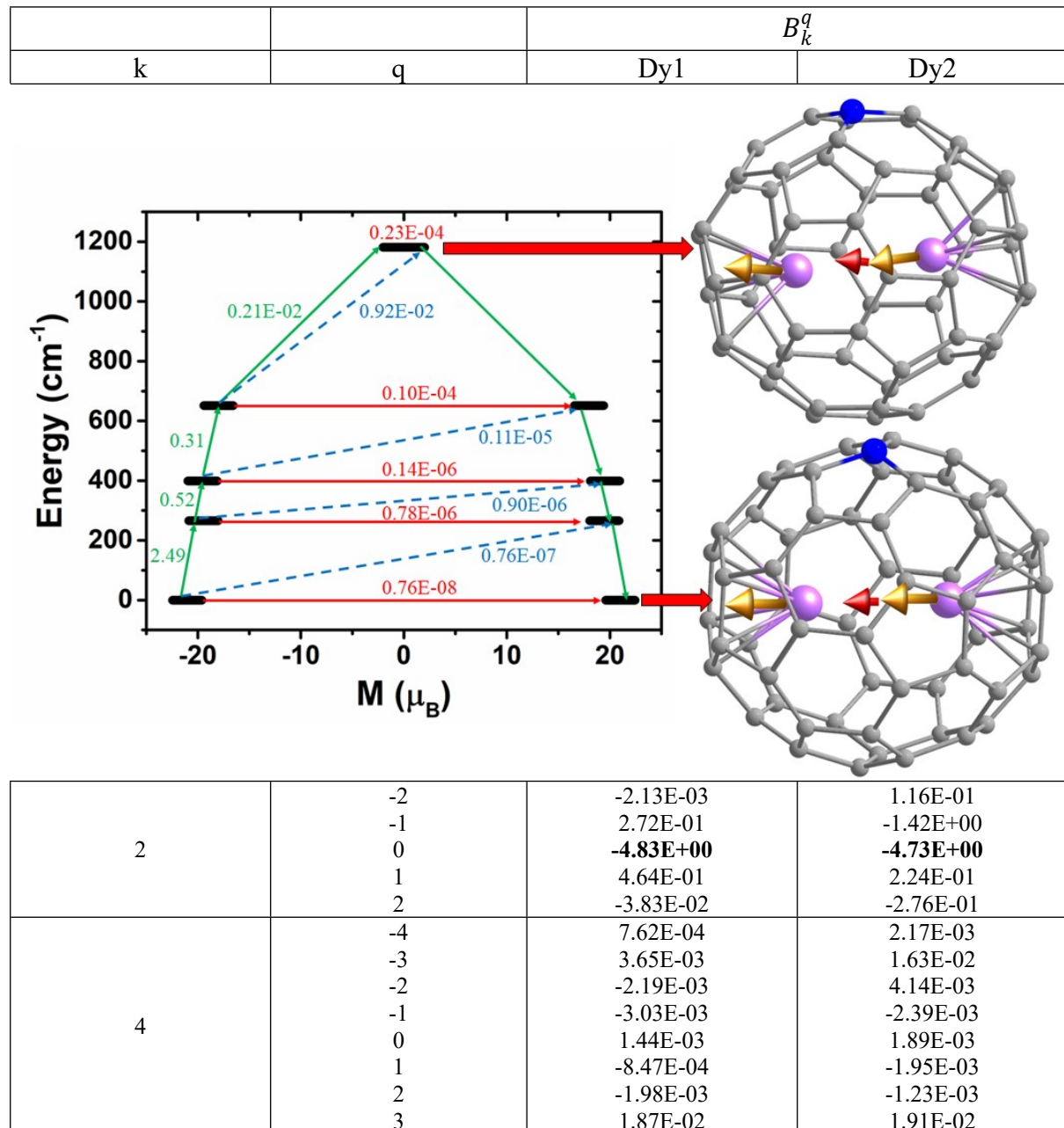
	4	-8.91E-04	-3.13E-03
6	-6	-1.90E-04	-1.70E-04
	-5	3.15E-06	-3.92E-04
	-4	1.45E-05	2.02E-05
	-3	4.57E-05	2.46E-05
	-2	1.46E-05	1.35E-05
	-1	2.04E-05	2.12E-04
	0	-4.98E-05	-4.41E-05
	1	-4.41E-05	6.98E-07
	2	-6.54E-05	-4.58E-06
	3	-4.53E-05	5.47E-05
	4	6.03E-05	-2.29E-05
	5	9.88E-05	-8.92E-04
	6	-2.72E-04	1.84E-04
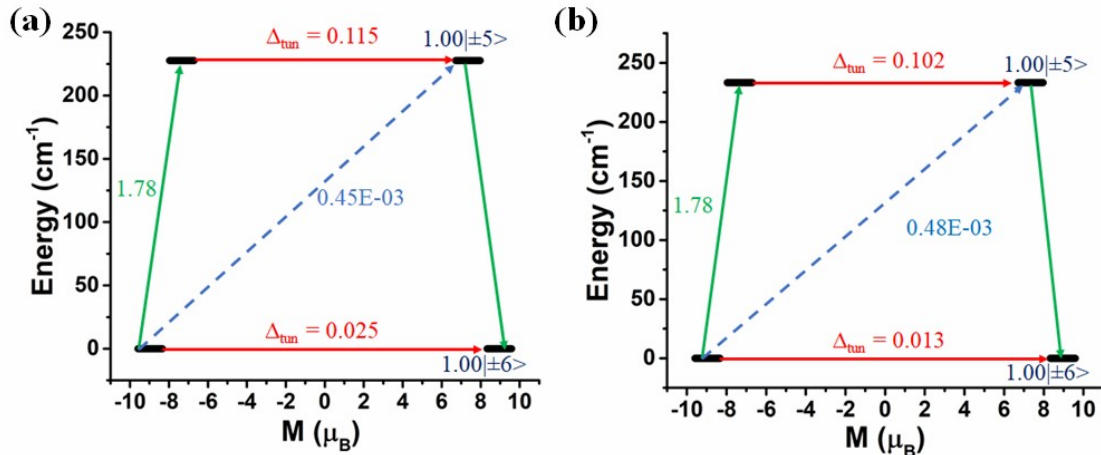
Figure S73: The mechanism of magnetic relaxation of Tb1 (a) Tb2 (b) centre of $Tb_2@C_{59}N$-C_s. The thick black line represents the magnetic moment of KDs. The red arrows imply the QTM for ground KD and TA-QTM for higher excited KDs. The blue dotted arrows indicate a possible Orbach process. The green arrows represent the mechanism of magnetic relaxation. The blue characters indicate the m_J composition of each pKDs.

Table S73: The computed energy (cm^{-1}) and g tensor of the four pKDs of Tb1 centre in $Tb_2@C_{59}N$-C_s.

Energy	g_x	g_y	g_z
0.000 0.025	0.000	0.000	17.921
227.569 227.684	0.000	0.000	14.682
453.711 454.086	0.000	0.000	11.448
621.650 661.529	0.000	0.000	8.494

Table S74: The computed energy (cm^{-1}) and g tensor of the four pKDs of Tb2 center in $Tb_2@C_{59}N$-C_s.

Energy	g_x	g_y	g_z
0.000 0.013	0.000	0.000	17.919

Energy (cm⁻¹)			
233.202 233.304	0.000	0.000	14.673
454.920 456.181	0.000	0.000	11.462
620.648 647.744	0.000	0.000	8.555

Table S75: The computed energy and g tensor of the six lowest pKDs of $Dy_2@C_{79}N$-C_s.

Energy (cm⁻¹)	g_x	g_y	g_z	Tunnel Splitting (cm⁻¹)
0.0	0.000	0.000	42.043	3.0E-10
265.7	0.000	0.000	39.174	1.6E-08
399.4	0.000	0.000	39.143	3.2E-08
651.8	0.000	0.000	36.324	7.0E-08
1183.3	0.000	0.000	11.021	2.2E-07
1227.6	0.000	0.000	5.436	1.1E-07

Table S76: The computed energy and g tensor of the six lowest KDs of $Tb_2@C_{79}N$-C_s.

Energy (cm⁻¹)	g_x	g_y	g_z	Tunnel Splitting (cm⁻¹)
0.0	0.000	0.000	37.938	4.9E-07
220.8	0.000	0.000	34.641	1.7E-08
461.8	0.000	0.000	34.690	2.9E-08
654.7	0.000	0.000	31.379	5.0E-07
1501.8	0.000	0.000	9.252	1.1E-06
1534.5	0.000	0.000	7.478	7.7E-07

Appendix S1: The optimised cartesian coordinates of $Gd_2@C_{30}$-D_{5h}.

```
C     2.807598000    1.250143000   -0.402711000
C     1.534614000    2.068110000   -0.669427000
C    -0.753251000    1.350141000   -1.859923000
C     0.755869000    1.349546000   -1.855560000
C     2.806755000    0.001443000   -1.309593000
C     1.533325000    0.000439000   -2.167860000
C     2.807636000   -1.246305000   -0.401937000
C    -0.752062000   -1.350803000   -1.858127000
C     0.756196000   -1.348302000   -1.853106000
C     1.535508000   -2.063716000   -0.666902000
C    -1.532198000   -0.001284000   -2.177581000
C     2.809402000   -0.768907000    1.065447000
C    -0.752708000   -2.183447000    0.710035000
C     0.757692000   -2.183168000    0.712371000
C     1.536667000   -1.275952000    1.762187000
C    -1.531378000   -2.068394000   -0.673334000
C     2.810250000    0.774326000    1.065494000
C    -0.752877000    0.001028000    2.292978000
C     0.756370000    0.002462000    2.300287000
C     1.534921000    1.280259000    1.762703000
C    -1.531306000   -1.276126000    1.755740000
C    -0.753510000    2.183060000    0.708383000
C     0.755668000    2.186311000    0.712755000
C    -1.532648000    2.066929000   -0.674038000
C    -1.532796000    1.276669000    1.755320000
C    -2.807441000    1.248895000   -0.409618000
C    -2.806532000    0.771637000    1.059973000
C    -2.805917000   -0.772940000    1.060741000
C    -2.807226000   -1.250836000   -0.408047000
C    -2.808113000   -0.001224000   -1.317519000
Gd   -1.111764000   -0.000375000   -0.006120000
```

Gd   1.109335000   0.003235000   0.007301000

Appendix S2: The optimized cartesian coordinates of Gd$_2$@C$_{30}$-C_{2v}.

C	2.800961000	-1.236000000	0.325564000
C	1.557068000	-2.060837000	0.723395000
C	2.836013000	0.011222000	1.232901000
C	-0.761378000	-1.322373000	1.852534000
C	0.789101000	-1.328420000	1.861213000
C	1.578861000	0.010023000	2.128639000
C	-1.527808000	-2.052491000	0.718790000
C	2.792303000	1.255609000	0.323209000
C	-0.766545000	1.347575000	1.853863000
C	0.784215000	1.347549000	1.857172000
C	1.547745000	2.074828000	0.720237000
C	-1.554116000	0.012595000	2.119654000
C	2.666459000	0.810468000	-1.186868000
C	2.672687000	-0.790786000	-1.187006000
C	1.296394000	-1.523353000	-1.691646000
C	1.288890000	1.537264000	-1.689951000
C	0.009122000	0.759746000	-2.243282000
C	0.010563000	-0.741438000	-2.242432000
C	-0.746840000	2.336076000	-0.549956000
C	0.755770000	2.329601000	-0.546296000
C	-1.536887000	2.080502000	0.718651000
C	-0.737924000	-2.310796000	-0.546490000
C	0.764682000	-2.315054000	-0.545705000
C	-1.271995000	-1.524666000	-1.695092000
C	-1.279436000	1.548268000	-1.699091000
C	-2.663765000	0.812710000	-1.190158000
C	-2.657339000	-0.793228000	-1.188355000
C	-2.781853000	1.256489000	0.323774000
C	-2.812048000	0.010357000	1.231071000
C	-2.773079000	-1.234983000	0.323597000
Gd	1.100611000	0.001193000	-0.032537000
Gd	-1.085037000	0.019067000	-0.051388000

Appendix S3: The optimized cartesian coordinates of Gd$_2$@C$_{32}$-C_2.

C	-0.260549136	2.109351427	1.346321575
C	-1.725812514	1.904931091	1.137796867
C	0.345097038	2.559769601	0.075960500
C	1.703747009	2.178470135	-0.361908452
C	2.641786217	1.398122895	0.572698807
C	-2.029822685	2.008954940	-0.314364875
C	-2.899425172	0.847260544	-0.742664777
C	-2.235719552	-0.087647030	-1.870358090
C	-0.663850181	2.293108671	-0.966051497
C	0.007667318	1.421401974	-1.961765252
C	-0.706027100	0.157522799	-2.348025575
C	-2.205205779	-1.462081443	-1.259808816
C	-0.827530488	-2.027204475	-1.376823807
C	-0.437998308	-2.545403825	-0.063416291

C	0.108250358	-1.121354224	-2.109140687
C	-2.661523009	-1.497132620	0.210347176
C	-3.136195504	-0.075680069	0.595857562
C	-2.224360979	0.667688314	1.779073903
C	-1.411977920	-2.124405281	0.963776051
C	-0.521756166	-1.370152787	1.995241269
C	-0.848711178	0.012832818	2.371484171
C	2.160848178	-0.791351079	1.730432957
C	1.908247715	0.690693549	1.903789280
C	0.337730297	1.051256268	2.151786420
C	0.944825113	-1.715609178	1.678311173
C	2.939683326	-1.051976473	0.413262091
C	2.070679111	-1.927934008	-0.478966091
C	0.950378500	-2.401292932	0.384035931
C	1.547346434	1.481666732	-1.686791820
C	2.446284735	0.205019199	-1.679797351
C	1.701840092	-1.146812884	-1.786063160
C	3.209103858	0.247400697	-0.289398963
Gd	-1.113897011	-0.018753843	0.014891712
Gd	1.092611105	0.029121342	-0.016282047

Appendix S4: The optimized cartesian coordinates of Gd$_2$@C$_{32}$-D_3.

C	-1.350355933	2.208864500	-0.608290592
C	1.355489529	2.208055626	0.608089504
C	0.132498584	1.837351961	1.449235565
C	-1.262445621	2.072945492	0.927625529
C	-2.493460506	1.375433404	-1.089359628
C	-3.183724940	0.746674919	0.105409464
C	-2.420334396	1.111371237	1.372351561
C	-1.979412451	0.299673788	-2.034475698
C	-0.517661573	0.577798441	-2.265045719
C	0.516798167	-0.578008736	-2.264482716
C	-2.424344369	-1.108871351	-1.371616650
C	-1.267155336	-2.072554642	-0.927366613
C	0.128093919	-1.837228011	-1.448967653
C	-3.185750721	-0.741570867	-0.103800552
C	1.978491195	-0.299173990	-2.034112698
C	2.493202236	-1.374944683	-1.089672626
C	1.350770030	-2.208767872	-0.608328592
C	2.423189445	1.107727524	-1.372661648
C	1.267438668	2.071565483	-0.928826613
C	-0.128158338	1.837008419	-1.449760657
C	3.185598535	0.741494417	-0.105527552
C	3.183877476	-0.746307866	0.104025464
C	2.496913398	1.371702123	1.089217539
C	1.980486649	0.296331599	2.033785614
C	-0.130959816	-1.836226157	1.450135568
C	1.263855186	-2.072561479	0.928421528
C	2.421297764	-1.111107501	1.371965563
C	-1.354419490	-2.207379067	0.609854501
C	-2.496066365	-1.371028200	1.090987541
C	0.519045531	0.578202224	2.264898629

S60

```
C    -0.517534793   -0.575864377    2.264872630
C    -1.979022320   -0.294859676    2.034183614
Gd    1.135461703    0.000400999    0.000653456
Gd   -1.136046645   -0.000939750   -0.000912544
```

Appendix S5: The optimized cartesian coordinates of Gd$_2$@C$_{34}$-*C*$_s$.

```
C    -1.611729000   -1.997620000    1.206895000
C     0.766943000   -0.538427000    2.334237000
C    -0.628887000    0.010549000    2.448254000
C    -1.853056000   -0.778641000    2.063114000
C    -0.849106000    1.407000000    2.028997000
C    -2.478255000   -1.861913000   -0.001290000
C    -2.847705000    0.134077000    1.351237000
C    -3.245897000   -0.555359000   -0.000903000
C    -1.612383000   -1.998255000   -1.211390000
C    -0.241869000   -2.323351000   -0.771621000
C     0.983362000   -1.798289000   -1.503365000
C    -1.853021000   -0.778187000   -2.065918000
C    -0.628660000    0.010934000   -2.449476000
C     0.766466000   -0.536682000   -2.338263000
C    -2.847608000    0.134206000   -1.355208000
C     2.301920000   -1.691676000   -0.801446000
C     2.919674000   -0.370660000   -1.217050000
C     1.948540000    0.395748000   -2.070787000
C     2.301534000   -1.692463000    0.795567000
C     0.982779000   -1.800188000    1.496951000
C    -0.241461000   -2.322677000    0.765735000
C     2.919740000   -0.372058000    1.212567000
C     3.280023000    0.441926000   -0.001085000
C     1.674140000    1.754294000    1.367989000
C     1.948263000    0.393549000    2.067569000
C     0.256154000    2.126703000    1.281277000
C    -0.375969000    2.515252000   -0.001655000
C     0.256305000    2.129303000   -1.285081000
C     1.674175000    1.755406000   -1.369911000
C     2.504698000    1.731619000   -0.000820000
C    -0.848996000    1.407084000   -2.031415000
C    -2.147546000    1.528740000    1.315514000
C    -1.823048000    2.182139000   -0.001689000
C    -2.147039000    1.528876000   -1.318441000
Gd   -1.150848000   -0.053836000   -0.001253000
Gd    1.131047000    0.032446000   -0.001676000
```

Appendix S6: The optimized cartesian coordinates of Gd$_2$@C$_{34}$-*C*$_2$.

```
C    -2.497343000   -1.292876000    1.227078000
C    -1.330208000   -2.191091000    0.847055000
C    -2.182364000    0.002828000    2.024241000
C     0.045141000   -1.974492000    1.440114000
C     1.301635000   -2.291701000    0.677722000
C    -2.385049000   -1.436897000   -1.200798000
C    -3.156696000   -0.828989000   -0.076561000
```

```
C     1.331353000    -2.200081000    -0.848202000
C    -0.045547000    -1.975705000    -1.440469000
C    -1.302049000    -2.284999000    -0.676624000
C    -3.149826000     0.675883000    -0.215756000
C    -2.596976000     1.200359000     1.158285000
C    -1.420352000     2.116226000     1.148786000
C    -2.242318000     0.984931000    -1.560546000
C    -1.055217000     1.924448000    -1.399006000
C    -0.740299000     2.529466000    -0.108848000
C    -1.817941000    -0.399515000    -2.097987000
C    -0.335799000     1.579907000     1.983359000
C    -0.730096000     0.249287000     2.453859000
C     0.346942000    -0.782868000     2.296746000
C     1.055483000     1.919378000     1.394449000
C     2.241382000     0.980161000     1.553394000
C     1.818410000    -0.402725000     2.097077000
C     0.740503000     2.525006000     0.106398000
C     3.158395000    -0.835841000     0.077719000
C     2.386268000    -1.442581000     1.202345000
C     2.594630000     1.193905000    -1.155160000
C     3.144417000     0.671077000     0.218056000
C     1.420282000     2.109627000    -1.147644000
C    -0.346049000    -0.783505000    -2.297564000
C     0.731096000     0.246964000    -2.455137000
C     0.336895000     1.577835000    -1.984744000
C     2.500461000    -1.300225000    -1.227937000
C     2.183848000    -0.001650000    -2.024961000
Gd    1.130453000    -0.036648000    -0.067736000
Gd   -1.132343000    -0.017383000     0.064608000
```

Appendix S7: The optimized cartesian coordinates of Gd₂@C₃₆-Cₛ.

```
C     3.424908000     0.437397000     0.012557000
C     2.684650000     1.700719000     0.012860000
C     3.083133000    -0.363303000     1.217598000
C     0.508360000     2.133087000     1.301859000
C     1.885449000     1.711261000     1.385581000
C     2.122707000     0.387020000     2.070680000
C     0.001424000     2.625304000     0.012009000
C     1.230877000    -1.816267000     1.518686000
C     2.519959000    -1.669519000     0.805094000
C     0.109041000    -2.382290000     0.764632000
C    -1.272629000    -2.177605000     1.208539000
C    -0.689962000     1.427646000     1.992903000
C    -0.513104000    -0.015829000     2.394474000
C     0.915892000    -0.552000000     2.340350000
C    -1.713096000    -0.982791000     2.026911000
C     0.109622000    -2.381948000    -0.743752000
C     1.232371000    -1.815701000    -1.496888000
C     2.520993000    -1.669359000    -0.781990000
C    -1.271764000    -2.176457000    -1.187753000
C    -3.115115000    -1.256773000     0.010199000
C    -2.097545000    -2.271026000     0.010083000
```

C	3.084985000	-0.362519000	-1.193366000
C	2.124976000	0.388408000	-2.046916000
C	0.509663000	2.134239000	-1.277819000
C	1.886824000	1.712446000	-1.361479000
C	-1.710953000	-0.981128000	-2.004552000
C	-0.511133000	-0.014772000	-2.371050000
C	0.918225000	-0.551296000	-2.318177000
C	-0.688373000	1.428063000	-1.969237000
C	-2.978782000	-0.449230000	-1.246176000
C	-3.020677000	0.976057000	-0.758069000
C	-1.911136000	1.870187000	-1.204233000
C	-3.021646000	0.976069000	0.779689000
C	-2.980149000	-0.450291000	1.267345000
C	-1.912324000	1.870241000	1.226786000
C	-1.411892000	2.504012000	0.011524000
Gd	1.210475000	0.008180000	0.010001000
Gd	-1.189336000	-0.038132000	0.012840000

Appendix S8: The optimized cartesian coordinates of Gd$_2$@C$_{36}$-D_{2d}.

C	-0.429263000	-0.623006000	-2.530441000
C	0.118204000	-1.921229000	-2.046180000
C	0.405056000	0.598231000	-2.537841000
C	-1.837161000	-0.587000000	-2.044310000
C	1.153564000	-2.610191000	-0.048574000
C	1.585170000	-1.958140000	1.161007000
C	2.408131000	-0.754184000	1.153104000
C	1.401204000	-1.866215000	-1.310213000
C	2.238532000	-0.640363000	-1.318423000
C	2.850425000	-0.126709000	-0.065720000
C	1.817222000	0.566716000	-2.063064000
C	2.077651000	1.653214000	1.472998000
C	1.868727000	0.252314000	2.043198000
C	0.783931000	2.535419000	1.474398000
C	2.799304000	1.360616000	0.049165000
C	0.457050000	-1.812813000	2.056599000
C	-0.775082000	-2.521516000	1.501333000
C	-2.066820000	-1.640272000	1.501479000
C	0.587562000	-0.384507000	2.551369000
C	-0.570314000	0.405998000	2.552226000
C	-1.855001000	-0.235143000	2.059180000
C	-0.444432000	1.830541000	2.044903000
C	-0.922197000	-2.701361000	-1.279198000
C	-2.183722000	-1.841028000	-1.277970000
C	-0.249147000	-3.102106000	0.080096000
C	-2.800646000	-1.361637000	0.083383000
C	-2.401743000	0.763111000	1.164914000
C	-2.853818000	0.124603000	-0.044650000
C	-1.579305000	1.967352000	1.156568000
C	-1.157418000	2.607894000	-0.062092000
C	2.169886000	1.827227000	-1.311287000
C	0.907740000	2.687586000	-1.309906000
C	0.246026000	3.101816000	0.050685000

C	-2.252748000	0.626980000	-1.306590000
C	-1.415161000	1.852382000	-1.314625000
C	-0.138078000	1.900361000	-2.060692000
Gd	-0.642597000	-0.937164000	-0.005621000
Gd	0.641164000	0.936635000	-0.014198000

Appendix S9: The optimized cartesian coordinates of Gd$_2$@C$_{38}$-C_1.

C	3.121529000	0.510511000	1.187088000
C	2.197566000	-0.201026000	2.089697000
C	2.509314000	1.744502000	0.681317000
C	2.459494000	1.650975000	-0.869149000
C	1.130212000	1.953939000	-1.472074000
C	1.262089000	1.911297000	1.472026000
C	0.118185000	2.485627000	0.814617000
C	0.116300000	2.632026000	-0.646453000
C	-1.236626000	2.210908000	1.264942000
C	-0.536525000	-1.331094000	2.132430000
C	-0.403963000	0.143680000	2.474541000
C	1.014275000	0.687970000	2.325488000
C	-1.572240000	1.033873000	2.133889000
C	2.232683000	-0.719801000	-1.970683000
C	0.866271000	-0.381458000	-2.469097000
C	3.066928000	0.302319000	-1.217460000
C	0.353184000	1.008164000	-2.319764000
C	-1.130576000	1.254768000	-2.097847000
C	-0.067540000	-1.443610000	-2.071572000
C	-1.549758000	-1.258619000	-1.979975000
C	-2.146888000	0.161157000	-2.052892000
C	-1.216876000	2.341556000	-1.110808000
C	0.688069000	-2.312104000	-1.094062000
C	2.092420000	-1.923468000	-1.092979000
C	0.014894000	-2.584896000	0.176117000
C	-1.418879000	-2.514597000	0.245597000
C	-2.221047000	-1.959244000	-0.881955000
C	3.466392000	-0.353924000	0.055968000
C	2.794249000	-1.667639000	0.234430000
C	0.590065000	-2.042003000	1.457767000
C	2.002412000	-1.602676000	1.506446000
C	-3.231107000	-1.086040000	-0.279965000
C	-2.097376000	2.232875000	0.087348000
C	-3.114833000	1.224564000	0.190058000
C	-3.236768000	0.233131000	-0.955855000
C	-1.800086000	-1.818565000	1.483984000
C	-2.953989000	-0.951504000	1.182265000
C	-2.863002000	0.488699000	1.503988000
Gd	-1.222463000	-0.019198000	0.032653000
Gd	1.219917000	-0.051237000	-0.011797000

Appendix S10: The optimized cartesian coordinates of Gd$_2$@C$_{38}$-D_{3h}.

| C | -1.245791000 | 1.805798000 | 1.527966000 |
| C | -2.519526000 | 1.868930000 | 0.793555000 |

C	2.527212000	-0.251895000	2.021694000
C	1.254199000	0.416500000	2.329863000
C	0.003958000	-0.376780000	2.285650000
C	-1.245255000	0.416314000	2.330843000
C	2.527416000	-1.596186000	1.246644000
C	-3.305666000	0.688269000	1.199999000
C	-2.518400000	-0.253391000	2.019624000
C	-2.518273000	-1.594231000	1.245637000
C	-1.244899000	-2.198783000	0.821978000
C	1.253963000	-2.198179000	0.821250000
C	0.003707000	-1.762697000	1.486675000
C	-3.813922000	0.007027000	0.019439000
C	-3.305492000	-1.355815000	0.020156000
C	-3.306357000	0.687534000	-1.161243000
C	-2.518797000	-1.595438000	-1.205597000
C	-2.519446000	-0.254986000	-1.980231000
C	-2.520505000	1.867930000	-0.755667000
C	0.003255000	2.162794000	0.816427000
C	1.253643000	1.805473000	1.527284000
C	-1.246775000	1.803738000	-1.491146000
C	1.254200000	1.803591000	-1.491159000
C	0.003340000	2.162378000	-0.781478000
C	2.527061000	1.871537000	-0.758225000
C	2.526281000	1.872209000	0.794147000
C	1.254214000	0.414171000	-2.293070000
C	-1.246658000	0.413947000	-2.292810000
C	0.003232000	-0.379533000	-2.247764000
C	3.313912000	0.691758000	1.202483000
C	3.809014000	0.008110000	0.018585000
C	3.314317000	0.690124000	-1.165325000
C	-1.245229000	-2.199244000	-0.782327000
C	0.003619000	-1.762751000	-1.448085000
C	2.526693000	-0.254035000	-1.984302000
C	2.526763000	-1.597896000	-1.206906000
C	1.253959000	-2.198634000	-0.781812000
C	3.314196000	-1.358975000	0.019662000
Gd	1.377943000	0.007623000	0.017983000
Gd	-1.356388000	0.007589000	0.019383000

Appendix S11: The optimized cartesian coordinates of Gd$_2$@C$_{40}$-C_{2v}.

C	2.548569000	-1.246976000	1.035823000
C	3.019553000	-0.006350000	0.532249000
C	2.543861000	1.232957000	1.035380000
C	1.453881000	1.313874000	2.000090000
C	0.763442000	-0.006068000	2.369149000
C	1.460795000	-1.328768000	2.004043000
C	1.192067000	3.049091000	0.274341000
C	2.304564000	2.145824000	-0.080004000
C	-0.729571000	2.597601000	1.645281000
C	0.732964000	2.592728000	1.642936000
C	-1.443204000	-1.325173000	1.999764000
C	-0.752836000	-0.004957000	2.369166000

```
C    -1.449884000    1.317336000    2.004207000
C     2.880194000   -0.006737000   -0.906182000
C     2.331636000   -1.318757000   -1.279368000
C     1.203646000   -1.350372000   -2.189419000
C     2.324483000    1.303617000   -1.276197000
C     1.199168000    1.338577000   -2.185503000
C     0.718064000   -0.005686000   -2.573533000
C     0.003178000    3.236625000   -0.664545000
C     0.004021000    2.270404000   -1.948505000
C     1.202288000   -3.070849000    0.276276000
C     0.008199000   -3.248934000   -0.664549000
C     2.313811000   -2.163220000   -0.081207000
C     0.007567000   -2.281130000   -1.947836000
C    -1.187477000   -1.349492000   -2.185875000
C    -1.181207000   -3.061115000    0.274300000
C    -2.293146000   -2.157188000   -0.080721000
C    -2.312892000   -1.314758000   -1.276797000
C    -0.706365000   -0.005281000   -2.574071000
C    -0.722174000   -2.604452000    1.643163000
C     0.740561000   -2.609176000    1.645442000
C    -1.192001000    1.339652000   -2.189815000
C    -2.320187000    1.307686000   -1.279866000
C    -2.868683000   -0.004415000   -0.906763000
C    -1.191083000    3.059277000    0.276096000
C    -2.302605000    2.151835000   -0.081285000
C    -2.532633000   -1.244275000    1.034704000
C    -3.008568000   -0.004942000    0.531662000
C    -2.537813000    1.235717000    1.035474000
Gd    0.026046000   -1.194023000    0.021591000
Gd   -0.015742000    1.181319000    0.021581000
```

Appendix S12: The optimized cartesian coordinates of Gd$_2$@C$_{40}$-D_2.

```
C   -0.925959000    2.375655000    1.150843000
C    0.529600000    2.470967000    1.261819000
C   -1.512572000    2.501175000   -0.168767000
C   -3.280901000    0.663527000    0.366828000
C   -2.692203000    1.688025000   -0.565785000
C    2.679378000    1.678330000    0.554462000
C    3.266383000    0.653467000   -0.376904000
C    1.502852000    2.495037000    0.157917000
C    2.580488000    0.447590000   -1.731158000
C    1.392423000    1.300891000   -2.091454000
C    0.916269000    2.371125000   -1.160814000
C   -0.538886000    2.471992000   -1.272370000
C    3.264354000   -0.667824000    0.376503000
C    2.680733000   -1.693518000   -0.557927000
C    2.319110000   -1.015855000   -1.826131000
C    1.004926000   -1.524490000   -2.241440000
C   -0.117228000   -0.718846000   -2.646501000
C    0.112293000    0.713335000   -2.647000000
C    1.380829000   -1.309435000    2.084809000
C    0.906465000   -2.379460000    1.153638000
```

```
C    2.571215000   -0.459730000    1.726653000
C    1.498817000   -2.505900000   -0.163637000
C    0.529316000   -2.477561000   -1.270565000
C    0.999226000    1.515520000    2.232772000
C   -0.125935000    0.714610000    2.636709000
C    2.311663000    1.002270000    1.820294000
C    0.100949000   -0.718331000    2.636706000
C   -1.022935000   -1.520472000    2.231016000
C   -1.404718000    1.306609000    2.082006000
C   -2.595188000    0.455847000    1.720943000
C   -2.335320000   -1.007832000    1.815292000
C   -0.926311000   -2.375642000   -1.162312000
C   -1.518671000   -2.499775000    0.154159000
C   -0.549527000   -2.475578000    1.261179000
C   -2.697469000   -1.683914000    0.547123000
C   -3.279429000   -0.658317000   -0.386899000
C   -1.398388000   -1.305254000   -2.093238000
C   -2.586763000   -0.452582000   -1.736055000
C   -1.011023000    1.517961000   -2.243597000
C   -2.325386000    1.009599000   -1.831465000
Gd  -1.207327000    0.003282000   -0.001780000
Gd   1.192336000   -0.009582000   -0.008834000
```

Appendix S13: The optimized cartesian coordinates of Gd$_2$@C$_{42}$-C_1.

```
C     0.587169000   -2.085190000   -1.934117000
C    -0.797395000   -1.680137000   -2.127420000
C    -1.016175000   -0.344550000   -2.599346000
C     1.793065000   -1.250187000   -2.055967000
C     2.452630000    1.170169000   -1.542823000
C     1.592177000    0.204194000   -2.345414000
C     0.146429000    0.597410000   -2.561649000
C     3.336702000    0.679753000   -0.387846000
C    -2.845495000   -1.530161000   -0.527992000
C    -3.183010000   -0.216176000   -1.169193000
C    -1.640278000   -2.245379000   -1.037518000
C    -2.243045000    0.344121000   -2.183077000
C     0.333850000    2.655621000   -1.172725000
C    -0.435228000    1.858012000   -2.041003000
C    -1.864779000    1.675897000   -1.766227000
C     1.750369000    2.334490000   -0.978905000
C    -0.657489000   -2.455486000    1.305721000
C    -1.784129000   -1.715005000    1.795781000
C    -0.636763000   -2.838820000   -0.089172000
C    -2.915581000   -1.294912000    0.941918000
C    -3.353804000    0.819926000   -0.105466000
C    -3.167690000    0.139215000    1.225068000
C     1.885674000   -2.559295000   -0.052645000
C     1.891032000   -2.051523000    1.311568000
C     0.643567000   -2.859011000   -0.722844000
C     0.584567000   -1.891098000    1.926880000
C     2.880090000   -0.928442000    1.359568000
C    -1.284535000   -0.573192000    2.528779000
```

S67

C	0.193227000	-0.633830000	2.582717000
C	3.402484000	-0.751082000	-0.034333000
C	2.692830000	-1.694889000	-0.918465000
C	-2.079311000	0.598420000	2.151044000
C	-1.277920000	1.764699000	1.826843000
C	0.210972000	1.774483000	2.063166000
C	1.028730000	0.576195000	2.449229000
C	2.448262000	0.426117000	1.911475000
C	-2.477515000	1.977671000	-0.440732000
C	-1.541969000	2.506575000	0.558439000
C	-0.254690000	3.012936000	0.115428000
C	2.001398000	2.432409000	0.434681000
C	0.752607000	2.689465000	1.092720000
C	2.882604000	1.380064000	0.849411000
Gd	-1.243159000	0.010393000	-0.016854000
Gd	1.248924000	-0.101641000	0.015055000

Appendix S14: The optimized cartesian coordinates of Gd$_2$@C$_{42}$-C_s.

C	-2.911030000	-0.006944000	1.661532000
C	-2.159284000	1.297879000	1.762600000
C	-0.827956000	1.250409000	2.336850000
C	-2.156145000	-1.310113000	1.761781000
C	-0.824824000	-1.260624000	2.336151000
C	-0.272487000	-0.004742000	2.840397000
C	0.134220000	-2.754999000	0.585209000
C	0.317447000	-2.030352000	1.825491000
C	-1.126362000	2.628337000	-0.164245000
C	0.127617000	2.747696000	0.586359000
C	-2.340085000	2.038429000	0.450528000
C	0.312375000	2.022356000	1.825895000
C	1.577938000	1.280492000	2.104332000
C	1.240367000	2.735745000	-0.332000000
C	2.500854000	2.073592000	-0.060060000
C	2.724442000	1.323675000	1.183201000
C	1.155587000	-0.003210000	2.696005000
C	-2.694115000	0.725950000	-1.745486000
C	-1.374649000	1.176375000	-2.235192000
C	-3.198841000	1.207746000	-0.408364000
C	-0.708912000	2.237915000	-1.538712000
C	0.744357000	2.303765000	-1.607830000
C	-1.371904000	-1.185434000	-2.235353000
C	-2.692366000	-0.738253000	-1.745694000
C	-0.703339000	-2.245605000	-1.539555000
C	0.750138000	-2.309405000	-1.609074000
C	1.618342000	1.255659000	-2.135959000
C	0.963629000	-0.002224000	-2.567819000
C	-0.546128000	-0.003517000	-2.620520000
C	1.622198000	-1.259509000	-2.137649000
C	-3.558738000	-0.007233000	0.354688000
C	-3.195972000	-1.221288000	-0.408639000
C	-1.120021000	-2.637369000	-0.165228000
C	-2.335160000	-2.050186000	0.449640000

C	2.821514000	1.243732000	-1.234493000
C	3.416503000	-0.000706000	-0.738709000
C	2.826162000	-1.246570000	-1.235853000
C	1.581945000	-1.286427000	2.105196000
C	2.729642000	-1.327814000	1.183949000
C	3.359997000	-0.000787000	0.754032000
C	1.247327000	-2.741563000	-0.333358000
C	2.507751000	-2.078360000	-0.060778000
Gd	1.246952000	-0.009079000	-0.027983000
Gd	-1.288391000	-0.004236000	-0.024540000

Appendix S15: The optimized cartesian coordinates of Gd$_2$@C$_{44}$-*C*$_s$.

C	-0.733888000	-2.350696000	1.598758000
C	-2.003074000	-2.277954000	0.941066000
C	-2.926219000	-1.187436000	1.265449000
C	0.362003000	-2.998086000	0.931021000
C	-3.513241000	-0.729925000	-0.014320000
C	-3.512634000	0.719646000	-0.014884000
C	-2.837086000	1.430512000	-1.136922000
C	-2.837615000	-1.441446000	-1.136248000
C	-1.984218000	-0.736205000	-2.161599000
C	-1.983724000	0.724958000	-2.161731000
C	-0.752210000	-2.543399000	-1.234022000
C	-2.008455000	-2.451550000	-0.521734000
C	1.678025000	-2.552791000	-0.961455000
C	0.379050000	-2.995724000	-0.530820000
C	-0.752018000	2.532971000	-1.235335000
C	-2.007996000	2.441094000	-0.523021000
C	0.379433000	2.985271000	-0.532345000
C	1.678672000	2.542655000	-0.962944000
C	1.881725000	1.460855000	-1.942886000
C	-0.659447000	1.412847000	-2.199617000
C	0.663435000	0.754313000	-2.462914000
C	-2.002320000	2.267825000	0.939625000
C	-2.925615000	1.177646000	1.264661000
C	-0.733384000	2.340755000	1.597215000
C	0.362463000	2.988099000	0.929505000
C	-0.193718000	1.208807000	2.362993000
C	-1.010622000	-0.004658000	2.539302000
C	-2.443750000	-0.004636000	2.074511000
C	-0.193963000	-1.218075000	2.363325000
C	1.591797000	2.394552000	1.365572000
C	1.311789000	1.225970000	2.190893000
C	2.147720000	-0.004657000	2.070844000
C	1.311458000	-1.235064000	2.190957000
C	1.591266000	-2.404106000	1.366663000
C	2.464372000	2.287935000	0.218792000
C	3.304195000	1.153659000	0.002685000
C	3.271966000	-0.004764000	0.956439000
C	-0.659829000	-1.423963000	-2.198864000
C	0.663109000	-0.765126000	-2.461898000
C	3.053060000	0.718315000	-1.402773000

C	3.052310000	-0.728597000	-1.402054000
C	1.880861000	-1.471095000	-1.941392000
C	3.302980000	-1.163254000	0.003242000
C	2.463529000	-2.297399000	0.219871000
Gd	-1.335240000	-0.006714000	0.030587000
Gd	1.269169000	-0.001758000	-0.104785000

Appendix S16: The optimized cartesian coordinates of Gd$_2$@C$_{44}$-*D*$_2$.

C	-2.766824000	-1.777187000	-0.572923000
C	-1.874678000	-2.546398000	0.276945000
C	-1.853999000	-1.994735000	1.590916000
C	0.668270000	-2.237722000	1.683573000
C	-0.580455000	-1.720808000	2.240745000
C	-3.395154000	-0.675350000	0.280912000
C	-3.397060000	0.672526000	-0.290405000
C	-2.753841000	0.852989000	-1.668880000
C	-2.754163000	-0.854117000	1.659953000
C	-1.881568000	2.547545000	-0.283915000
C	-1.856924000	1.995963000	-1.598161000
C	-1.957928000	0.207192000	2.363499000
C	-1.981608000	1.530912000	1.815032000
C	-2.773355000	1.776203000	0.564345000
C	0.623593000	-0.376873000	-2.738713000
C	-0.629627000	0.383279000	-2.739931000
C	-0.581376000	1.725491000	-2.245654000
C	-0.633119000	2.854156000	0.378441000
C	0.614136000	2.856090000	-0.381797000
C	0.665239000	2.245646000	-1.686026000
C	1.966266000	1.536362000	-1.818239000
C	1.946369000	0.212813000	-2.367227000
C	-0.682549000	2.243368000	1.682584000
C	-1.973778000	-1.529654000	-1.821282000
C	-0.672968000	-2.239523000	-1.687242000
C	-1.952838000	-0.206420000	-2.370382000
C	0.574310000	-1.719011000	-2.244289000
C	1.848744000	-1.989630000	-1.594679000
C	-0.624351000	-2.850269000	-0.383162000
C	0.621395000	-2.848464000	0.379375000
C	1.870946000	-2.541431000	-0.280643000
C	3.384134000	0.681508000	0.286871000
C	3.386642000	-0.666593000	-0.283768000
C	2.745836000	-0.846756000	-1.663857000
C	2.757083000	1.783444000	-0.567919000
C	2.761008000	-1.769801000	0.569370000
C	2.739899000	0.860108000	1.665036000
C	1.840135000	2.000575000	1.594527000
C	1.863262000	2.552351000	0.280516000
C	-0.633526000	-0.378847000	2.735264000
C	0.617397000	0.384741000	2.736689000
C	0.565398000	1.726769000	2.242356000
C	1.967080000	-1.524658000	1.817889000
C	1.942375000	-0.201422000	2.366771000

Gd	-1.279804000	0.003386000	-0.002445000
Gd	1.269430000	0.004837000	-0.001684000

Appendix S17: The optimized cartesian coordinates of Gd$_2$@C$_{46}$-C_1.

C	-2.704197000	-0.401838000	1.916434000
C	-3.478156000	0.157834000	0.795494000
C	-3.122963000	1.550120000	0.345080000
C	-1.955269000	-1.699124000	1.764946000
C	-3.559179000	-0.644712000	-0.453380000
C	-2.816607000	-1.924798000	-0.577054000
C	-1.993539000	-2.419920000	0.503943000
C	-3.152765000	0.187884000	-1.589940000
C	-2.902108000	1.539493000	-1.104238000
C	0.295876000	2.925758000	0.017517000
C	-1.121928000	2.746468000	-0.166277000
C	-1.639475000	2.194978000	-1.407617000
C	-2.095528000	-0.519954000	-2.348344000
C	-0.865798000	0.169874000	-2.701647000
C	-0.662680000	1.551444000	-2.301556000
C	0.770413000	1.761178000	-2.137418000
C	1.249865000	2.567673000	-1.043520000
C	-1.965091000	-1.833611000	-1.755534000
C	-1.325294000	1.759351000	2.086843000
C	0.145055000	1.837901000	2.221817000
C	-1.974379000	2.291970000	0.929197000
C	0.914086000	2.555853000	1.265169000
C	2.285917000	2.133903000	1.009676000
C	3.300859000	1.096685000	-0.848381000
C	2.511346000	2.242103000	-0.419812000
C	-1.754228000	0.488415000	2.625044000
C	-0.556905000	-0.229600000	2.961901000
C	0.571379000	-2.128947000	1.928405000
C	-0.644713000	-1.538098000	2.421930000
C	2.865736000	0.888744000	1.531000000
C	1.945208000	0.003768000	2.354521000
C	0.648350000	0.585431000	2.753555000
C	1.893400000	-1.435127000	2.006135000
C	3.625418000	0.318149000	0.368762000
C	3.480950000	-1.088147000	0.010852000
C	2.670186000	-1.937909000	0.857478000
C	1.496442000	0.514854000	-2.510063000
C	2.966989000	-1.177487000	-1.362899000
C	2.800314000	0.200174000	-1.901707000
C	-0.652201000	-2.396955000	-1.466891000
C	1.830586000	-2.128444000	-1.354845000
C	0.574462000	-1.827715000	-2.036631000
C	0.454146000	-0.510873000	-2.686731000
C	1.755567000	-2.658925000	-0.005255000
C	0.501475000	-2.839131000	0.683308000
C	-0.702262000	-2.835365000	-0.080561000
Gd	1.368161000	-0.011884000	-0.049344000
Gd	-1.359607000	0.003134000	-0.053660000

Appendix S18: The optimized cartesian coordinates of Gd$_2$@C$_{46}$-C_s.

C	3.419609000	-0.732839000	-1.036584000
C	3.418976000	0.735447000	-1.036058000
C	2.357025000	-1.463573000	-1.743031000
C	2.355979000	1.466213000	-1.742057000
C	1.331226000	0.741602000	-2.496827000
C	1.331978000	-0.738999000	-2.497259000
C	-0.067202000	-1.181721000	-2.467004000
C	-1.915939000	-2.224075000	-1.103008000
C	-0.534781000	-2.252457000	-1.569102000
C	3.429393000	1.169889000	0.370817000
C	2.482552000	2.274494000	0.479311000
C	1.868949000	2.478054000	-0.818301000
C	2.202643000	0.000047000	2.284175000
C	1.289000000	1.175986000	2.375993000
C	3.321533000	0.000566000	1.268034000
C	1.423244000	2.278316000	1.455613000
C	0.207358000	2.764874000	0.783284000
C	-0.077248000	0.712458000	2.669242000
C	-1.283097000	1.432915000	2.256826000
C	-1.096695000	2.462951000	1.269852000
C	-2.195431000	2.418021000	0.323935000
C	-0.067766000	1.183328000	-2.466844000
C	-0.536394000	2.253381000	-1.568190000
C	0.463533000	2.774301000	-0.644693000
C	-1.917285000	2.223972000	-1.102423000
C	2.484067000	-2.273181000	0.478041000
C	1.424616000	-2.278210000	1.454348000
C	3.430311000	-1.168115000	0.370302000
C	1.289791000	-1.176359000	2.375446000
C	-0.076638000	-0.713623000	2.668786000
C	0.209224000	-2.765644000	0.782013000
C	-1.094991000	-2.463904000	1.268432000
C	-1.281875000	-1.434506000	2.255795000
C	0.465364000	-2.773835000	-0.646256000
C	1.870526000	-2.476437000	-0.819714000
C	-2.193957000	-2.418943000	0.322792000
C	-3.168756000	-1.445786000	0.779476000
C	-3.632187000	-0.720031000	-0.424590000
C	-3.169831000	1.444054000	0.779875000
C	-2.565401000	0.728846000	1.949211000
C	-2.564986000	-0.730987000	1.948695000
C	-3.632335000	0.718585000	-0.424117000
C	-0.924541000	0.000490000	-2.652961000
C	-2.311391000	0.000105000	-2.283707000
C	-2.841447000	1.182515000	-1.573602000
C	-2.840617000	-1.183013000	-1.573931000
Gd	-1.402174000	0.000059000	-0.019692000
Gd	1.394101000	-0.000544000	-0.006561000

Appendix S19: The optimized cartesian coordinates of Gd$_2$@C$_{48}$-C_1.

C	0.991921000	2.863464000	-0.365905000
C	2.307935000	2.278200000	-0.570243000
C	0.315333000	2.798943000	0.926697000
C	3.025945000	1.664687000	0.513244000
C	3.723784000	0.365658000	0.242110000
C	3.440176000	-0.473569000	1.389942000
C	-1.931439000	2.565080000	-0.192598000
C	-1.209307000	2.347687000	-1.457478000
C	-1.122343000	2.640061000	1.013823000
C	0.195858000	2.561797000	-1.536375000
C	0.984062000	1.761523000	-2.431898000
C	2.295573000	1.590228000	-1.893082000
C	-2.581698000	0.842972000	2.072337000
C	-3.482464000	0.906286000	0.915251000
C	-1.416578000	1.708531000	2.128621000
C	-3.124638000	1.758537000	-0.236563000
C	-3.066955000	0.905626000	-1.431347000
C	0.446713000	0.494013000	-2.867958000
C	-0.979781000	0.199291000	-2.731950000
C	-1.837693000	1.246261000	-2.171180000
C	-1.354306000	-1.177155000	-2.454341000
C	-2.351652000	-0.586590000	2.343346000
C	-3.692706000	-0.457215000	0.398700000
C	-3.006602000	-1.379867000	1.323562000
C	-1.009583000	-1.107864000	2.547237000
C	0.103020000	-0.216594000	2.814152000
C	-0.123689000	1.211684000	2.611333000
C	0.934147000	2.014751000	1.958916000
C	2.282907000	1.515953000	1.813656000
C	1.438382000	-0.746722000	2.595355000
C	2.541103000	0.175972000	2.305925000
C	-0.827186000	-2.241820000	1.649433000
C	-1.884708000	-2.522929000	-0.588058000
C	-2.049777000	-2.348889000	0.833918000
C	-0.586644000	-2.889324000	-1.065350000
C	0.612956000	-2.944613000	-0.252948000
C	0.503319000	-2.588129000	1.137499000
C	1.643926000	-1.947894000	1.770466000
C	-2.460510000	-1.520901000	-1.530807000
C	-3.376676000	-0.481863000	-1.046739000
C	1.503007000	-0.489806000	-2.645277000
C	1.109880000	-1.806513000	-2.241567000
C	-0.290116000	-2.128470000	-2.240155000
C	2.899779000	-1.804862000	-0.469841000
C	3.423859000	-0.483626000	-0.977023000
C	2.662456000	0.176740000	-2.031713000
C	1.729377000	-2.412556000	-1.079257000
C	2.886878000	-1.743793000	0.994113000
Gd	-1.425078000	0.061251000	0.110447000
Gd	1.409048000	-0.038208000	0.090518000

Appendix S20: The optimized cartesian coordinates of Gd$_2$@C$_{48}$-C_{2v}.

C	2.596674000	-0.933119000	-1.985577000
C	2.482607000	-2.175588000	-1.186353000
C	2.146333000	1.900824000	-1.441663000
C	3.247335000	1.280868000	-0.754025000
C	3.595357000	-0.074253000	-1.204810000
C	1.269015000	2.808348000	-0.718681000
C	1.268509000	2.808415000	0.717812000
C	0.001069000	2.824225000	-1.388590000
C	3.287201000	-2.051192000	-0.000454000
C	3.957227000	-0.796842000	-0.000148000
C	2.481714000	-2.175567000	1.184848000
C	1.195124000	-2.650327000	0.745540000
C	0.002770000	-2.262668000	1.439257000
C	-1.188365000	-2.650774000	0.744890000
C	-2.475347000	-2.176662000	1.182815000
C	3.593936000	-0.074265000	1.204246000
C	2.595005000	-0.932777000	1.983801000
C	0.002296000	-1.054113000	2.325692000
C	-1.188033000	-2.650832000	-0.749224000
C	-2.474880000	-2.176559000	-1.187484000
C	-3.280527000	-2.053439000	-0.002406000
C	0.003733000	-2.263055000	-1.442704000
C	1.195657000	-2.650595000	-0.748060000
C	-2.589000000	-0.934764000	-1.986319000
C	-1.338635000	-0.326279000	-2.490557000
C	0.003881000	-1.054392000	-2.328905000
C	1.345282000	-0.325599000	-2.489979000
C	1.280711000	1.135419000	-2.392864000
C	-1.276470000	1.134966000	-2.394743000
C	0.002004000	1.783740000	-2.378761000
C	-3.589511000	-0.076509000	-1.206618000
C	-3.951151000	-0.799813000	-0.002209000
C	-3.245053000	1.278567000	0.753022000
C	-3.244719000	1.278592000	-0.756944000
C	-2.143831000	1.900036000	-1.443764000
C	-2.144751000	1.900012000	1.440549000
C	-3.589926000	-0.076915000	1.202215000
C	1.279073000	1.135453000	2.391447000
C	1.343588000	-0.325343000	2.487538000
C	0.000413000	1.783892000	2.376955000
C	-1.278126000	1.135086000	2.392026000
C	-1.340088000	-0.326270000	2.486799000
C	-2.589893000	-0.934826000	1.981765000
C	2.145315000	1.900785000	1.440977000
C	3.246358000	1.280471000	0.753694000
C	-1.267366000	2.807654000	-0.719831000
C	-1.267930000	2.808010000	0.717378000
C	0.000173000	2.824594000	1.386975000
Gd	-1.498107000	-0.143719000	-0.002320000
Gd	1.504295000	-0.151659000	-0.002227000

Appendix S21: The optimized cartesian coordinates of Gd$_2$@C$_{52}$-C_s.

C	1.212416000	3.136035000	1.154679000
C	-0.134864000	3.110420000	0.738434000
C	2.034570000	3.340408000	0.000100000
C	3.094701000	2.408986000	0.000336000
C	-2.369374000	2.311741000	-0.755684000
C	-3.378961000	1.392651000	-1.195615000
C	1.212849000	3.135422000	-1.154502000
C	-0.134563000	3.110010000	-0.738822000
C	-1.098070000	2.336144000	-1.433695000
C	-4.075313000	0.978940000	-0.000753000
C	-4.239394000	-0.429646000	-0.000387000
C	-3.641428000	-0.966017000	-1.204417000
C	-1.600240000	-2.303794000	-1.419032000
C	-2.836563000	-2.078465000	-0.758791000
C	1.723028000	2.008186000	-1.899973000
C	0.836700000	0.973291000	-2.399571000
C	-0.653475000	1.187629000	-2.276994000
C	-1.633780000	0.052144000	-2.471925000
C	-3.028470000	0.186228000	-2.001903000
C	-1.018787000	-1.273593000	-2.329426000
C	-3.379362000	1.393039000	1.194336000
C	-2.369682000	2.312127000	0.754490000
C	-1.098818000	2.337000000	1.433138000
C	-3.029333000	0.187043000	2.001140000
C	-1.019769000	-1.272730000	2.329253000
C	-1.634750000	0.053240000	2.471755000
C	-0.654663000	1.188543000	2.276964000
C	0.835522000	0.973970000	2.399342000
C	1.722041000	2.008675000	1.900158000
C	-1.600815000	-2.302966000	1.419465000
C	-2.836824000	-2.078208000	0.758841000
C	-3.642038000	-0.965505000	1.203941000
C	-0.538142000	-2.984347000	0.745910000
C	-0.537922000	-2.983791000	-0.744468000
C	0.412701000	-1.476779000	2.319843000
C	1.400687000	-0.429069000	2.509007000
C	2.782958000	-0.703572000	2.036040000
C	3.524957000	0.360498000	1.305178000
C	3.016843000	1.670331000	1.255289000
C	3.002331000	-1.940682000	1.202534000
C	3.715611000	-1.562763000	0.000678000
C	1.912064000	-2.742306000	0.755980000
C	0.666767000	-2.635982000	1.409486000
C	0.667403000	-2.635456000	-1.408015000
C	3.003210000	-1.941159000	-1.201412000
C	1.912391000	-2.742416000	-0.754652000
C	3.017471000	1.670146000	-1.254890000
C	3.525657000	0.360282000	-1.304055000
C	2.783851000	-0.704149000	-2.035277000
C	1.401995000	-0.429623000	-2.509005000
C	0.413531000	-1.477416000	-2.319640000
C	3.997399000	-0.177480000	0.000718000

Gd	1.556941000	-0.292123000	-0.000418000
Gd	-1.711089000	0.016009000	0.000031000

Appendix S22: The optimized cartesian coordinates of Gd$_2$@C$_{52}$-D_{2d}.

C	3.270379000	-1.949410000	0.022150000
C	3.667713000	-1.182529000	-1.178015000
C	1.987256000	-2.555591000	0.029561000
C	1.121471000	-2.458253000	1.209998000
C	0.237997000	-0.698623000	2.656491000
C	1.398674000	-1.440585000	2.227388000
C	1.120520000	-2.484153000	-1.152429000
C	1.397286000	-1.491402000	-2.194000000
C	2.658514000	-0.779963000	-2.158858000
C	0.236330000	-0.761043000	-2.642604000
C	-0.238362000	-2.656160000	-0.698012000
C	-2.660411000	-2.175596000	-0.728271000
C	-1.399577000	-2.227836000	-1.439612000
C	-1.122876000	-1.209776000	-2.457277000
C	-3.668488000	-1.176495000	1.182940000
C	-2.659952000	-2.158039000	0.780456000
C	-0.237964000	-2.643023000	0.761385000
C	-1.121066000	-1.152220000	2.484484000
C	-1.398569000	-2.193878000	1.491894000
C	2.658774000	0.728779000	-2.176012000
C	3.668671000	1.153657000	-1.205485000
C	0.236600000	0.698382000	-2.655331000
C	1.397964000	1.440040000	-2.227630000
C	1.121819000	2.457739000	-1.209811000
C	1.988525000	2.555007000	-0.029991000
C	3.271381000	1.948324000	-0.023314000
C	-3.271800000	-0.022169000	-1.947732000
C	-1.988860000	-0.029232000	-2.554486000
C	-1.122110000	1.152979000	-2.482923000
C	-1.398263000	2.194942000	-1.490051000
C	-0.237104000	2.644048000	-0.760687000
C	-3.669765000	-1.204061000	-1.153249000
C	4.359790000	-0.009354000	-0.721442000
C	4.360187000	0.007511000	0.719303000
C	3.669253000	1.181106000	1.176542000
C	2.659767000	-0.729643000	2.175236000
C	3.668867000	-1.155111000	1.203905000
C	1.122325000	2.484302000	1.152587000
C	1.399391000	1.491133000	2.194147000
C	2.660334000	0.778971000	2.158144000
C	0.238472000	0.760772000	2.642430000
C	-0.236489000	2.657685000	0.699159000
C	-2.658567000	2.175926000	0.729853000
C	-1.397264000	2.227843000	1.440381000
C	-1.120675000	1.210150000	2.457590000
C	-3.668699000	1.178044000	-1.180511000
C	-2.659292000	2.159137000	-0.778064000

C	-4.360606000	-0.719533000	0.009756000
C	-4.359868000	0.721217000	-0.007020000
C	-1.987069000	0.030296000	2.555428000
C	-3.668174000	1.205370000	1.155558000
C	-3.270216000	0.023409000	1.949500000
Gd	1.661991000	0.000510000	0.000348000
Gd	-1.661632000	-0.000800000	-0.001609000

Appendix S23: The optimized cartesian coordinates of Gd$_2$@C$_{60}$-I_h.

C	2.473712188	1.925435149	1.715088129
C	3.427478264	1.040546080	1.033019079
C	1.629059122	1.502388117	2.789096214
C	3.428558261	-0.380755029	1.414961109
C	3.420105263	-1.438089107	0.358487027
C	3.418637262	1.426747108	-0.410533032
C	3.409861260	0.385206030	-1.449938111
C	3.410879259	-1.057366080	-1.062829083
C	-0.246285019	2.929842222	1.997965151
C	0.589444045	3.366115256	0.896944070
C	0.282287022	1.999813154	2.926428225
C	1.911291146	2.856067220	0.753280057
C	2.460482185	2.530685194	-0.550241044
C	-0.259220020	3.535992271	-0.265875021
C	0.256577020	3.193612241	-1.539403119
C	1.603579121	2.698269205	-1.683696128
C	-1.882045144	0.769408056	2.866118216
C	-2.444741189	1.733443134	1.939323146
C	-0.557620045	0.904995068	3.368830258
C	-1.597023123	2.801749212	1.509584113
C	-1.605766121	3.178058240	0.107056008
C	-3.409547262	1.057971083	1.063311079
C	-3.419827260	1.438463109	-0.357140027
C	-2.462452190	2.464637190	-0.789649060
C	-0.244495019	-1.534321117	3.196236246
C	-1.595226122	-1.668792126	2.710375208
C	0.283467022	-0.263700020	3.533871270
C	-2.444092185	-0.529802038	2.547842195
C	-3.408935258	-0.384653029	1.450734110
C	-1.603860125	-2.697698206	1.685338128
C	-2.460753188	-2.530303192	0.551796041
C	-3.418764259	-1.426157108	0.411913032
C	2.474154189	-0.804594062	2.447637185
C	1.912455145	-2.091871162	2.081686156
C	1.629799124	0.099209008	3.166017241
C	0.591367043	-2.462419186	2.461422189
C	-0.256843020	-3.193196245	1.541050119
C	2.462579188	-2.464014189	0.790999060
C	1.605747123	-3.177436240	-0.105612008
C	0.259087020	-3.535288270	0.267391020
C	-2.474774189	-1.925261145	-1.713663129
C	-1.911805146	-2.855668220	-0.751777056
C	-0.589625044	-3.365267255	-0.895370070

S77

C	-1.629618124	-1.501736113	-2.787338213
C	-2.475261190	0.805457061	-2.446734187
C	-3.429873262	0.381322029	-1.413935108
C	-3.429122264	-1.040599077	-1.031957078
C	-1.630475126	-0.098546007	-3.164613243
C	0.244050019	1.534991119	-3.194533243
C	-0.591640046	2.463279189	-2.460148190
C	-1.912819145	2.092548160	-2.080322160
C	-0.284015022	0.264368020	-3.532412271
C	1.881530143	-0.768657059	-2.863949219
C	2.443659185	0.530247039	-2.546103196
C	1.594767124	1.669196126	-2.708714206
C	0.556921044	-0.904032071	-3.366730255
C	0.246075019	-2.929037222	-1.996229153
C	1.596962120	-2.801249214	-1.508369117
C	2.444712185	-1.732741133	-1.938376147
C	-0.282710022	-1.998691150	-2.924302223
Gd	1.528674119	-0.001683000	-0.003599000
Gd	-1.527741116	-0.000016000	-0.000461000

Appendix S24: The optimized cartesian coordinates of Gd$_2$@C$_{80}$-C_{2v}.

C	-4.393641000	-0.894393000	-0.739457000
C	-4.145187000	0.357982000	-1.436851000
C	-4.393602000	-0.894266000	0.740586000
C	-4.016356000	1.589660000	-0.739750000
C	-1.119131000	0.617630000	-3.634991000
C	-3.212408000	0.127048000	-2.529597000
C	-2.265062000	1.120961000	-2.971421000
C	-2.177534000	2.405624000	-2.283949000
C	-0.920141000	3.151161000	-2.285109000
C	-3.095329000	2.592368000	-1.182475000
C	-0.654808000	4.037878000	-1.186511000
C	-2.938158000	-2.951426000	0.743731000
C	-2.938229000	-2.951543000	-0.742012000
C	-3.590880000	-1.890859000	1.421304000
C	-3.590966000	-1.891016000	-1.419815000
C	-2.874093000	-1.275100000	-2.520704000
C	-1.597123000	-1.757629000	-2.973961000
C	-0.793062000	-0.796401000	-3.643238000
C	0.373873000	-3.974537000	0.000886000
C	-1.699628000	-3.467172000	1.194665000
C	-0.992708000	-3.883649000	0.000950000
C	-0.958979000	-2.886636000	-2.304108000
C	-1.699680000	-3.467230000	-1.192811000
C	1.136810000	-3.660694000	-1.188375000
C	0.484479000	-2.989098000	-2.307879000
C	1.136993000	-3.660610000	1.190011000
C	0.484752000	-2.988593000	2.309320000
C	-0.958713000	-2.886279000	2.305776000
C	-1.596784000	-1.757086000	2.975389000
C	-2.873734000	-1.274750000	2.521955000
C	-0.792662000	-0.795437000	3.644058000

C	2.449474000	-3.353065000	0.740836000
C	3.250312000	-2.393196000	1.431337000
C	2.630670000	-1.703530000	2.546816000
C	1.284193000	-1.982606000	3.003434000
C	0.625042000	-0.918421000	3.684229000
C	3.250553000	-2.393884000	-1.430591000
C	2.449420000	-3.353225000	-0.739499000
C	0.624640000	-0.919453000	-3.683428000
C	1.283872000	-1.983443000	-3.002388000
C	2.630527000	-1.704370000	-2.546059000
C	-1.118660000	0.618616000	3.635348000
C	-2.264453000	1.121776000	2.971546000
C	-3.211005000	0.127568000	2.529159000
C	-4.144330000	0.358245000	1.437241000
C	-4.016372000	1.589995000	0.740221000
C	-0.919951000	3.151894000	2.284940000
C	-2.177339000	2.406444000	2.284030000
C	-3.095384000	2.592892000	1.182700000
C	-0.654698000	4.038260000	1.186008000
C	-1.478852000	3.994355000	-0.000171000
C	-2.660132000	3.296441000	-0.000036000
C	0.102769000	1.360331000	3.674695000
C	1.559610000	2.966035000	2.573595000
C	0.240350000	2.616577000	3.001576000
C	3.163128000	-0.370158000	2.570160000
C	2.438435000	0.719487000	3.152059000
C	1.180591000	0.418513000	3.737010000
C	2.635602000	2.011192000	2.610587000
C	2.929835000	3.319793000	0.703141000
C	1.777105000	3.806516000	1.419962000
C	0.676321000	4.312720000	0.729276000
C	2.929742000	3.319576000	-0.703730000
C	4.020658000	-0.196013000	1.414974000
C	4.043729000	1.089855000	0.739404000
C	3.459777000	2.194939000	1.420001000
C	4.020754000	-0.196489000	-1.414759000
C	4.128089000	-1.471855000	-0.731896000
C	4.128022000	-1.471578000	0.732383000
C	3.459590000	2.194455000	-1.420274000
C	4.043660000	1.089630000	-0.739416000
C	1.180154000	0.417470000	-3.736566000
C	2.635315000	2.010403000	-2.610745000
C	2.438063000	0.718570000	-3.151812000
C	3.162871000	-0.370918000	-2.569725000
C	0.676238000	4.312509000	-0.729997000
C	1.776987000	3.806083000	-1.420609000
C	1.559375000	2.965297000	-2.573972000
C	0.240054000	2.615759000	-3.001765000
C	0.102341000	1.359291000	-3.674399000
Gd	-2.144421000	-0.219454000	-0.000744000
Gd	1.884265000	-0.825408000	-0.001173000

Appendix S25: The optimized cartesian coordinates of Gd$_2$@C$_{80}$-*D*$_{5h}$.

C	3.473972000	2.122521000	0.841453000
C	4.094360000	0.865460000	0.541608000
C	4.129350000	0.459671000	-0.861085000
C	3.912417000	-0.190510000	1.518924000
C	3.091933000	0.048858000	2.695587000
C	2.442722000	1.302632000	2.971851000
C	2.730427000	2.363498000	2.062448000
C	3.700405000	-1.592709000	1.117320000
C	3.666882000	-1.990693000	-0.273507000
C	3.919195000	-0.942945000	-1.261465000
C	2.686477000	-2.980842000	-0.622024000
C	1.238904000	-1.198504000	3.753142000
C	2.456804000	-1.186703000	3.056207000
C	2.750644000	-2.172288000	2.062645000
C	1.752248000	-3.143349000	1.697971000
C	1.804083000	-3.615025000	0.353623000
C	0.235769000	2.361875000	3.418133000
C	1.155806000	1.297610000	3.677857000
C	0.592713000	0.042261000	4.075231000
C	1.985175000	-2.997641000	-1.891186000
C	2.155917000	-1.939382000	-2.825271000
C	3.120565000	-0.918734000	-2.472028000
C	1.049438000	-1.574375000	-3.635727000
C	-0.616999000	-4.040188000	0.337521000
C	0.624525000	-4.039386000	-0.331401000
C	0.701763000	-3.622896000	-1.700219000
C	-0.460959000	-3.157339000	-2.405538000
C	-0.243160000	-2.191687000	-3.434357000
C	0.247260000	-2.186335000	3.437754000
C	0.466838000	-3.153114000	2.410365000
C	-0.695024000	-3.621974000	1.705793000
C	0.826386000	-0.197455000	-4.021574000
C	1.713871000	0.834393000	-3.604955000
C	2.872935000	0.441441000	-2.837994000
C	1.176913000	2.122721000	-3.359017000
C	-2.454518000	-1.195497000	-3.054162000
C	-1.236627000	-1.206174000	-3.751213000
C	-0.592698000	0.035344000	-4.074943000
C	-1.158111000	1.290257000	-3.679472000
C	-0.240020000	2.356592000	-3.421206000
C	-1.797321000	-3.618911000	-0.348147000
C	-1.746355000	-3.148994000	-1.693136000
C	-2.746426000	-2.180114000	-2.059106000
C	1.738985000	2.981152000	-2.324793000
C	2.847543000	2.561631000	-1.539653000
C	3.458539000	1.287041000	-1.843124000
C	2.898327000	2.988910000	-0.185544000
C	-1.769465000	3.384953000	-1.793956000
C	-0.541586000	3.377878000	-2.452953000
C	0.666966000	3.737851000	-1.742843000

C	0.642712000	4.059326000	-0.351971000
C	1.829104000	3.746662000	0.392971000
C	-3.092055000	0.039373000	-2.695383000
C	-2.445019000	1.293915000	-2.973416000
C	-2.734668000	2.355504000	-2.065464000
C	-1.835948000	3.742692000	-0.397981000
C	-0.650091000	4.058643000	0.346492000
C	-0.673756000	3.739027000	1.737776000
C	0.535448000	3.382347000	2.448402000
C	1.763315000	3.390848000	1.789464000
C	-2.903758000	2.983815000	0.181639000
C	-3.461100000	1.283412000	1.841750000
C	-2.852234000	2.558590000	1.536408000
C	-1.744408000	2.981251000	2.320881000
C	-3.912370000	-0.199797000	-1.518432000
C	-4.130443000	0.453405000	0.860796000
C	-4.096576000	0.857285000	-0.542578000
C	-3.477813000	2.114816000	-0.844069000
C	-2.680793000	-2.984964000	0.626608000
C	-3.916935000	-0.948153000	1.263003000
C	-3.662402000	-1.996677000	0.276637000
C	-3.697172000	-1.600899000	-1.114695000
C	-1.046449000	-1.571152000	3.638252000
C	-3.118563000	-0.920850000	2.473533000
C	-2.152236000	-1.939362000	2.828322000
C	-1.979549000	-2.998648000	1.895772000
C	-1.180722000	2.125355000	3.356340000
C	-2.873722000	0.440301000	2.837738000
C	-1.715358000	0.836390000	3.604133000
C	-0.825948000	-0.193248000	4.022142000
Gd	-1.908670000	-0.250820000	0.010768000
Gd	1.908832000	-0.250742000	-0.011603000

Appendix S26: The optimized cartesian coordinates of Gd$_2$@C$_{59}$N-*C*$_s$.

C	-2.444125000	-2.397096000	1.038764000
C	-3.417370000	-1.385014000	0.586997000
C	-1.642777000	-2.251581000	2.220399000
C	-3.501897000	-0.122661000	1.345441000
C	-3.508801000	1.184348000	0.615877000
C	-3.335285000	-1.358474000	-0.896804000
C	-3.349400000	-0.081352000	-1.612635000
C	-3.436201000	1.202610000	-0.850698000
C	0.321609000	-3.344482000	1.136409000
C	-0.467512000	-3.486624000	-0.069232000
C	-0.273353000	-2.716651000	2.261408000
C	-1.820241000	-3.000746000	-0.106375000
C	-2.323321000	-2.351692000	-1.279555000
C	0.405540000	-3.249085000	-1.169615000
N	-0.076046000	-2.604613000	-2.319756000
C	-1.419167000	-2.145677000	-2.376382000
C	1.844398000	-1.448519000	2.619486000
C	2.478985000	-2.103458000	1.498077000
C	0.507280000	-1.762617000	3.017905000

C	1.683932000	-3.049238000	0.758052000
C	1.736161000	-2.997425000	-0.683108000
C	3.438650000	-1.183808000	0.874161000
C	3.521726000	-1.164777000	-0.602075000
C	2.612290000	-2.058195000	-1.326038000
C	0.085948000	0.621357000	3.486798000
C	1.449931000	0.932219000	3.106667000
C	-0.384016000	-0.709895000	3.448848000
C	2.346981000	-0.090655000	2.683103000
C	3.345560000	0.102781000	1.618956000
C	1.445261000	2.197571000	2.406699000
C	2.330794000	2.371700000	1.301432000
C	3.330612000	1.373973000	0.904265000
C	-2.586993000	0.033115000	2.485158000
C	-2.068559000	1.390544000	2.500599000
C	-1.713313000	-1.004136000	2.943804000
C	-0.769054000	1.681542000	3.006512000
C	0.075342000	2.660898000	2.343729000
C	-2.601857000	2.084305000	1.343463000
C	-1.743056000	3.032380000	0.694302000
C	-0.412972000	3.315088000	1.197397000
C	2.439501000	2.406464000	-1.035906000
C	1.812463000	3.022701000	0.115784000
C	0.473348000	3.509810000	0.063832000
C	1.646001000	2.259731000	-2.217029000
C	2.582075000	-0.025503000	-2.476934000
C	3.503266000	0.140457000	-1.334995000
C	3.408488000	1.401898000	-0.584753000
C	1.716472000	1.017744000	-2.952489000
C	-0.086240000	-0.614089000	-3.455225000
C	0.746198000	-1.650841000	-2.954058000
C	2.073464000	-1.375449000	-2.471064000
C	0.394756000	0.727156000	-3.451902000
C	-1.845156000	1.454207000	-2.610733000
C	-2.363255000	0.111287000	-2.668963000
C	-1.446066000	-0.926760000	-3.093105000
C	-0.504681000	1.770788000	-3.020308000
C	-0.313223000	3.354217000	-1.136243000
C	-1.676644000	3.052293000	-0.747305000
C	-2.470809000	2.116873000	-1.485002000
C	0.272062000	2.721823000	-2.260650000
Gd	-1.535003000	-0.001067000	-0.001103000
Gd	1.533594000	-0.013621000	0.002157000

Appendix S27: The optimized cartesian coordinates of Gd$_2$@C$_{79}$N-C_s-1.

C	2.054910000	-0.244430000	3.618190000
C	0.797210000	0.144470000	4.205450000
C	-0.292630000	-0.842700000	4.136610000
C	0.430140000	1.526990000	3.971150000
C	1.310800000	2.456710000	3.267200000
C	2.552950000	2.041410000	2.675310000
C	2.952450000	0.697670000	2.944140000
C	-0.939560000	1.926500000	3.655290000

C	-1.998320000	0.968480000	3.508160000
C	-1.657010000	-0.418870000	3.775080000
C	-3.005280000	1.254140000	2.541700000
C	0.908630000	4.008330000	1.413400000
C	0.484270000	3.424090000	2.616240000
C	-0.885810000	3.084160000	2.799650000
C	-1.836130000	3.323600000	1.754620000
C	-2.958520000	2.447580000	1.708090000
C	3.820110000	1.944600000	0.534290000
C	3.007350000	2.686440000	1.440710000
C	2.163350000	3.691910000	0.850530000
C	-3.638600000	0.211910000	1.764310000
C	-3.232810000	-1.141310000	1.908580000
C	-2.232560000	-1.423860000	2.916070000
C	-3.264940000	-1.980130000	0.759350000
C	-3.170790000	2.753160000	-0.713420000
C	-3.603770000	2.136910000	0.471530000
C	-3.981840000	0.752560000	0.470050000
C	-3.868730000	-0.040060000	-0.716170000
C	-3.598870000	-1.434180000	-0.536930000
N	-0.010350000	4.291180000	0.395450000
C	-1.374190000	3.931140000	0.510620000
C	-2.072790000	3.680480000	-0.687640000
C	-2.300300000	-3.035060000	0.566300000
C	-1.260940000	-3.262130000	1.511040000
C	-1.264220000	-2.459250000	2.714260000
C	-0.003980000	-3.713060000	1.035710000
C	-2.411980000	-1.557100000	-2.685360000
C	-2.872880000	-2.188960000	-1.513750000
C	-2.034740000	-3.140800000	-0.850400000
C	-0.727220000	-3.446470000	-1.351250000
C	0.258310000	-3.824130000	-0.381620000
C	-3.103020000	2.000920000	-1.930190000
C	-3.408490000	0.612480000	-1.950790000
C	-2.696220000	-0.177670000	-2.929680000
C	1.219460000	-3.306810000	1.687570000
C	1.209440000	-2.477410000	2.843680000
C	-0.067580000	-2.104800000	3.426890000
C	2.273460000	-1.539070000	2.988370000
C	2.066300000	-2.916460000	-1.771930000
C	1.646070000	-3.539870000	-0.582690000
C	2.241460000	-3.169970000	0.668170000
C	3.232270000	-2.146560000	0.747060000
C	3.284300000	-1.398760000	1.970500000
C	-1.162120000	-1.901430000	-3.302600000
C	-0.275680000	-2.805690000	-2.598930000
C	1.122260000	-2.584940000	-2.793620000
C	3.092070000	-1.914060000	-1.735160000
C	3.686850000	-1.498950000	-0.492540000
C	4.160350000	-0.155330000	-0.432580000
C	4.160630000	0.581780000	0.800750000
C	3.721560000	-0.032850000	1.987770000

C	2.827090000	-0.983630000	-2.797930000
C	2.326910000	1.342630000	-3.307260000
C	3.192360000	0.390130000	-2.668000000
C	3.903400000	0.786970000	-1.501330000
C	-0.696510000	-0.739130000	-4.084170000
C	1.122680000	0.946640000	-4.019420000
C	0.737480000	-0.450390000	-4.163830000
C	1.607950000	-1.383260000	-3.486840000
C	-2.008920000	2.534050000	-2.729560000
C	0.142960000	2.007610000	-3.783550000
C	-1.256560000	1.717520000	-3.633290000
C	-1.661470000	0.341060000	-3.805950000
C	0.681460000	4.197200000	-0.839690000
C	0.764020000	3.026410000	-2.979290000
C	0.006570000	3.798350000	-2.031040000
C	-1.381020000	3.569950000	-1.961020000
C	3.686800000	2.084610000	-0.908000000
C	2.108950000	2.618860000	-2.699450000
C	2.760120000	2.989820000	-1.474140000
C	2.022940000	3.828810000	-0.571250000
Gd	0.000000000	0.000000000	-1.915390000
Gd	0.000000000	0.000000000	1.915380000

Appendix S28: The optimized cartesian coordinates of Gd$_2$@C$_{79}$N-C$_s$-2.

C	-0.939940000	-0.829890000	4.199420000
C	-1.622560000	0.428530000	3.964320000
C	0.544170000	-0.837600000	4.291500000
C	-0.926480000	1.666420000	3.936960000
C	-3.607440000	0.800840000	0.822950000
C	-2.669150000	0.236510000	2.964640000
C	-3.041140000	1.276210000	2.037600000
C	-2.370520000	2.549330000	2.052230000
C	-2.296640000	3.323680000	0.821480000
C	-1.320440000	2.705510000	3.044980000
C	-1.204590000	4.249830000	0.649480000
C	0.611120000	-2.832180000	2.744850000
C	-0.872060000	-2.828670000	2.667790000
C	1.257740000	-1.805040000	3.476020000
C	-1.573330000	-1.790080000	3.321870000
C	-2.640150000	-1.149650000	2.576740000
C	-3.024400000	-1.590370000	1.268400000
C	-3.621730000	-0.576110000	0.458530000
C	0.037990000	-3.725190000	-0.640050000
C	1.122950000	-3.300110000	1.510510000
C	-0.031110000	-3.687420000	0.727050000
C	-2.332880000	-2.688010000	0.620640000
C	-1.261600000	-3.298020000	1.389240000
C	-1.109260000	-3.385720000	-1.452020000
C	-2.263020000	-2.736120000	-0.839170000
C	1.266100000	-3.379750000	-1.328460000
C	2.355520000	-2.744150000	-0.590510000
C	2.274450000	-2.698610000	0.855220000
C	2.914780000	-1.602200000	1.572660000

C	2.395980000	-1.167490000	2.845990000
C	3.624370000	-0.612420000	0.844560000
C	0.894750000	-3.032650000	-2.652920000
C	1.630710000	-2.042340000	-3.382300000
C	2.707380000	-1.377230000	-2.670150000
C	3.091340000	-1.712510000	-1.310660000
C	3.736540000	-0.676360000	-0.573770000
C	-1.230180000	-2.030750000	-3.518450000
C	-0.586660000	-3.019700000	-2.724370000
C	-3.588600000	-0.644960000	-0.957220000
C	-2.908460000	-1.716190000	-1.636170000
C	-2.384690000	-1.371570000	-2.935980000
C	3.605540000	0.787790000	1.231280000
C	2.881790000	1.248510000	2.358070000
C	2.393600000	0.219520000	3.248950000
C	1.257190000	0.415980000	4.144220000
C	0.563870000	1.661800000	4.023530000
C	2.268110000	3.334280000	1.071490000
C	2.207470000	2.541430000	2.284930000
C	1.044320000	2.679950000	3.150190000
C	1.177130000	4.244560000	0.783960000
C	-0.047660000	4.151310000	1.530330000
C	-0.111850000	3.404590000	2.679260000
C	3.697730000	1.578220000	0.044620000
C	2.670870000	3.241500000	-1.399550000
C	3.036490000	2.843870000	-0.072350000
C	2.758230000	-0.020950000	-3.141910000
C	3.298560000	1.039410000	-2.340620000
C	3.816360000	0.682360000	-1.068690000
C	2.771250000	2.339010000	-2.509840000
C	0.874020000	3.662800000	-2.848030000
C	1.525900000	4.092690000	-1.642230000
C	0.785910000	4.557680000	-0.552240000
C	-0.540500000	3.663800000	-2.922160000
C	1.650320000	0.190680000	-4.050850000
C	0.970380000	1.478030000	-4.049110000
C	1.613510000	2.557930000	-3.381530000
C	-1.177190000	0.192750000	-4.193280000
C	-0.487510000	-1.071550000	-4.318700000
C	0.978180000	-1.079980000	-4.252770000
C	-1.220330000	2.563220000	-3.540910000
C	-0.505120000	1.477280000	-4.126580000
C	-3.585970000	0.685490000	-1.441380000
C	-2.454560000	2.341490000	-2.803840000
C	-2.981550000	1.050790000	-2.671770000
C	-2.384920000	-0.020410000	-3.411730000
C	-0.679140000	4.561680000	-0.629520000
C	-1.310690000	4.098870000	-1.792540000
C	-2.457580000	3.231000000	-1.664790000
C	-2.914050000	2.817600000	-0.391730000
N	-3.581380000	1.566490000	-0.339910000
Gd	0.000000000	0.000000000	2.053640000

Gd   0.196460000   -0.533620000   -2.014080000

References:

1.   O. Kahn, *VCH Publishers, Inc.(USA), 1993*, 1993, 393.
2.   G. Blondin and J. J. Girerd, *Chem. Rev.*, 1990, **90**, 1359-1376.
3.   R. Bastardis, N. Guihéry, N. Suaud and C. de Graaf, *J. Chem. Phys.*, 2006, **125**, 194708.
4.   J. D. Hilgar, M. G. Bernbeck, B. S. Flores and J. D. Rinehart, *Chem Sci*, 2018, **9**, 7204-7209.
5.   J. J. Le Roy, M. Jeletic, S. I. Gorelsky, I. Korobkov, L. Ungur, L. F. Chibotaru and M. Murugesu, *J Am Chem Soc*, 2013, **135**, 3502-3510.
6.   L. Ungur, J. J. Le Roy, I. Korobkov, M. Murugesu and L. F. Chibotaru, *Angew. Chem. Int. Ed.*, 2014, **126**, 4502-4506.